WASHINGTON UNIVERSITY IN ST. LOUIS

School of Engineering and Applied Science

Department of Energy, Environmental and Chemical Engineering

Dissertation Examination Committee:
Milorad Duduković, Chair
Muthanna Al-Dahhan, Co-chair
Pratim Biswas
Berthold Breman
Guy Genin
Cynthia Lo
Palghat Ramachandran

FLUID DYNAMICS AND SCALE-UP OF BUBBLE COLUMNS WITH INTERNALS

by

Ahmed Abouelfetouh Youssef

A dissertation presented to the Graduate School of Arts and Sciences of Washington University in partial fulfillment of the requirements of the degree of

DOCTOR OF PHILOSOPHY

August 2010

Saint Louis, Missouri

copyright by

Ahmed Abouelfetouh Youssef

2010

ABSTRACT OF THE DISSERTATION

Fluid Dynamics and Scale-up of Bubble Columns with Internals

by

Ahmed Abouelfetouh Youssef

Doctor of Philosophy in Energy, Environmental and Chemical Engineering

Washington University in St. Louis, 2010

Research Advisors: Professor Muthanna Al-Dahhan

Professor Milorad Duduković

Bubble columns and slurry bubble columns, as multiphase reactors, are favored for a wide range of applications in the chemical, biochemical, petrochemical and metallurgical industries. They are considered the reactor of choice for the Fischer Tropsch synthesis, among other applications, offering an alternative energy source and providing clean liquid fuels as compared to other reactors.

Most of the industrial applications of bubble column reactors require the utilization of heat exchanging tubes, the effect of which on the reactor's performance is not fully understood.

This study proposes detailed investigations of selected local hydrodynamics in bubble columns with and without internal heat exchanging tubes. The main focus of this dissertation is to enhance the understanding of the phenomena associated with the local gas holdup and the bubble dynamics (specific interfacial area, frequency, velocity, and chord length) and their radial profiles via detailed experimentations by means of the four-point

optical fiber probe as a measuring technique. In addition, the liquid phase mixing is investigated. The effects of the presence of cooling tubes, which are commonly used in industrial applications of bubble columns, are thoroughly investigated in columns of different diameters to assess the effect of scale.

Based on the insights gained from the above, one of the main limitations in bubble columns, scale up, is to be tackled in this study. A new approach, yet simple, for designing the reactor in order to reduce the scale-up risk is developed making use of the *necessary* heat exchanging vertical internals in controlling the effect of scale through reactor compartmentalization leading to an optimized, yet efficient, design of large scale bubble columns.

The main findings of this work can be summarized as follows:

- The impact of vertical internals on bubble dynamics and liquid phase mixing is assessed:
    - Increase in gas holdup, interfacial area.
    - Decrease in bubble size due to higher break-up rates.
    - Enhancement in the large scale recirculation cells.
    - Increase in the liquid phase mixing.
- The new scaling methodology was proposed and proven viable.

Acknowledgements

Thanks God.

I would like to express my sincere gratefulness to my advisors, Prof. Milorad Duduković and Prof. Muthanna Al-Dahhan.

Prof. Al-Dahhan has catalyzed my work with his devotion, enthusiasm, encouragement and advice, and I thank him for giving me the chance of pursuing my studies in CREL at WUSTL. His help on many issues, even those extra-curricular ones, showed me how much of a great individual he is.

Prof. Duduković has taught me how to think when facing research problems and how to tackle those efficiently meeting high standards. He has provided comments, time, mentorship and support when most needed. His timely reviews and profound fundamental understanding added new insights and perspectives to this work.

I want to extend my thanks to all members of my dissertation examination committee; Prof. Palghat Ramachandran has always been available for discussions with an open-door policy to answer questions and to provide useful comments; Dr. Berthold Breman has accepted my application as an intern at Sasol and added industrial viewpoints to the work as well as shared with me many extensive discussions; Prof. Cynthia Lo has provided mentorship on many occasions and complemented my Fischer-Tropsch understanding through DFT simulations in her class.

Special thanks are due to Prof. Guy Genin from the Mechanical, Aerospace and Structural Engineering for the aspects he added to this study and to Prof. Pratim Biswas, the EECE Department Chairman, for agreeing to take part of the Ph.D. committee on very short notice.

No words can describe the gratitude I maintain for my lifetime friend Mohamed E. Hamed. He is not just the basketball fellow with whom I grew up, the undergraduate classmate with whom I competed and hung out, the roommate I lived with, the countryman with whom I worked on the same doctorate project, and the advocate with whom I debated matters of scientific and social nature. He is probably the brother I never had. So, Thanks or better Shokran!

The Consortium project on bubble columns (Slurry Bubble Column Reactors for Clean Alternative Energy "SBCR-CAE") introduced me to a number of great individuals that I am proud of knowing and thankful for all their help and guidance with my start and more. Dr. Ashfaq Shaikh is my first roommate. We prayed together, ate for Iftar in Ramadan and talked about almost everything! I thank him for his continuous flow of advice and greatly owe him. Dr. Lu Han is my first officemate and the person through whom, apart from helping in many matters, I observed and tried to pick consistent hard working as a lifestyle. Dr. Chengtian Wu walked me to the laboratory for the first time in CREL and I want to thank him for answering all my questions even after his graduation.

In a major part of my work, I have utilized the four-point optical probe. I could not learn how to use it and fabricate it without Dr. Sean Mueller and Dr. Fadha Ahmed and I am grateful for the time they provided and the patience they had shown.

I would also like to thank those who helped me with the design, the manufacturing and the building of the experimental setups; those who simply taught me that Engineering is one way of *doing* things yet "back-engineering" is the way to *fix* those things. The technical support of Mr. Steven Picker, Mr. Jim Linders, Mr. John Krietler, and Mr. Pat Harkins was invaluable.

Since Arabic is my mother tongue and French is my 1st foreign language, I could use all the help I can get with my English writing. The Engineering Communications Center (ECC) and its director Dr. James Ballard provided more than what I asked for in terms of reviewing my manuscripts, presentations and this dissertation. I am very thankful for all their help. Along the same lines, the French say "Petit a petit, l'oiseau fait son nid" or "Step by step, a bird builds its own nest", as I stepped into this *terra incognita* of my studies, I relied heavily on available state-of-the-knowledge to start where others ended. The hundreds of references I read were mainly made available by the WUSTL Libraries including those hard-to-find articles and theses.

When I first received Prof. Al-Dahhan's e-mail early 2006 explaining the details of the project I would work on for my doctorate studies, I quickly realized how useful it would be to interact with the sponsoring companies. However, only after I actually started the research work, I sensed the magnitude of benefits. The financial support of ConocoPhillips, Eni, Johnson Matthey, Sasol, and Statoil, made my continuation in the program possible. Moreover, the review meetings and extended discussions widened my boundaries and

perspectives about the field and the realistic industrial needs. I would like to specifically express my gratitude to Dr. Berthold Breman and Dr. Gary Combes for their comments and feedback as well as understanding. My first year was sponsored by the Ruth and August Homeyer Scholarship to whom I am deeply thankful.

The Chemical Reaction Engineering Laboratory (CREL) is more than a lab where one does research for a scientific degree. The gathering of such bright minds made my studies a lifetime experience. The weekly and annual meetings were truly pleasant and challenging.
Amongst these colleagues, Wisam Khudayer hosted me and invited me for dinner on my first night in USA; Daniel Combest and Evgeniy Redekop shared the first year's ups and downs; Dr. Rajneesh Varma helped with the CT system and showed me the way into students activities with AGES; Mehmet Morali shared the window-less office for almost 2 years and with whom I enjoyed many constructive discussions; Dr. Bia Henriques-Thomas organized our CREL annual meetings to perfection and gave me an opportunity to visit her homeland Brasil; Dr. Debangshu Guha, Dr. Radmila Jevtic, Dr. Subramania Nayak, Arnaud Denecheau, Zeljko Kuzeljevic, and Vesna Havran were more close 'pals' rather than just labmates.
I always enjoyed the company of my roommate and classmate, Luis B. Modesto. The conversations we had before and after our qualifying exams made sleepless nights of hard work enjoyable.

Our Energy, Environmental, and Chemical Engineering Department administrative assistant, Rose Baxter, set a great example of a professional yet very friendly secretary. She could resolve all issues even before my arrival to St. Louis. I appreciate her devotion and thank her for everything she did to make my life easier.

At times when I seemed tough for everyone around, those, thousands miles away, knew I was more brittle than ever. My parents and sister never hesitated in giving me the support and encouragement. I owe them more than I can try to payback. Their calls and visits were a motivation for me to move forward. As I thank them for continued bearing with my problems and being good listeners, I ask for their forgiveness for not being there and available when needed.

"What we call the beginning is often the end. And to make an end is to make a beginning. The end is where we start from." T. S. Eliot.

As I head towards other places to meet other peoples, I hope I left a good memory as I gathered many.

Ahmed Abouelfetouh Youssef

Washington University in St. Louis

August 2010

To Mami, Papi, Alaà, Mama, and Geddo

Contents

Abstract iii

Acknowledgments v

List of Tables xiii

List of Figures xiv

Nomenclature xviii

List of Abbreviations xxiii

1 Introduction 1
- 1.1 Overview 6
- 1.2 Motivation 8
- 1.3 Research Objectives 10
- 1.4 Dissertation Structure 13

2 Background 15
- 2.1 Internals 15
- 2.2 Bubble Dynamics 21
  - 2.2.1 Local gas holdup 23
  - 2.2.2 Specific interfacial area 24
  - 2.2.3 Bubble velocity 25
  - 2.2.4 Bubble chord length 28
  - 2.2.5 Bubble frequency 31
- 2.3 Scale-up 32
- 2.4 Liquid Mixing 36

3 Bubble Dynamics in 8" Bubble Column with Vertical Internals 39
- 3.1 Scope 39
- 3.2 Measurement Technique 40
- 3.3 Selection of Heat Exchanger Bundle Configuration 43
- 3.4 Impact of Internals on Gas Holdup and Bubble Properties in an 8" Bubble Column 45
  - 3.4.1 Experimental setup 45
  - 3.4.2 Results and discussion 48
    - 3.4.2.1 Overall gas holdup 48
    - 3.4.2.2 Local gas holdup 49
    - 3.4.2.3 Specific interfacial area 52
    - 3.4.2.4 Bubble chord length 54
    - 3.4.2.5 Bubble velocity 56

4 Impact of Internals on Gas Holdup and Bubble Properties in a Pilot Plant Scale Bubble Column 61
4.1 Experimental Setup 61
4.2 Results and Discussion 64
4.2.1 Overall gas holdup 64
4.2.2 Local gas holdup 70
4.2.3 Specific interfacial area 73
4.2.4 Bubble chord length 78
4.2.5 Bubble velocity 81
4.3 Guidelines for the Design of Heat Exchangers for Fischer-Tropsch Slurry Reactors 86

5 Liquid Phase Mixing in Bubble Columns with Internals 88
5.1 Scope 88
5.2 Experimental Setup 89
5.3 Measurement Technique 90
5.4 Experimental Procedure 92
5.5 Results and Discussion 93
5.5.1 Preview 93
5.5.2 Notes on the data analysis procedure 94
5.6 Conclusions 100

6 Scale-up of Bubble Column Reactors 102
6.1 Scope 102
6.2 Preview 103
6.3 Hypothesis 106
6.4 Experimental Setup 107
6.5 Preliminary Considerations 108
6.6 Proof of Concept 110
6.7 Results and Discussion 112
6.8 Conclusions 119

7 Conclusions and Recommendations 120
7.1 Summary 120
7.2 Conclusions 120
7.2.1 Impact of internals on overall gas holdup 120
7.2.2 Study of bubble dynamics in columns with and without internals 120
7.2.3 Effect of internals on liquid mixing behavior 121
7.2.4 Scale-up of bubble columns 121
7.3 Recommendations for Future Work 121

Appendix A - Tabulated Listing of Studies of Bubble Columns with Internals 123

Appendix B - Design, Setting and Construction of Internal Structures for Bubble Columns 132

Appendix C - The Estimation of Lumped Parameters from the 4-Point Optical Probe Data 139

References 144

Vita 158

List of Tables

Table 1.1 - Advantages and disadvantages of bubble column reactors 4

Table 2.1 - Sample reaction systems operated in bubble column reactors (after Schlüter et al., 1995) 16

Table 2.2 - Measurement techniques used in bubbly flows 22

Table 2.3 - Summary of liquid mixing studies in columns with horizontal internals 37

Table 2.4 - Summary of liquid mixing studies in columns with vertical internals 38

Table 3.1 - Statistical measures of the chord length distribution for different internals arrangements at Ug=20 cm/s 56

Table 3.2 - Statistical measures of the upward velocity at 5% internals for different superficial gas velocities 59

Table 4.1 - Effect of internals and gas velocity on the overall gas holdup (%) 69

Table 4.2 - Statistical measures of the chord length distribution for different investigated conditions 81

Table 5.1 - Measures of response curves from Figure 5.7 97

Table 5.2 - Measures of response curves from Figure 5.8 98

Table 5.3 - Measures of response curves from Figures 5.9 and 5.10 99

List of Figures

Figure 1.1 - Global energy consumption by region (Source: International Energy Outlook 2008) 1

Figure 1.2 - World oil prices in three price cases 1980-2030 (IEO 2009) 2

Figure 1.3 - Bubble columns for laboratory use 8

Figure 1.4 - Research structure 14

Figure 2.1 - Effect of internals on the profile of the axial component of the liquid velocity (modified from Bernemann, 1989) 17

Figure 2.2 - Enhancement of large recirculation scale and decrease of radial dispersion due to internals (Forret et al. (2003)) 18

Figure 2.3 - CFD simulations of time-averaged contour plots of the axial liquid velocity component over a cross-sectional slice taken in the fully developed region with different internals configurations (Larachi et al., 2006) 19

Figure 2.4 - Typical radial gas holdup radial profiles at different superficial gas velocities (after Hills, 1974) 24

Figure 2.5 - Terminal velocity of air bubbles in water at 20°C (after Clift et al., 1978) 29

Figure 2.6 - Schematic representation of an elliptic bubble (Xue, 2004) 30

Figure 2.7 - The chord length distributions for both homogeneous and heterogeneous regimes against the triangular bubble size density at the probe (y is the chord length, and R is equivalent to OC from Figure 2.6) – (Liu et al., 1998) 31

Figure 2.8 - Radial bubble frequency profile (Hills, 1974) 32

Figure 2.9 - Bubble frequency for different spargers (Xue, 2004) 32

Figure 2.10 - Scheme of characterization/scaling of churn turbulent bubble columns (Degaleesan, 1997) 33

Figure 2.11 - Overall gas holdup as a function of superficial gas velocity in different columns' scales (Forret et al., 2006). 35

Figure 3.1 - Configuration of the four-point optical probe (not to scale) (a) picture of the probe, (b) side view of probe tip, (c) bottom view of probe tip 41

Figure 3.2 - Response of a bubble passing by the four-point optical probe 42

Figure 3.3 - Schematic diagram of the bubble column setup 46

Figure 3.4 - Internals configuration: (a) 5% covered cross-sectional area and (b) 22% covered CSA (dimensions in inches). 47

Figure 3.5 - Effect of internals on overall gas holdup (Courtesy of Hamed and Al-Dahhan (2010) - experiments performed by Mohamed Hamed) 49

Figure 3.6 - Radial gas holdup profiles at different superficial gas velocities (5% internals) 50

Figure 3.7 - Effect of internals on local gas holdup at Ug=20cm/s 51

Figure 3.8 - Effect of superficial gas velocity on interfacial area with 5% internals 52

Figure 3.9 - Effect of internals on specific interfacial area at Ug=20cm/s 53

Figure 3.10 - Effect of internals on interfacial area radial profile (Ug= 8 cm/s). 54

Figure 3.11 - Bubble passage frequency as a function of radial position at various conditions 54

Figure 3.12 - Bubble chord length distribution at the column's center at Ug=20 cm/s and different percentages of internals: (a) no internals, (b) 5% internals, and (c) 22% internals 55

Figure 3.13 - Bubble velocity distribution at the column's center at Ug= 20 cm/s and different percentages of internals: (a) no internals, (b) 5% internals, and (c) 22% internals 57

Figure 3.14 - Bubble upward velocity distribution at the column's center at Ug=3 cm/s and 5% internals 58

Figure 3.15 - Bubble velocity distribution at 20 cm/s in the wall region and the column's center with different percentage of internals; (a) 22% internals, (b) no internals 60

Figure 4.1 - Schematic diagram of the pilot plant experimental setup (dimensions in inches) 62

Figure 4.2 - Design of internals bundle; (a) 5% coverage and (b) 25% coverage (dimensions in inches) 63

Figure 4.3 - Configurations of internals bundles covering (a) 20%, (b) 15%, and (c) 10% of the total column's CSA 65

Figure 4.4 - Overall gas holdup profiles with various internals coverage 66

Figure 4.5 - Overall gas holdup profile comparison with literature data at 10% covered CSA 67

Figure 4.6 - Effect of superficial gas velocity for open area on overall gas holdup at different internals arrangements 68

Figure 4.7 - Effect of gas velocity on overall gas holdup at different internals arrangements 68

Figure 4.8 - Effect of internals on gas holdup at Ug=20 cm/s 70

Figure 4.9 - Effect of internals on gas holdup at Ug=30 cm/s 71

Figure 4.10 - Effect of column diameter on the gas holdup radial profile at Ug=20 cm/s and with dense internal structures 72

Figure 4.11 - Effect of internals on the specific interfacial area at different superficial gas velocities (a) Ug= 20 cm/s, (b) Ug= 30 cm/s, and (c) Ug= 45 cm/s .. 77

Figure 4.12 - Radial interfacial area profile at Ug= 20 cm/s and 25% internals 78

Figure 4.13 - Bubble chord length probability distribution at Ug= 20 cm/s and column's center with (a) No internals, (b) 25% internals 79

Figure 4.14 - Bubble chord length probability distribution at Ug= 20 cm/s and r/R= 0.9 with (a) No internals, (b) 25% internals 80

Figure 4.15 - Bubble chord length probability distribution at Ug= 45 cm/s and column's 80

Figure 4.16 - Bubble chord length probability distribution at Ug= 45 cm/s and 25% internals (wall region) 81

Figure 4.17 - Bubble velocity probability distribution at Ug= 30 cm/s and no internals for (a) Column's center, (b) Wall region 82

Figure 4.18 - Bubble velocity probability distribution at Ug= 30 cm/s and 25% internals for (a) Column's center, (b) Wall region 83

Figure 4.19 - Bubble direction angle probability distribution at Ug=30cm/s in the wall region for (a) No internals, and (b) 25% internals 84

Figure 4.20 - Bubble velocity probability distribution at Ug= 20 cm/s and 25% internals in 18" diameter column for (a) Column's center, (b) Wall region 85

Figure 5.1 - Flow profile of the liquid phase in a bubble column (Ueyama and Miyauchi, 1979) 88

Figure 5.2 - Schematic diagram of the bubble column for the tracer experimental setup 90

Figure 5.3 - Tracer injection device 91

Figure 5.4 - Conductivity probe (#2) inside a PVC tube at the liquid outlet 92

Figure 5.5 - Filtered output signal from conductivity probes at Ug=45 cm/s and U_l=0.5 cm/s in a column with no internals 95

Figure 5.6 - Filtered output signal from conductivity probes at Ug=20 cm/s and U_l=0.5 cm/s in a column with 25% internals 95

Figure 5.7 - System response curves with and without internals (Ug=20 cm/s and U_l=1 cm/s) 96

Figure 5.8 - System response curves with and without internals (Ug=30 cm/s and U_l=1 cm/s) 97

Figure 5.9 - System response curves with and without internals (Ug=30 cm/s and U_l=1.5 cm/s) 98

Figure 5.10 - System response curves with and without internals (Ug=45 cm/s and U_l=1.5 cm/s) 99

Figure 6.1 - Various designs of slurry phase bubble column compartmentalized by means of shafts and with the presence of internal heat exchanging tubes (Kölbel and Ackermann, 1958) 105

Figure 6.2 - Schematic diagram of 6" diameter internals bundle inside 18" diameter column 107

Figure 6.3 - Experimental setup for scale-up approach, (a) Photo of 6" circular bundle inside 18" bubble column and (b) Photo of top supporting plate 108

Figure 6.4 - Radial gas holdup profiles inside the tube bundle 110

Figure 6.5 - Specific interfacial area radial profiles inside the tube bundle 111

Figure 6.6 - Comparison of rods vs. solid wall effect 112

Figure 6.7 - Radial gas holdup profiles inside circular bundle and in a steel bubble column of 6" diameter at 20 cm/s 113

Figure 6.8 - Radial gas holdup profiles inside circular bundle and in a steel bubble column of 6" diameter at 30 cm/s 113

Figure 6.9 - Radial gas holdup profiles inside circular bundle and in a steel bubble column of 6" diameter at 45 cm/s 114

Figure 6.10 - Bubble chord length distributions at the column's center and Ug=45 cm/s 116

Figure 6.11 - Bubble chord length distributions at the wall and Ug=45 cm/s 117

Figure 6.12 - Bubble velocity distributions at the column's center and Ug=45 cm/s 118

Figure 6.13 - Bubble velocity distributions at the wall and Ug=45 cm/s 118

Figure B.1 - Spacer for 5% internals and lower part of internal rods 135

Figure B.2 - Lower spacer for 25% internals attached to distributor 136

Figure B.3 - Top plate hooked to top crane 137

Figure B.4 - Attachment of the PVC initial rods to the spacers via threaded pins 138

Figure C.1 - Effect of internals on k_la in 8" column (Ug= 20cm/s) 141

Figure C.2 - Axial dispersion coefficients from Degaleesan (1997) for (a) D=14 cm and (b) D=44 cm 143

Nomenclature

a	Specific interfacial area, cm^2/cm^3
A	Gas phase component, interfacial area, cm^2
A	Total surface area of tube bundle (m^2)
a_1, a_2, A, B	Constants, m/s
AB	Arbitrary chord of a bubble
A_f	Relative free cross sectional area
a_L	Thermal diffusivity of the liquid phase, m^2/s
A_{tot}	Total cross sectional area of the column
c	Parameter for non-zero void fraction at the wall
c	Parameter in Fan–Tsuchiya equation reflecting surface tension effect
C	Concentration, g/ml
C'	Fluctuating tracer concentration, mol/cm^3
$\bar{C}$	Average liquid tracer concentration, mol/cm^3
C_p	Specific heat capacity of the liquid phase, J/kg.K
D	Diameter of column, m
D_{AB}	Liquid phase diffusivity, m^2/s
D_{ax}	Axial dispersion coefficient based on ADM (cm^2/s)
$D_{ax,\ 2D}$	Axial dispersion coefficient (from 2D model), m^2/s
$\overline{D_{rr}}$	Average radial eddy diffusivity, cm^2/s
$\overline{D_{xx}}$	Average eddy diffusivity in x direction, cm^2/s
D_{Taylor}	Taylor-type diffusivity, cm^2/s
d_b	Bubble diameter, m
$d_{b,\ max}$	Maximum bubble diameter, m
d_b'	Dimensionless bubble diameter
$D_{c,\ min}$	Minimum column diameter to avoid wall effects, m
d_e	Volume equivalent diameter, m
d_i	Internal's diameter, m

d_o	Orifice diameter, m
d_R	Internal's diameter, m
$D_{rad, 2D}$	Radial dispersion coefficient (from 2D model), m^2/s
d_s	Sauter mean diameter, m
Eo	Eötvös number ($g\ \Delta\varrho d_b^2/\sigma$)
Fr	Froude number
Fr_G	Froude number of the gas phase ($U_g^2/(gD_R)$)
g	Gravitational acceleration, m/s^2
H_{dyn}	Dynamic height of the bed, m
$H_{st.}$	Static Height of the bed, m
h_{tube}	Height of tube, m
J	Average concentration flux, mol/cm^2s
K_b	Parameter in Fan-Tsuchiya equation reflecting viscous nature of surrounding medium thickness of the liquid film between two coalescing bubbles
K_{bo}	K_b at the orifice
k_G	Gas side mass transfer coefficient, cm/s
k_L	liquid side mass transfer coefficient, cm/s
L	Height of column, m
l_e, l_z	Size of turbulent eddy, m
Mo, M	Morton number ($g\ \Delta\varrho\mu_L^4/(\varrho_l^2\sigma^3)$)
m	Constant
n	Parameter in Fan–Tsuchiya equation reflecting system purity
n	# moles/s
n, N	Number of data points
N_c	Capacitance number ($4V_{ch}g\varrho_l/\pi d_o^2 p_h$)
n_R	# tubes (internals)
N_{tube}	# tubes in column
OD	Outer Diameter, m

P	Pressure, bar
Pe	Péclet number ($U_lL/[D_{ax}(1-\varepsilon_g)]$)
P/V	Energy dissipation or power input W/m^2
p_h	Hydrostatic pressure at the orifice plate, MPa
Pr_L	Prandtl number of the liquid phase (ν_L/a_l)
Q	Heat generation rate (kj/s)
R	Column radius, m
R	Ideal gas constant (8.314×10^{-5} m^3bar/K.mol)
r	Radial coordinate
r/R, φ	Dimensionless radial coordinate
Re	Reynolds number
Re_G	Reynolds number of the gas phase (U_gD_R/ν_L)
Re_L	Reynolds number of the liquid phase ($\rho_lU_Ld_p/\mu_L$)
R_{max}	Maximum response signal, mvolt
R_{min}	Minimum response signal, mvolt
R_{norm}	Normalized response signal
r_{tube}	Radius of tube, m
St	Stanton number ($\alpha/(U_gC_p\rho_L)$)
T	Temperature, K
t	Time, s
t_e	Contact time, s
$\bar{t}$	Mean residence time of tracer, s
t_R	Tube pitch, m
U	Overall heat transfer coefficient ($kcal/m^2$.s.K)
u_b	Bubble velocity, m/s
u_b'	Dimensionless bubble rise velocity, m/s
U_g	Superficial gas velocity, m/s
U_{ge}	Equivalent gas superficial velocity, cm/s
$U_{O.A.}$	Superficial gas velocity for open area, m/s

u_l	Liquid velocity, m/s
$u_{l,\ wall}$	Liquid velocity at the wall formed by the tubes bundle, m/s
u_l^*	Liquid velocity in the annular region (from locus of maximum downward liquid velocity to the wall), m/s
U_l	Superficial liquid velocity, m/s
u_{slip}	Slip velocity, m/s
U_{sup}	Superficial gas velocity, m/s
$\overline{u_e}$	Average fluctuating velocity (average velocity of turbulent eddy), m/s
$\overline{u_{rec}}$	Mean recirculation velocity, cm/s
V	Volume, m^3
Var(x)	Variance of the distribution
V_{ch}	Volume of the plenum chamber, m^3
V_D	Dispersion volume, cm^3
V_l	Liquid phase velocity, m/s
V_{LZ}	Centerline liquid velocity, m/s
$\dot{V}$	Volumetric flow rate (m^3/s)
$\overline{(v_z'^2)}^{0.5}$	Root mean square of fluctuating velocity, cm/s
We	Weber number ($Re^2Mo^{0.5}/Eo^{0.5}$)
We_c	Critical Weber number
x, y	Value of parameter of interest in AARD relation
X_v	Covered volume fraction
$\bar{x}$	Mean of the distribution
y, L_i	Chord length, m

Greek symbols

ρ	Density, kg/m^3
μ	Dynamic viscosity, Pa.s
σ	Surface tension, N/m
τ	(turbulent) shear stress, N/m^2
φ'	Dimensionless column diameter (d_R/D_R)

σ^2	Variance (measure of spread of RTD curve), s^2
β_d	Ratio of densities (ρ_p/ρ_l)
$\sigma_D{}^2$	Dimensionless variance
$\varepsilon_g(r)$	Local gas holdup
ε_g, ϵ_g	Overall gas holdup
η_L	Dynamic viscosity of the liquid phase, Pa.s
ν_L, ν_m	Kinematic viscosity of the liquid phase, m^2/s
η_{LW}	Dynamic viscosity of the liquid phase at the wall, Pa.s
λ	Dimensionless radial position where the downward liquid velocity is maximum
ρ_p	Particle density (kg/m^3)
ρ_{sl}	Slurry phase density, kg/m^3
ν_t	Turbulent viscosity, m^2/s
$\nu_{t,\,z}$	Turbulent viscosity in Z direction, m^2/s
β_U	Ratio of superficial velocities (U_g/U_l)
τ_w	Wall shear stress, N/m^2
$\bar{\varepsilon}$	Cross-sectional average gas holdup
α	Heat transfer coefficient, $W/m^2.K$
$\Delta\rho$	Density difference between liquid and gas phases, kg/m^3

List of Abbreviations

2D	Two Dimensional
3D	Three Dimensional
AARD	Average Absolute relative Difference
ADM	Axial Dispersion Model
AFDU	Alternative Fuel Development Unit
BTL	Biomass to Liquid
CARPT	Computed Automated Radioactive Particle Tracking
CFD	Computational Fluid Dynamics
CREL	Chemical Reaction Engineering Laboratory
CSA	Cross Sectional Area
CT	Computed Tomography
CTL	Coal to Liquid
DGD	Dynamic Gas Disengagement
ECVT	Electrical Capacitance Volume Tomography
EIA	Energy Information Administration
FT	Fischer Tropsch
GTL	Gas to Liquid
IEO	International Energy Outlook
LED	Light Emitting Diode
LPMeOH	Liquid Phase Methanol
RTD	Residence Time Distribution
UBC	University of British Columbia
WUSTL	Washington University in Saint Louis

Chapter 1

Introduction

The discoveries of petroleum (oil) and natural gas, along with the developments in related technologies for coal conversion, have provided most of the energy consumed in the 20th century. However, these fossil fuel-based sources of energy have also contributed to a complex problem. From a global perspective, this problem is three-fold: a growing world population, the depletion of finite resources and volatile fuel prices. An additional concern is the anthropogenic climate change driven by carbon combustion and pollutants.

A growing population: Energy consumption and damage to the environment are proportional to population. The United Nations estimates that the world's population will reach 9.1 billion inhabitants by 2050, as compared to 5.3 billion in 1990 and 6.1 billion in 2000. Striking boosts in the populations of countries like China (almost triple since WW II) and India (almost quadruple since WW II) add to the problem.

The depletion of finite resources: Increases in population and continuous improvement in the standards of living raise energy consumption and depletion of natural resources accordingly. However, this growth in consumption will be globally unevenly distributed, as estimated by the Energy Information Administration (EIA) (Figure 1.1) (IEO 2008), which leads to potential tension and instability among regions and nations.

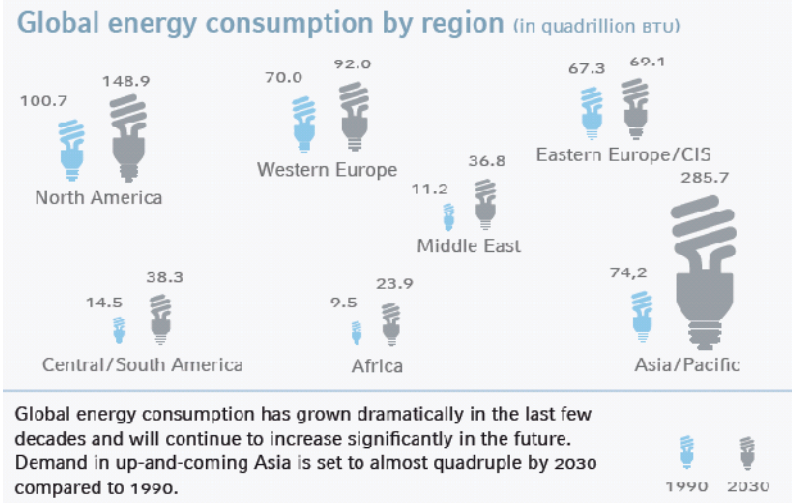

Fig.1.1 – Global energy consumption by region (Source: International Energy Outlook 2008)

Volatile fuel prices: As an example, consider the market for oil, whose price fluctuates widely. The EIA assumes three different prices reflecting the uncertainty in future scenarios (Figure 1.2).

Ultimately, an energy 'crisis' can be avoided by utilizing novel, clean, and renewable energy sources. Suggestions include solar, wind, geothermal, and biomass. However, limitations ranging from economics and efficiency to safety still need to be addressed thoroughly before switching to these alternatives. In the mean time, we must bridge the gap between complete dependency on oil and the utilization of non-fossil developing technologies.

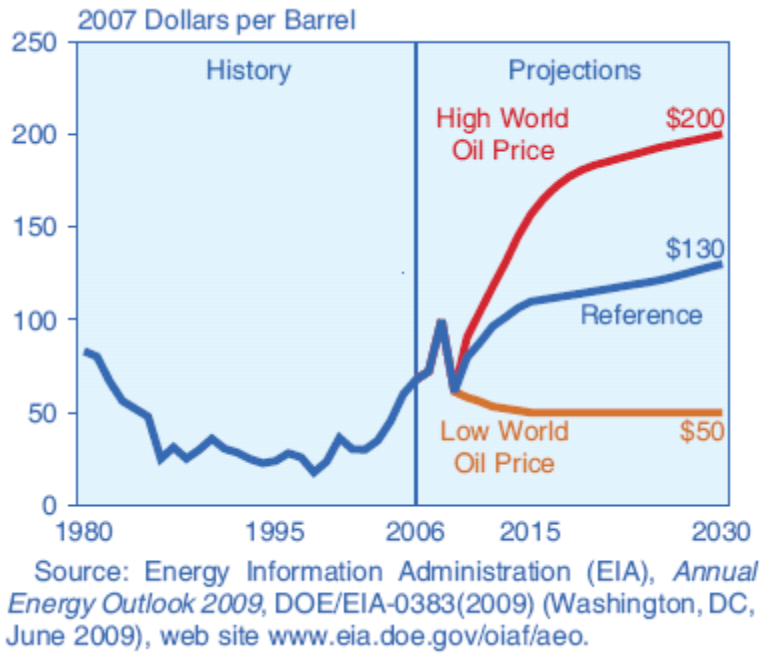

Fig. 1.2 – World oil prices in three price cases 1980-2030 (IEO 2009)

One of the more promising solutions lies in the generation of liquid fuels from natural gas and coal which has been practiced since World War II and recently from biomass. Among the processes considered, one of the most discussed is the Fischer Tropsch synthesis for conversion of syngas to liquid fuels and chemicals. The Fischer-Tropsch (FT) primary chemical reaction can be expressed as follows:

$$CO + 2H_2 \rightarrow -CH_2 - + H_2O.$$

This reaction is typically accompanied by the water gas shift reaction.

The primary reaction, which is highly exothermic, involves contacting a mixture of carbon monoxide and hydrogen (syngas) over fine solid catalysts to produce hydrocarbons and water. FT produces sulfur-free and aromatics-free liquid fuels, and can use many different sources of syngas. The abundant reserves of coal, the uncommitted reserves of natural gas, and the renewable resources of biogas and biomass are the three major syngas sources. Their conversion processes to liquid fuels are called CTL (Coal-to-Liquid), GTL (Gas-to-Liquid), and BTL (Biomass-to-Liquid).

The reactor of choice for such conversions is the slurry bubble column reactor (Krishna and Sie, 2000). Bubble columns, in their simplest form, are cylindrical vessels in which gas is injected as bubbles through a distributor (sparger), into a liquid (a 2-phase column) or into a suspension of fine solids in a liquid (a 3-phase column). The flow in a 3-phase column is sometimes approached as a pseudo 2-phase flow: the fine solids follow the liquid phase, so a pseudo homogeneous assumption can be made for the slurry (liquid-solid) phase. In a continuous flow system, the gas may flow either with or counter to the liquid flow direction. In a semi-batch system, gas is sparged into a static liquid (slurry) medium. In either case, a high interfacial contacting area is provided between the liquid (or slurry) and gas phases. Bubble columns for laboratory use can be classified on the basis of design and operating conditions. Some examples of such variations are shown in Figure 1.3.

Bubble columns as multiphase reactors (or contactors) are favored for a wide range of applications in the chemical, biochemical, petrochemical, and metallurgical industries (Dudukovic, 2000). Chlorination, oxychlorination, carbonylation, and alkylation are examples of 2-phase bubble column applications. On the other hand, 3-phase slurry bubble columns are used for hydrogenation, polymerization, coal liquefaction, and Fischer-Tropsch synthesis among many other uses.

Bubble columns are preferred to other types of multiphase reactors in these applications for a number of reasons. Compared to fixed beds, their superior heat transfer properties allow close to isothermal operation, leading to improved selectivity (Shetty et al., 1992). Unlike agitated tanks, they provide good mass and heat transfer without moving parts. Moreover, their ease of construction and operation put bubble columns ahead of both fluidized bed (or ebulated three phase fluid beds) and fixed bed (or trickle bed) reactors. However the

backmixing of the phases and the scale up issues are the main limitations of these multiphase reactors. The advantages and disadvantages of bubble column reactors are summarized in Table 1.1.

Table 1.1 - Advantages and disadvantages of bubble column reactors

Pros	**Cons**
Good heat transfer	Significant phase back-mixing and Difficult scale-up and design
Ease of construction and operation	
Absence of moving parts	
Low maintenance costs	
Good mass transfer	

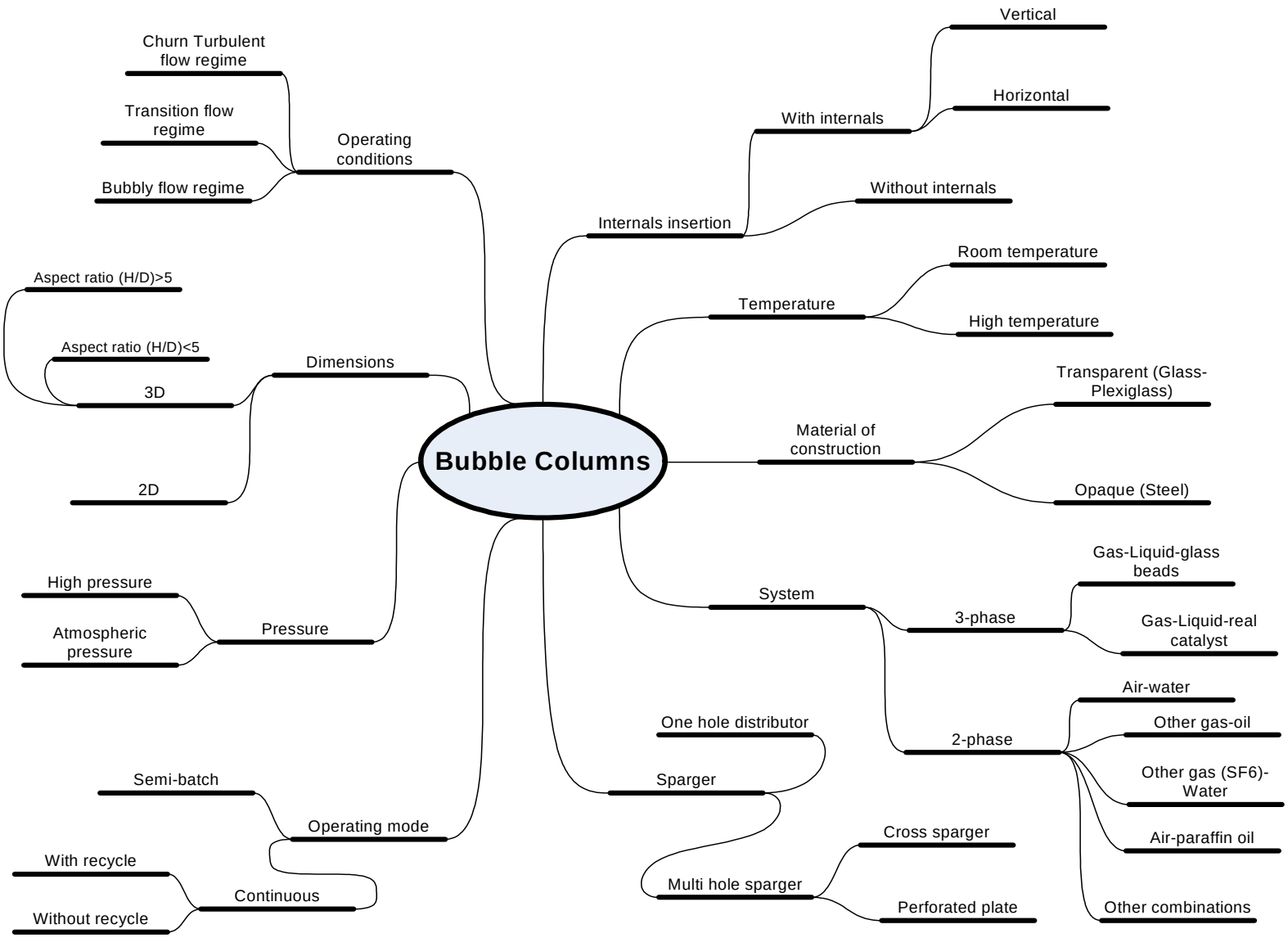

Fig. 1.3 – Bubble columns for laboratory use

1.1 – Overview

To scale-up and optimize bubble columns, the molecular scale, bubble scale, and reactor scale must be carefully considered.

At the reactor scale, gas holdup, its radial distribution, the liquid's recirculation, and fluid back mixing are important measured (or modeled) parameters. Investigations of bubble scale phenomena include the quantification and understanding of various transport steps as well as the understanding of models of breakup and coalescence. At the molecular scale, fundamental chemistry is required to study the catalysts and the gas conversion processes (Dudukovic, 2000).

Recently, Shaikh and Al-Dahhan (2007) reviewed the various flow regimes in bubble column reactors and noted four patterns: homogeneous (bubbly flow), heterogeneous (churn turbulent) flow, slug flow, and annular flow. In addition, a grey region that exists between the bubbly and the churn turbulent flow regimes is referred to as the transition regime. These different regimes exhibit very distinctive flow characteristics. As higher superficial gas velocities are applied for some bubble column applications (e.g. Fischer-Tropsch synthesis (Deckwer, 1992 and Steynberg and Dry, 2004), the non-uniformity of the interwoven gas holdup and liquid velocity radial profiles becomes more significant. The following phenomena are observed with increasing superficial gas velocity (i.e., gas flow rate divided by the cross sectional area of the empty column):

- A narrow distribution of small spherical bubbles, characteristic of the homogeneous flow regime, is replaced by a broader bubble size distribution.
- Bubbles tend to coalesce, and the large ones (no longer spherical) move towards the core region of the column.
- A difference in mixture density between the core and the wall regions develops due to a parabolic gas holdup profile along the column radius.
- This density difference results in a difference in the buoyancy forces in the cross-section of the column. The magnitude of these buoyancy forces is much larger in the churn turbulent flow regime and induces a strong liquid recirculation.

- Liquid flow is driven upwards by the above mentioned large bubbles in the column's center, and for liquid continuity (the overall conservation equation) to be ensured, a downward liquid stream flows along the walls of the reactor.
- A strong recirculation cell is thus produced.

Liquid recirculation might be viewed as advantageous in processes requiring good mass and heat transfer capabilities, in order to maintain isothermal conditions inside the reactor (Alvaré and Al-Dahhan, 2006b). It may, however, lead to a decrease in overall conversion, promotion of undesired secondary reactions, and problems with maintaining uniform catalyst suspension. Many researchers have used advanced measuring and modeling tools to investigate the effects of operating conditions (gas and liquid flow rates, catalyst renewal rate, temperature, pressure and feed composition), design parameters (column diameter, sparger design, catalyst size and loading), and physical properties on global gas holdup, holdup radial profile, bubble dynamics, liquid recirculation profiles and intensities, liquid turbulent eddy mixing, and gas and liquid dispersion (Rados, 2003).

In spite of a significant improvement in understanding the flow dynamics in churn turbulent flows, there is general agreement that a full understanding of bubble column performance is only beginning to emerge. Recent developments in computational tools are reflected in the substantial increase in the number of publications dealing with the computational fluid dynamics (CFD) of bubble column flows (Svendsen et al., 1992, Ranade, 1992, Grienberger and Hofmann, 1992, Sokolichin and Eigenberger, 1994, Lapin and Lubbert, 1994, Delnoij et al., 1997, Pan et al., 1999, 2000, Sanyal et al., 1999, Krishna and van Baten, 1999, Olmos, 2002, Lapin et al., 2002, and Chen et al., 2005 and 2006). These studies provide a promising foundation for phenomenological models (Gupta et al., 2001, Degaleesan et al., 2001, Wild et al., 2003, and Yang et al., 2007). Nevertheless, 'a prori' prediction of bubble column churn turbulent flows is still not possible. Better turbulence closures are needed (Mudde, 2005 and Diaz et al., 2008), as well as deeper understanding of detailed hydrodynamics, transports and bubble interactions, including coalescence and breakup phenomena (Jakobsen et al., 2005, Chen et al., 2005 and 2006 and Rafique et al., 2004).

1.2 – Motivation

The performance of bubble column reactors is affected by a number of interrelated parameters including, but not limited to, gas holdup, bubble velocity, gas-liquid interfacial area, bubble chord length, and bubble passage frequency) as well as various phenomena (e.g., mass and heat transfer, liquid phase backmixing and many others). These, in turn, depend upon several factors, including operating variables (e.g., gas and liquid flow rates, pressure, and temperature), design variables (e.g., column geometry, sparger design, and internals), kinetics, and thermodynamic as well as physical properties. Obviously, the hydrodynamic behavior in a bubble column reactor is complex, since the fluid phases involved are characterized by very different densities, and one is more compressible than the other (Shaikh, 2007). In order to achieve reliable scale-up, further experiments and the integration of generated databases into fundamentally based models are needed (Devanathan et al., 1991, Kumar et al., 1995, Dudukovic, 2000, and Rados, 2005).

Many industrial applications for which bubble column reactors are preferred, such as FT and liquid phase methanol synthesis, require high superficial gas velocities, high solids (catalyst) loading, high temperature, high pressure, and large reactor diameters and heights (Krishna and Ellenberger, 1996). To remove the heat generated by the chemical reaction, most of these applications use heat exchanging internals. However, most of the work done on bubble columns so far has not accounted for the presence of the cooling tubes (Yamashita, 1987, Forret et. al., 2003, and Larachi et al., 2006). This lack can be attributed to the scrupulously protected know-how of internals design and a lack of published unified geometrical standards, coupled with the complexity imposed on laboratory scale columns by internals insertion. In the early 1990's, Saxena and his coworkers published a series of studies on bubble columns with internals (e.g. Saxena et. al., 1991, Saxena and Chen, 1993, Thimmapuram et. al., 1993, and Saxena and Chen, 1994). However, these studies focused on investigating the heat transfer rather than the impact of the internals on the hydrodynamics. It is believed that the flow dynamics in the column are affected when large parts of the cross-sectional area of the reactor are obstructed by internals (Soraker et. al., 2005). Even the few studies that reported experimental findings involving internal heat exchange tubes do not provide an insight into this belief as they were mostly concerned with the global parameters, with no thorough interpretation of the local parameters. De et al. (1999)

reported overall gas holdup based on the bed expansion method as a function of the internals. Others investigated only limited cross sectional area coverage (5%) by the internals (Chen et al., 1999).

Therefore, there is a need for close investigation of the effects of the heat exchanging internals on the local parameters, such as local gas holdup and bubble properties, in a variety of systems at a wide range of experimental conditions. Measuring techniques such as optical probes have exhibited a huge improvement in recent years (Xue et al., 2003) and can be of help in this regard.

It is noteworthy that Larachi et al., 2006 performed 3D simulations of the liquid circulation and mixing patterns in columns with internals but lacked any experimental evidence to compare with their model predictions. The current study seeks to begin providing the necessary database for validation of such CFD simulations.

Furthermore, the liquid phase mixing behavior within bubble columns with heat exchanging internals has not been reported before. Several models have been reported for bubble columns without internals, including one dimensional (e.g., Ueyama and Miyauchi, 1979 and Kumar et al., 1994) and two dimensional models (e.g., Degaleesan, 1997). However, the applicability of these models was never tested in columns with internals, probably due to the lack of a relevant database. The huge difference between industrial scale reactors (e.g., Sasol's slurry column of 10 m diameter and 60 m height) and laboratory scale units (about 25 cm diameter on average) indicates that reliable scale-up methodologies are essential for approaching industrial applications. However, scale-up is considered one of the main challenges of bubble columns, one that has yet to be tackled in more detail. In general, the scaling rules are derived from mass and momentum balances, resulting in dimensionless hydrodynamic numbers such as Reynolds (Re) and Froude (Fr) numbers. Earlier scale-up attempts (van den Bleek and Schouten, 1993) suggested that for a proper scaling these numbers should be kept constant, together with dimensionless geometric numbers such as L/D, to ensure both dynamic and geometrical similarity. Using the latter principle, Safoniuk et al. (1999), followed by Macchi et al. (2001), used the pi Buckingham theorem to identify up to five dimensionless groups to be matched, and proposed a scale-up methodology for gas-liquid-solid fluidized beds. Macchi et al. (2001) concluded, based on their pressure fluctuations studies, that more than five dimensionless numbers are needed to fully

characterize the system. Since that is very hard to do in practice, the main motivation for this work is to look into different routes to provide a firm scale-up methodology.

The lack of open literature on the design aspects of large scale reactors burdens researchers of bubble column scale-up and renders the process even harder to achieve. None of the aforementioned studies has accounted for the presence of internals while scaling the reactor up, although a commercial FT slurry reactor can have up to thousands of cooling tubes spanning most of the vertical extent of the reactor. Kölbel and Ackermann (1958) proposed a design in which multiple vertical shafts (either circular or hexagonal) are inserted in the reactor, compartmentalizing the external column shell into smaller columns of 5 to 30 cm diameter or more, which imposes extra costs and difficulties during construction.

In summary, there has been no previous study that made use of the *necessary* heat exchange vertical internals to control the effect of scale, or in the validation of a scale-up methodology leading to an optimized, yet efficient, design of large scale bubble columns. Therefore, this study seeks to quantify the hydrodynamic effects of reactor compartmentalization achieved by arranging the vertical internal heat exchanging tubes.

1.3 – Research Objectives

The first goal of this study is to assess the impact of internals on bubble column hydrodynamics. This will be accomplished via extensive experimental investigations of gas holdup and bubble dynamics. The second goal is to explore the effects of internals on liquid mixing. The knowledge generated above will enhance the database whose quantification and assessment will guide the design of bundles of internals. The final goal is to simplify the scale up process by compartmentalizing the column using the vertical internals. The details of these goals are as follows:

Investigation of the impact of heat exchanging internals in bubble columns

Only few earlier studies examined global parameters in bubble columns with internals. However, Youssef et al. (2010) show that the reported data is contradictory and insufficient in extracting conclusions on such systems. In this study, for the first time, insight will be presented on local bubble dynamics and liquid phase mixing behavior in a pilot plant scale unit with and without internals. This task focuses on studying the effect of vertical heat

exchanger tubes in two columns of 8" (19 cm) and 18" (44 cm) in diameter. It is to be noted that two researchers from the University of Dortmund (Korte, 1987 and Bernemann, 1989) have studied heat transfer and liquid phase velocity profiles, respectively, in columns of 19 cm and 45 cm diameter with internals. The two columns utilized in the present work were specifically chosen to complement a database for bubble columns with internals in these scales. This is especially true since the internals configurations are designed to be as close as possible to those in the above studies. Moreover, due to high industrial significance of the methanol and Fischer-Tropsch syntheses, the configurations of the tube bundles are proposed to meet the corresponding heat transfer requirements for each process. The details of the design criteria are emphasized in Chapters 2 and 3. Finally, the choice of the above columns allows the assessment of the effect of scale and dynamic similarities between the two systems. The column's diameter was reported to have no effect on the overall gas holdup (Wilkinson et al., 1992) for column diameters larger than 15 cm. Deen et al. (2010) assert no effect of column diameter on heat and mass transfer as well. However, these conclusions are limited to columns without internals. Whenever possible, this study, therefore, will evaluate the differences in parameters between both units to help in the scaling process. It will assess how gas holdup and bubble dynamics, their radial distributions, and liquid mixing characteristics all depend on the following parameters:

Gas velocity: covering bubbly and/or churn turbulent flow regimes.

Column diameter and aspect ratio: Two units of different scales (8" and 18" diameters).

Internals: 0% (without), 5%, 22-25% covered Cross Sectional Area (CSA) [as needed for Methanol and FT syntheses, respectively], different diameter (0.5" OD (d_i) (for the smaller column) and 1" OD (d_i) (similar to Korte (1987) and Bernemann (1989) to mimic industrial conditions in the pilot plant column). Note that the internals diameters were chosen to maintain the ratio d_i/D close for both columns.

Gas dynamics: The overall gas holdup will be measured via the bed expansion method. The local gas holdup, and the bubble dynamics distributions (velocity, chord length, specific interfacial area, and passage frequency) will be studied using a four-point fiber optical probe.

These bubble parameters explain variations in coalescence and break-up rates as a result of internals and their configurations.

Liquid mixing: Since the behaviors of the gas and liquid phases are linked within the flow field, it is important to study the liquid phase mixing as a function of the addition of internals. A standard liquid tracer/conductivity probe utilized in a semi-batch mode (continuous gas flow and batch liquid) will identify the effect of vertical internal structures on the concentration and residence time distributions of the liquid phase in the system.

Scale-up of bubble columns

Using the experimentally generated holdup profiles and understanding of bubble scale phenomena, the scale up part of this work includes the assessment of a new methodology for scaling up bubble column with internals. It is well known that the exothermic Fischer-Tropsch reaction requires heat exchanging internals that cover ~25% of the Cross-Sectional Area (CSA) of the reactor to remove the resulting heat. The positions of these tubes, usually kept undeclared by companies, might be configured in multiple arrangements. Can they be arranged so that they in effect form small internal bubble columns within the large scale reactor walls? If so, can they, in such a configuration, mimic the behavior of columns of the same small diameter having a solid wall instead? The answer to this question forms the basis of the hypothesis of the newly proposed scale-up methodology. Note that the reactor does not need to be compartmentalized into columns with circular cross sections; more intelligent designs (such as honeycombed geometries) may eliminate dead spaces between the compartments.

To assess the new scale-up methodology, the hydrodynamics (gas holdup and bubble dynamics) inside the above mentioned structured column will be investigated and compared with those generated in a solid wall column of the same diameter. Once there is a match, the following step is the replication of structured compartments by adding more vertical internals.

Figure 1.4 shows a schematic summary of the research, demonstrating the network of investigations and their linkage.

1.4 – Dissertation Structure

This thesis consists of the following chapters:

Chapter 1 introduces the FT process as an alternative solution to cleaner liquid fuels and chemicals from more abundant resources than oil, bubble column reactors are key part of the process. The motivation for this study and objectives are presented as well.

The pertinent literature review is outlined in Chapter 2.

Chapter 3 reports the results for the investigated hydrodynamics in 8" bubble column with internals.

Chapter 4 discusses the impact of the internals in a pilot plant scale column.

Chapter 5 highlights the effect of heat exchanging internals on the liquid phase mixing behavior.

Chapter 6 proposes a new scale-up methodology for bubble column reactors, based on reactor compartmentalization.

Finally, Chapter 7 summarizes the recommendations for future work on the topic.

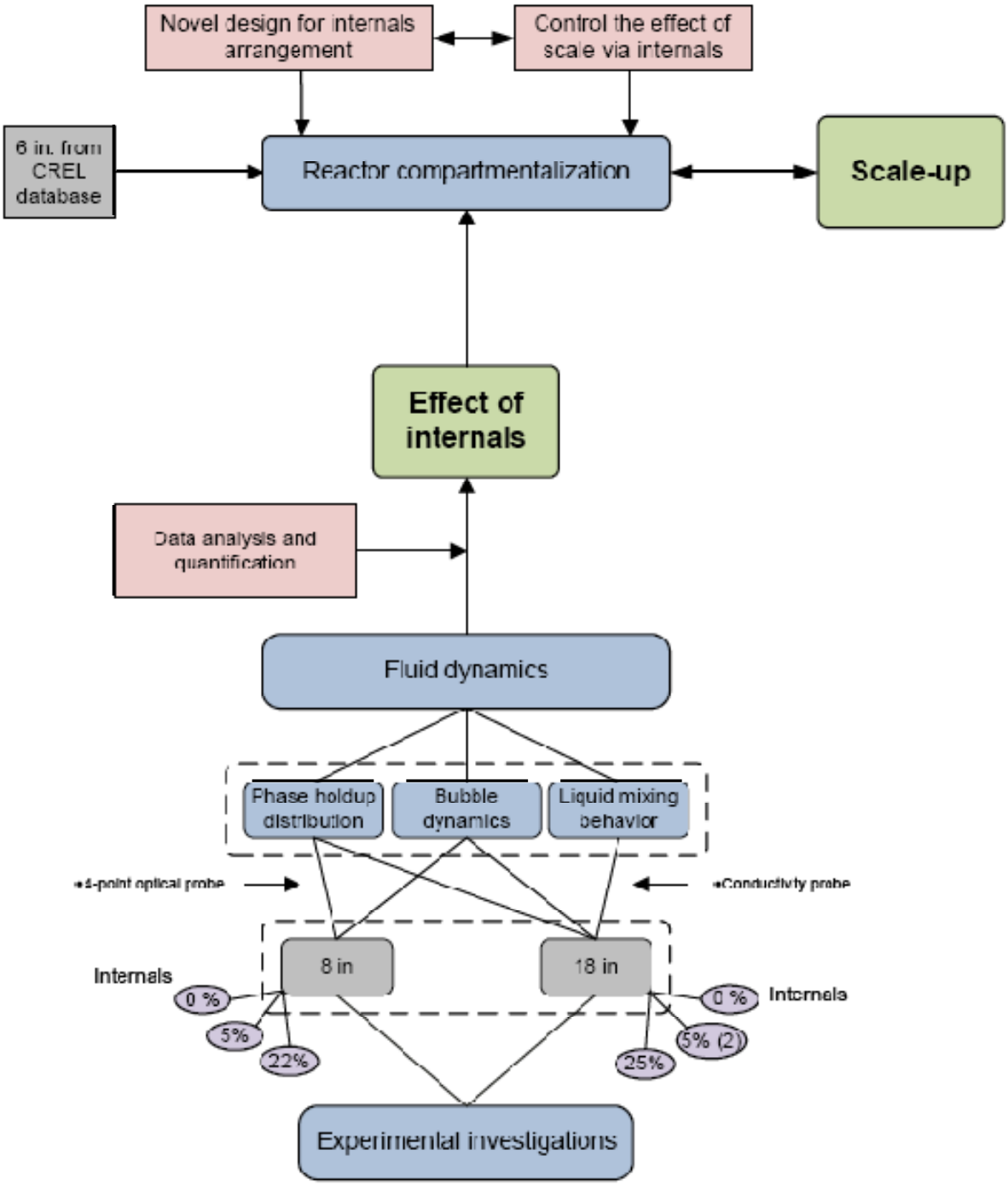

Fig. 1.4 – Research structure

Background

2.1 – Internals

Krishna et al. (2001) listed the typical conditions for an industrial Fischer-Tropsch conversion including heat removal by means of cooling tubes inserted in the reactor. The conversion process is highly exothermic, as are most processes conducted in bubble columns. Table 2.1 indicates a number of examples. However, most researchers have not studied the effect of internals as a design parameter impacting bubble column performance.

Recently, Hulet et al. (2009) reviewed the heat transfer studies in bubble columns and recommended that more work involving bubble columns with internals needs to be done to develop reliable models for predicting large scale unit performance. There also is no definitive guidance on the design of the internals. Kölbel and Ralek (1980) in their "Notes on the Development of Large-Scale Reactors" suggested the insertion of honeycombed cross section vertical shafts inside the column, with the cooling pipes located in corners or around the shafts. They claim this design will be able to eliminate unfavorable backmixing. They, however, do not provide experimental data for such a design. Chapter 6 of this dissertation will discuss their study further.

Korte (1987) comprehensively studied heat transfer from horizontal and vertical tube bundles with an embedded heat transfer probe in columns of 19 and 45 cm diameter and concluded that the heat transfer coefficient is very sensitive to the bundle's configuration and density. It was shown that even with high viscosity liquids, which promote bubble coalescence, the presence of internals may inhibit any impact (decrease) on the values of the heat transfer by enhancing the bubble break-up rate. Taking into account the internals, Korte then correlated his results as follows:

$$St=0.139\left[\left(Re_G Fr_G Pr_L^{2.26}\right)^{-\frac{1}{3}}\right]^{0.84} .A_f^{-0.2}.\left(\frac{t_R}{d_R}\right)^{0.14}.\left(\frac{\eta_L}{\eta_{LW}}\right)^{0.3},$$

Table 2.1 - Sample reaction systems operated in bubble column reactors (after Schlüter et al., 1995)

Product	Feed	Heat of Reaction (kJ/mol)	Pressure (bar)	Temperature (°C)
Acetaldehyde	Ethylene, Oxygen	**-243**	3	120-130
Acetone	Propene, Oxygen	**-255**	10-14	110-120
Ethyl Benzene	Benzene, Ethylene	**-113**	2-4	125-140
Benzoic Acid	Toluene, Air (or Oxygen)	**-628**	2-3	110-120
n-, iso-butyraldehyde	Propene, Hydrogen, Oxygen	**-118/-147**	7-25	90-120
Cumene	Benzene, Propene	**-113**	7	35-70
Cyclohexane	Benzene, Hydrogen	**-214**	50	200-225
Cyclohexanol Cyclohexanone	Cyclohexane, Air	**-294**	8-15	125-165
1,2 - Dichloroethane	Ethylene, Chlorine, Oxygen	**-239**	15-20	170-185
	Ethylene, Chlorine	**-180**	4-5	40-70
Acetic Acid	Acetaldehyde, Oxygen	**-294**	2.3-2.5	50-70
Acetic Acid, Methyl ethyl	n-Butane, Air	**-1270**	15-20	180
Vinyl Acetate	Ethylene, Ethyl Acid, Oxygen	**-176**	30-40	110-130
Wet Air oxidation of Sewage Sludge	Sewage Sludge, Air	**-435**	50-150	200-300
Fischer-Tropsch Synthesis	Hydrogen, Carbon Monoxide	**-210**	30-40	250-290
Methanol synthesis	Hydrogen, Carbon Monoxide	**-91**	50-100	220-270

From a fundamental standpoint, it is expected that, similar to the heat transfer coefficient, various hydrodynamic and transport coefficients are altered by the presence of internals. In other words, correlations and models developed in empty columns need to be revisited.

Bernemann (1989) used a flywheel anemometer and found the axial component of the liquid phase velocity to be higher in a column with internals than in a column without internals,

regardless of the gas velocity used (Figure 2.1). However, the inversion point (zero liquid flow) between the positive and negative liquid velocities in the radial profile was maintained at about the same dimensionless radius of ~0.7.

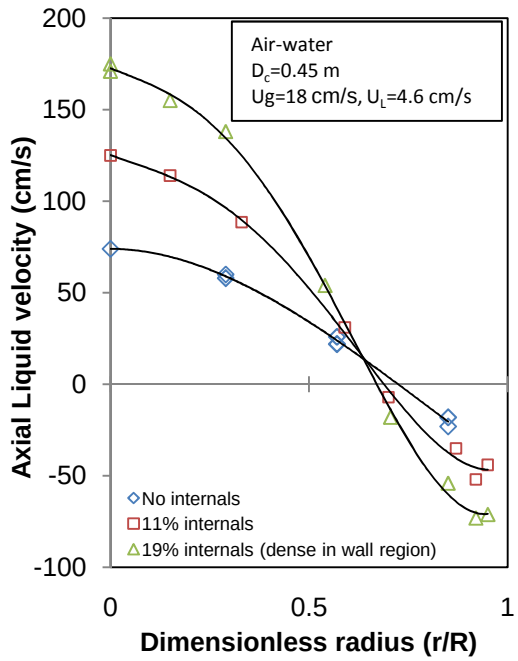

Fig. 2.1 - Effect of internals on the profile of the axial component of the liquid velocity (modified from Bernemann, 1989)

Saxena et al. (1992) investigated the effect of internal tubes in 0.305 m diameter column, blocking 1.9, 2.7 and 14.3% of the total column's cross sectional area (CSA) with a 3 phase system (air-water-glass beads). The gas holdup was found to be higher for 37 tubes than for 7 tubes. However, they reported the overall gas holdup as a global parameter, with no mention of the resulting radial profile. Thus, the effect of internals on liquid recirculation is impossible to assess from their data.

Similarly, Pradhan et al. (1993) studied six different covered volume fractions (X_v) of the column ranging from 0.014 to 0.193, and their results showed that gas holdup increased with an increase of X_v (up to a maximum of 55%). Moreover, helical coil internals provided higher gas holdup than vertical tubes, a finding attributed to the fact that vertically inter-tubes gaps allowed large bubbles to escape, decreasing the gas holdup, while with helical coils, smaller gaps were present.

Chen et al. (1999) assessed the effect of internals covering ~5% of the column's CSA, using gamma ray Computed Tomography (CT) and Computer Automated Radioactive Particle Tracking (CARPT) facilities available in the Chemical Reaction Engineering Laboratory (CREL) at Washington University in St. Louis. They studied gas holdup, liquid recirculation, and turbulent parameters in an 18" diameter column. Such internals were found to have no significant effect on liquid recirculation velocity, while gas holdup increased slightly (~10% at the column's center and less towards the wall region). The turbulent stresses and eddy diffusivities were lower with the internals added.

Modeling bubble columns with internals was attempted by Forret et al. (2003) based on a 2D approach, and by Larachi et al. (2006), using computational fluid dynamics codes (CFD), who employed full 3D simulation..

Forret et al. (2003) observed that internals decreased the liquid fluctuating velocity and enhanced large scale liquid recirculation (Figure 2.2) following their liquid tracer experiments. Hence, the 1D Axial dispersion Model (ADM) could not be used in a column with internals. They developed a 2D model to predict the effect of internals on liquid mixing by accounting for an axial dispersion coefficient $D_{ax,2D}$, a radially dependent axial velocity profile, and a radial dispersion coefficient $D_{rad,2D}$.

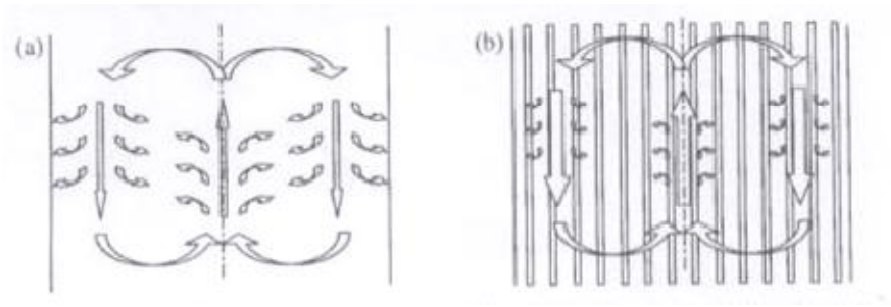

Fig. 2.2 - Enhancement of large recirculation scale and decrease of radial dispersion due to internals (Forret et al. (2003))

Larachi et al. (2006) carried out CFD simulations for the flow behavior in a column without internals and with four different internal arrangements (see Figure 2.3). The occluded cross sectional areas ranged between 2 to 16.2%. The well known core-annulus flow was predicted by the simulation of the uniform internals configurations, which confirmed the results

highlighted earlier by Bernemann (1989). However, for non-uniform internals, a complex flow behavior was detected (Figure 2.3).

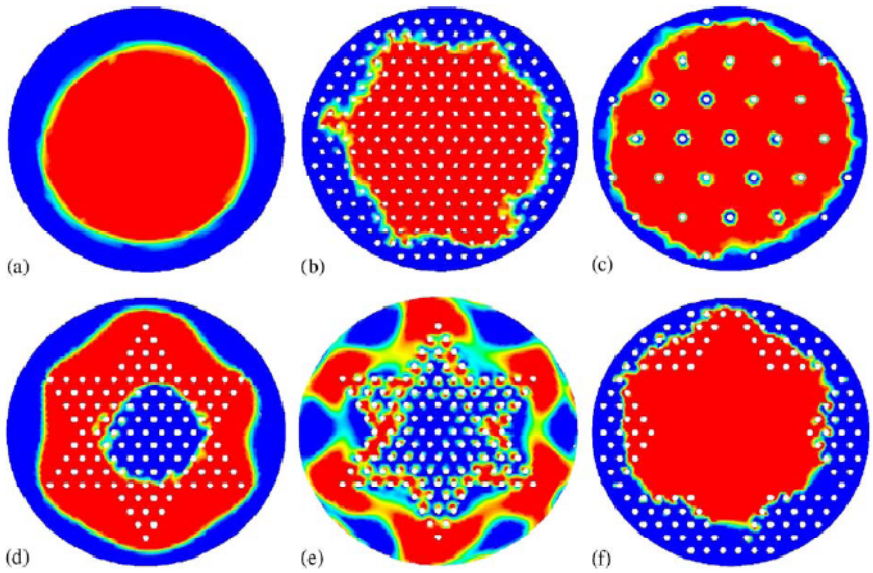

Fig. 2.3 – CFD simulations of time-averaged contour plots of the axial liquid velocity component over a cross-sectional slice taken in the fully developed region with different internals configurations (Larachi et al., 2006)

A review of bubble column reactors with internals (Youssef et al., 2010) leads to the following summary of the state-of-knowledge of the effect of horizontal and vertical internals in bubble and slurry bubble column reactors:

- Sectionalizing bubble columns via perforated trays leads to an increase in gas holdup (Fair et al., 1962, Kawasaki, 1994, Kemoun et al., 2001, and Alvaré and Al-Dahhan, 2006a). A similar increase in gas holdup was observed when utilizing horizontal tubes instead (Colmenares et al., 2001).

- Blass and Cornelius (1977) reported a decrease in bubble coalescence upon the addition of horizontal sectionalizing plates ranging from 1.1% to 46% open CSA in a 3-phase system (14 cm diameter). Kemoun et al. (2001) used ~5% open CSA sieve trays in an air-water system (19 cm diameter) and claimed that the trays induce bubble coalescence and present an obstacle to the uniform bubbles.

- Horizontal internals in bubble columns tend to reduce the overall back-mixing, so that the benefits of reactor operation as an ideal cascade can be approached (Westerterp, van Swaaij and Beenackers, 1987, Mashelkar, 1970, Palaskar et al., 2000, Nosier, 2003, and Alvaré and Al-Dahhan, 2006b).

- Some researchers (Sekizawa and Kubota, 1974 and Blass and Cornelius, 1977) found that with an increase in the plate open free area, the backflow ratio increases approaching mixed stirred vessel behavior. Others (Palaskar et al., 2000, and Doshi and Pandit, 2005) observed that decreasing the open free area reduced the liquid recirculation and increased the pressure drop.

- The mass transfer coefficient was found to increase upon sectionalization with perforated trays (Kawasaki, 1994), and to decrease upon addition of more horizontal tube rows (Nosier, 2003).

- Because they inhibit bubble coalescence, vertical internals break bubbles into tiny ones (Saxena et al., 1992 and Pradhan et al., 1993). However, O'Dowd et al. (1987) reported an increase in bubble size upon insertion of the baffles.

- Longitudinal tube internals tend to decrease the area available for flow and causing an increase in gas holdup values over those of the 'empty' reactors (Yamashita, 1987, Chen et. al., 1999, and Balamurugan and Subbarao, 2006). The same applies when helical coils are used (Pradhan et al., 1993).

- The gap size between internals is important in the longitudinal funneling of liquid flow. Because internals contain the large scale eddies, this gap length scale is also responsible for the decrease of the liquid kinetic turbulent energy (Larachi et al., 2006).

- The large scale liquid recirculation increases when vertical tube internals cover a large CSA (~22%) (Forret et al., 2006), while a less covered CSA (5%) does not affect liquid recirculation (Chen et al., 1999).

- A 2D model fitted the large columns well with and without vertical tube internals. (Forret et al., 2003).

- Vertical tubes increase the heat transfer coefficient more than horizontal internals do, because the angle of attack provided for the two-phase flow changes from 90° to 0° (Aksel'rod, 1976). The axial dispersion coefficient also increases, especially in the bubbly flow regime, where it is a strong function of the gas velocity distribution at the bottom of the column. This distribution is largely affected by the internals (Shah et al. 1978).

It should be noted that a tabulated list summarizing the studies on bubble columns with internals is provided in Appendix A.

To our knowledge, the recent study by Youssef and Al-Dahhan (2009) is the only investigation where the bubble dynamics and the gas holdup radial distribution were reported experimentally for a bubble column unit equipped with internals.

2.2 – Bubble Dynamics

Bubble column reactor performance depends greatly on the characteristics of the bubbles. The bubble size, residence time, frequency, and velocity are the key factors that affect transport steps between the system's phases. Performance is also affected by the complex coalescence and break-up events that commonly occur in bubble column reactors.

Several researchers have reviewed the bubble dynamics, and detailed studies can be found elsewhere (Yang et al., 2007 and Wu, 2007). In this section, the different bubble parameters are briefly introduced and defined, and the state of knowledge related to each is identified. The factors impacting the bubbles' motion, shape, and holdup are also presented.

A number of techniques have been utilized over the years for the measurement and quantification of above parameters. Table 2.2 (extended from Kumar et al., 1998) gives a summarized comparison among these techniques. In addition, the group of Prof. L.-S. Fan at OSU used a 3D ECT or Electrical Capacitance Volume Tomography (ECVT), incorporating a geometrically configured sensor design and a neural network image reconstruction, to capture the dynamic 3D multiphase flow behavior (Warsito and Fan, 2005). Although the ECVT technique has been commercialized through an OSU spin-off start-up, some concerns about the true resolution of the resulting images remain to be addressed.

Table 2.2 - Measurement techniques used in bubbly flows

	Conductivity or resistivity probe	**Optical Fiber probe**	**Dynamic Gas Disengagement (DGD)**	**Cameras**	**X-ray or γ-ray Tomography**	**Ultrasound Doppler**
Intrusive	Yes	Yes	No	Internal (Borescope): Yes External: No	No	Yes
Applicability	3-phase systems following statistical, chaos, etc. analysis	3-phase systems, hydrocarbon and high P and T	3-phase systems, high T and P	2D units, close to wall in 3D units (transparent)	3-phase systems, high P, T and hydrocarbons	3-phase systems and hydrocarbons
Drawbacks	Requires high difference between conductivity of phases	Needs high difference in refractive index between phases and fragile	No local measurement	Not useful in highly churning systems	Time consuming and poses safety concerns	Low holdup cases
Costs	Low	low	Low	Medium	High	High

2.2.1 – Local gas holdup

The gas holdup is defined as the fraction of gas in a gas-in-liquid (or gas-liquid-solid) dispersion (Deckwer, 1992). It is probably considered as the main parameter in bubble column reactors' design. Hence, it is not surprising that the literature is full of studies on gas holdup (e.g., Schügerl et al., 1977, Reilly et al., 1986, and de Swart, 1996). These studies, however, have focused on the evaluation of the overall gas holdup (with a few exceptions, e.g., Hills, 1974) and have gone a long way toward the development of correlations for the estimation of gas holdup in columns operating under a wide range of conditions (also see Fan et al. (1999) and Krishna and Sie (2000)). The evaluation of reliable radial (and axial) profiles of gas holdup was achieved by the advances in probe techniques (Matsuura and Fan, 1984, Lee and De Lasa, 1987, Frijlink, 1987, and Xue, 2004) and in tomography imaging (Kumar et al., 1994).

The radial non-uniformity of the gas holdup profiles is manifested by a higher gas holdup in the column's axis and lower values in the vicinity of the wall. This difference drives the liquid recirculation, as briefly described earlier, accelerates the bubbles in the column's center, and hinders those at the wall region. Consequently, a broad residence time distribution of the gas phase exists in the column, and the analysis of various processes becomes more complicated (Mudde, 2005). Hence, the investigation of radial gas holdup profiles is pertinent. Typical gas holdup radial profiles are shown in Figure 2.4.

It is obvious from Figure 2.4, and was pointed out by many investigators (e.g., Yasunishi et al., 1986), that the radial profiles are parabolic and are found, in most cases, to be axisymmetric (Ong et al., 2009). A mechanism governing the radial profile of the gas holdup in multiphase reactors was suggested by Bankoff (1960) and Koide and Kubota (1966), positing that a balance exists between the horizontal drag force acting on the bubbles and the radial diffusion of bubbles. However, this explanation cannot be valid in bubble column systems due to the recirculating turbulent flow. Ueyama (2006) successfully derived the parabolic distribution of gas holdup radial profiles by balancing the total effect of the drag force at the interface between gas and liquid phases with an apparent force composed of time-averaged physical quantities. The latter was accomplished on the basis of time-averaged Navier-Stokes equations for the liquid and gas phases.

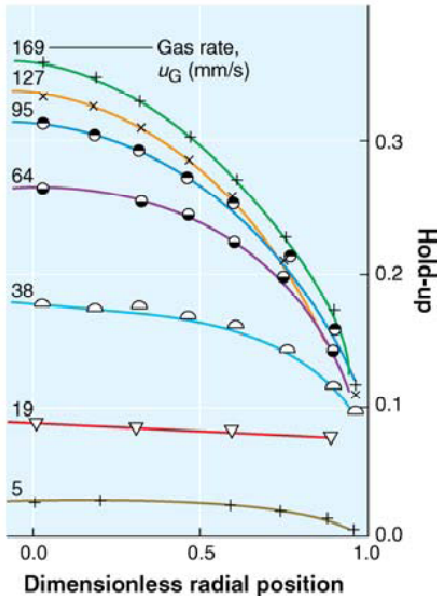

Fig. 2.4 – Typical radial gas holdup radial profiles at different superficial gas velocities (after Hills, 1974)

The local gas holdup, similar to the overall gas holdup, is affected by many parameters. Radial gas holdup exhibits higher values with an increase in the superficial gas velocity (Xue et al., 2008), with an increase in the system's pressure (Rados, 2003), and with a decrease in the system's viscosity (Shaikh, 2007). Wu (2007) found the local gas holdup to decrease with an increase in the solids loading. The effect of internals on local gas holdup profiles has not been reported.

It is noteworthy that an improved model of bubble column reactor performance requires the radial holdup profile, as opposed to a lumped value of an overall gas holdup.

2.2.2 – Specific interfacial area

Specific interfacial area ($a = A/V_D$) and its distribution in the column are important. In bubble column reactors, there exists a large interfacial area between the dispersed gas phase and the continuous liquid phase, which is a key in determining the bubble column reactor's productivity. In fact, bubble column reactors are favored when the mass transfer resistance lies in the liquid phase (i.e., $(k_La) << (k_Ga)$). Fan (1989), Patel et al. (1990), and Behkish et al. (2002) agreed that the variation in the observed volumetric mass transfer coefficient k_La values is mainly due to changes in the interfacial area (a) This area can be calculated

(assuming spherical bubbles) from the gas holdup values by using the Sauter mean bubble diameter: $a=6\varepsilon_g/d_s$. Although the calculation may be valid for a single bubble in a pool of liquid, this assumption is highly debatable for bubble column systems, where a bubble population balance equation best captures the widely distributed bubble size (Chen et al., 2004). Hibiki and Ishii (2001 and 2002) reviewed the interfacial area studies and showed that even the widely used correlations in the literature, given by Akita and Yashida (1974), come short in predicting data sets outside of the range of conditions in their own study.

The specific interfacial area largely depends on the shape of the bubbles. Spherical bubbles generally exist at low superficial gas velocities, while ellipsoidal, spherical cap, and skirted bubbles (Bhaga and Weber, 1981), as well as very irregular bubble shapes, are found deep in the churn turbulent flow regime as a result of coalescence and break-up phenomena. More details are given in the bubble chord length section in this chapter. The experimental measurement of gas-liquid interfacial area can be accomplished via a variety of chemical and physical methods, the details of which can be found elsewhere (Deckwer, 1992). Generally, the interfacial area increases with an increase in pressure (Wilkinson et al, 1992) and in the superficial gas velocity (Xue et al., 2008), but decreases with higher solids loading (Wu, 2007).

Typical radial profiles of the specific interfacial area exhibit higher values at the column's core and lower values in the wall region (Xue, 2004), similar to the local gas holdup trends, but these findings were not verified with the presence of internals before.

2.2.3 – Bubble velocity

The bubble velocity directly influences the residence time of the gas phase in the system, and hence determines the gas holdup. The bubble velocity's significance also stems from its relation with the slip velocity, which is defined as

$$u_{slip}=u_b-u_l.$$

The slip velocity is very relevant for CFD simulations due to its impact on various forces acting upon the bubble-liquid interface (lift, drag, etc.) (Xu et al., 2005). Photographic techniques (Krishna et al., 1999) have been used for the measurement of bubble velocity, as well as electro-resistivity probes (Matsuura and Fan, 1984 and Yasunishi et al., 1986) and

optical probes (Chabot and De Lasa, 1993, Groen et al., 1995, Guet et al., 2003, Xue, 2004 and Wu et al., 2008). Wu (2007) tabulated some correlations for the estimation of bubble velocity. He observed that they were limited to a certain range of superficial gas velocities, pressures, and/or bubble size. For example, Fan and Tsuchiya (1990) proposed a correlation for the bubble rise velocity in two-phase systems. Later, Tsuchiya et al. (1997) extended its applicability for slurry systems, and finally, Luo et al. (1997) generalized it for high-pressure systems. This correlation can be represented in a dimensionless form as follows:

$$u_b^{'} = u_b \left(\frac{\rho_{sl}}{\sigma g}\right)^{1/4} = \left\{\left[\frac{Mo^{-1/4}}{K_b}\left(\frac{\Delta\rho}{\rho_{sl}}\right)^{5/4} d_b^{'2}\right]^{-n} + \left[\frac{2c}{d_b^{'}} + \left(\frac{\Delta\rho}{\rho_{sl}}\right)\frac{d_b^{'2}}{2}\right]^{-n/2}\right\}^{-1/n},$$

with the dimensionless bubble diameter being

$$d_b^{'} = d_b(\rho_{sl} g/\sigma)^{1/2}.$$

The three empirical parameters (n, c, K_b) respectively account for the contamination level of the liquid phase, the dynamic effects of the surface tension, and the viscous nature of the surrounding medium:

$$n = \begin{cases} 0.8 & for\ contaminated\ liquids \\ 1.6 & for\ pure\ liquids \end{cases}$$

$$c = \begin{cases} 1.2 & for\ contaminated\ liquids \\ 1.4 & for\ pure\ liquids \end{cases}$$

$$K_b = max(K_{b0} M_o^{-0.038}, 12)$$

Although, when compared against the famous Re vs. Eo plot (Clift et al., 1978), the above correlation seems to predict well the rise velocity over a wide range of temperatures, pressures, and bubble sizes, it is still limited to single bubbles. Extrapolation to bubble swarms where coalescence and break-up occur is not possible. Ueyama et al. (1980) and Yoshida and Akita (1965) both asserted that the bubble velocity is little affected by the column's diameter, in columns 0.6 m to 5.5 m diameter for the former study and 0.077 m to 0.6 m for the latter study. Kulkarni and Joshi (2005) concluded that only the rise velocity of small bubbles is drastically affected by the liquid's viscosity (it decreases with an increase in viscosity) and surface tension (it decreases with a decrease of surface tension), while large

bubbles are insensitive to these liquid properties. This may not be surprising if one notes that small bubbles move with rise velocities ranging from 3 to 22 cm/s (Kölbel et al., 1961), while large bubbles can reach up to 2 m/s. For example, Figure 2.5 shows the relation between the terminal velocity of air bubbles in water as a function of bubble equivalent diameter. The curves converge for very small rigid (spherical) bubbles and for large (spherical-cap) bubbles. Theoretically, for the former case, even distilled water contains enough surfactants to prevent bubble internal circulation, while for the latter, the liquid's physicochemical properties cease to be important (Clift et al., 1978). However, for the range in-between, the deviation between the two curves is clear. For other systems, similar convergence occurs for large bubbles, regardless of physical and operating conditions (Luo et al., 1997).

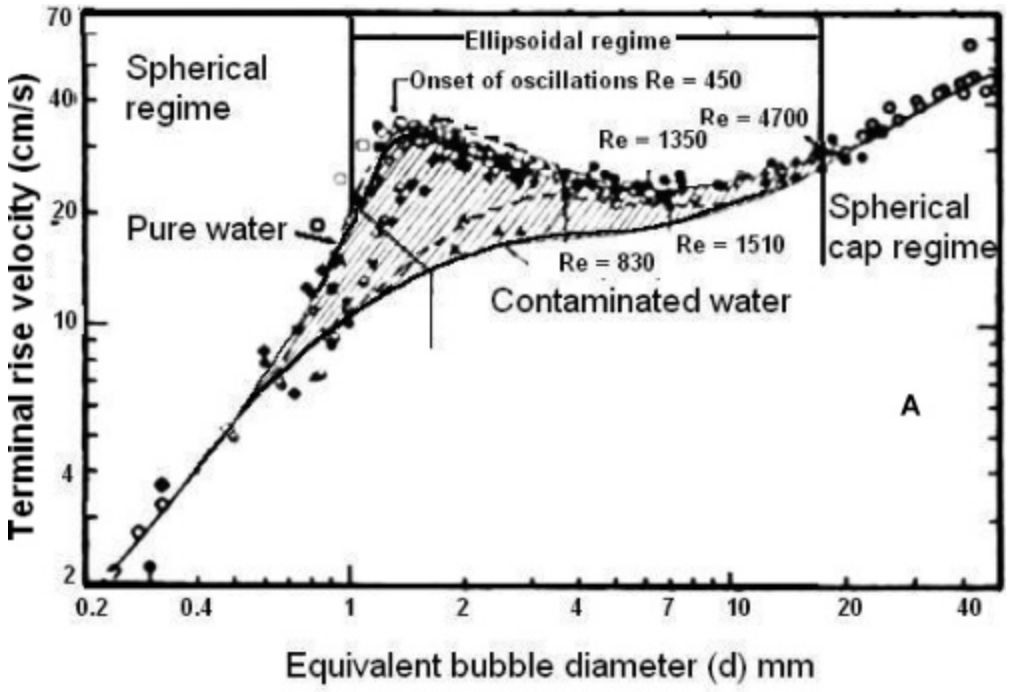

Fig. 2.5 – Terminal velocity of air bubbles in water at 20°C (after Clift et al., 1978)

It is generally agreed that bubble velocity, which is highly dependent on the flow regime, exhibits the broadest probability distributions in the slug flow regime. In the literature, bubble velocity has been erroneously confused with bubble rise velocity, but bubbles in bubble columns move downward as well. In other words, the bubble velocity should be represented by a bi-modal probability distribution highlighting the upward (positive) velocity

and downward (negative) velocity components of the bubbles. The latter are due to recirculation in bubble columns as higher superficial gas velocities are applied. This approach will be followed in the current work.

2.2.4 – Bubble chord length

Bubble size and shape have been the subject of numerous studies (e.g., Clift et al., 1978, and Bhaga and Weber, 1981). The characteristics of a bubble in motion can be described by both the bubble shape and its velocity. The bubble shape and size are interrelated, and the observed bubble shape, and hence its dynamics, results from a balance among the forces acting on a moving bubble. As the dominant forces change with bubble size, the bubble shape undergoes an accordant change (Yang et al., 2007). For example, when the bubble size is small (less than 1 mm) the shape is spherical, and viscous forces and surface tension forces dominate. If the bubble is of an intermediate size, both the surface tension and the inertia (buoyancy) force are important, and bubbles tend to be ellipsoidal. Large rising bubbles are of a spherical cap shape because the inertia forces dominate and the effects of viscosity and surface tension are negligible (Fan and Tsuchiya, 1990). In addition, the largest stable bubble size in static equilibrium is obtained by equating both the buoyancy and surface tension forces. As a rough rule of thumb, small bubbles are those with a volume equivalent bubble diameter d_e<1mm in water, while large bubbles are those with volumes larger than 3 cm^3 (i.e., d_e>18mm).

The above forces are usually grouped in three commonly used dimensionless numbers when the bubble shape, size, and motion are to be characterized. These numbers are the Reynolds number (ratio of inertial force/viscous force), the Eötvös number (ratio of buoyancy/surface tension), and the Morton number (a combination of inertial, gravitational, surface tension and viscous forces). These numbers can be represented as follows:

$$\mathrm{Re} = \frac{\rho d_b \mathrm{v}}{\mu}$$

$$Eo = \frac{g d_b^2 \rho}{\sigma}$$

$$Mo = \frac{g \mu^4}{\rho \sigma^3}$$

It is worth noting that the Weber number is not independent of Re, Eo, and Mo, as it is given by Xue (2004):

$$We = \frac{\rho d_b \mathrm{v}^2}{\sigma} = \frac{\mathrm{Re}^2 Mo^{0.5}}{Eo^{0.5}}$$

Due to the absence of a reliable measuring technique to assess the properties of large bubbles in the heterogeneous regime, the Sauter mean diameter, defined as the diameter of a sphere that has the same volume to surface area ratio as would all the bubbles in the distribution if they were uniform, has been utilized by several researchers to represent the bubble size (Deckwer, 1992). In other words, while the Sauter mean diameter can be effectively representative for low superficial gas velocities, it will not be valid at higher superficial gas velocities of industrial importance. There are many correlations to estimate the Sauter mean diameter (Calderbank, 1976, Akita and Yoshida, 1974, and Fukuma et al., 1987), which are reviewed elsewhere (Saxena and Chen, 1994). The main issue is that these are mostly limited to low superficial gas velocities of less interest for industrial applications.

The bubble size can also be probed by measuring the bubble chord length (Kwon et al., 1994), but a model for the bubble shape is then needed to fully infer bubble size. Figure 2.6 shows an arbitrary chord length, AB (L_i), for an ellipsoidal bubble.

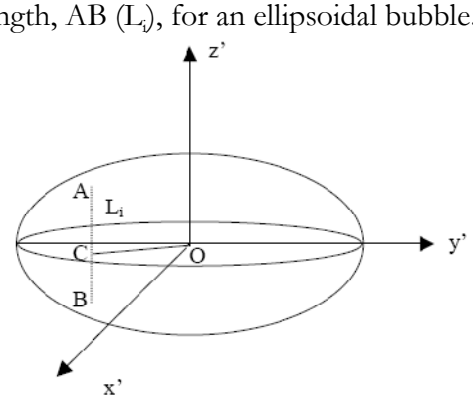

Fig. 2.6 – Schematic representation of an elliptic bubble (Xue, 2004)

The fiber optical probe utilized in the current work determines the bubble chord length as an indication of the bubble size, for irregular bubbles or a gas stream and for lack of more accurate representative parameters, especially over the wide range of superficial gas velocities applied as discussed above. It is evident that the characteristics of both flow regimes vary greatly. For instance, Liu et al. (1998) showed that the chord length probability distribution, obtained from an optical probe, in the heterogeneous regime differs from that of the bubbly flow regime, as shown in Figure 2.7. Many authors (e.g., Luewisutthichat et al., 1997 and Pohorecki et al., 2001) have reported the bubble chord length distributions to be best represented by a log-normal distribution, with its upper value at the maximum stable bubble size. Such a distribution implies the coincidence of a relatively large number of disintegrated small bubbles and a small number of coalesced large bubbles, that is a very asymmetric bubble size distribution.

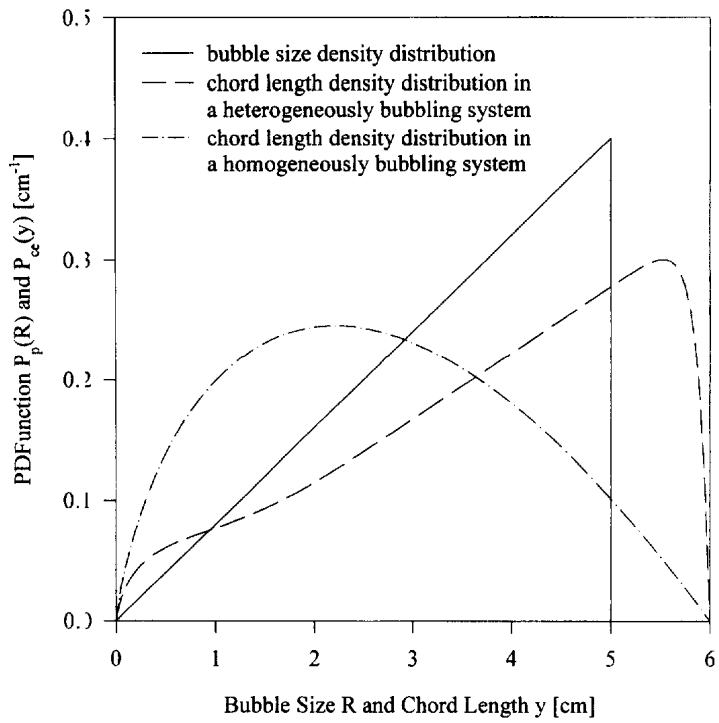

Fig. 2.7 – The chord length distributions for both homogeneous and heterogeneous regimes against the triangular bubble size density at the probe (y is the chord length, and R is equivalent to OC from Figure 2.6) – (Liu et al., 1998)

The initial bubble size is mainly determined by the gas sparger design. Thus, the effect of the gas sparger, its design, and the pressure drop across it have been subject to a number of

studies (e.g., Ong et al., 2009). However, the initial bubble size is limited only to the gas distributor region at the bottom of the column. This is especially true for the higher superficial gas velocity conditions, when several coalescence and break-up phenomena associated with the flow lead to variations in the bubble growth and equilibrium size. It is important to note that there still are many uncertainties with regard to such phenomena. The bubble size was found to increase with an increase in the solids loading, to decrease with an increase in pressure, and to be independent of the column's diameter for reactor diameters ≥15 cm. The bubble size distribution broadens as the superficial gas velocity increases.

2.2.5 – Bubble frequency

In the current study, and where a fiber optical probe is utilized as a measuring technique, the bubble frequency can be defined as the number of bubbles that hit the central tip of the probe per second. Since the bubble frequency, gas holdup, and specific interfacial area are interwoven parameters, one can confidently expect an increase in both gas holdup and interfacial area with an increase in bubble frequency. Accordingly, the bubble frequency typically exhibits parabolic profiles as shown in Figure 2.8. It is clear from the figure that the bubble frequency increases with superficial gas velocity.

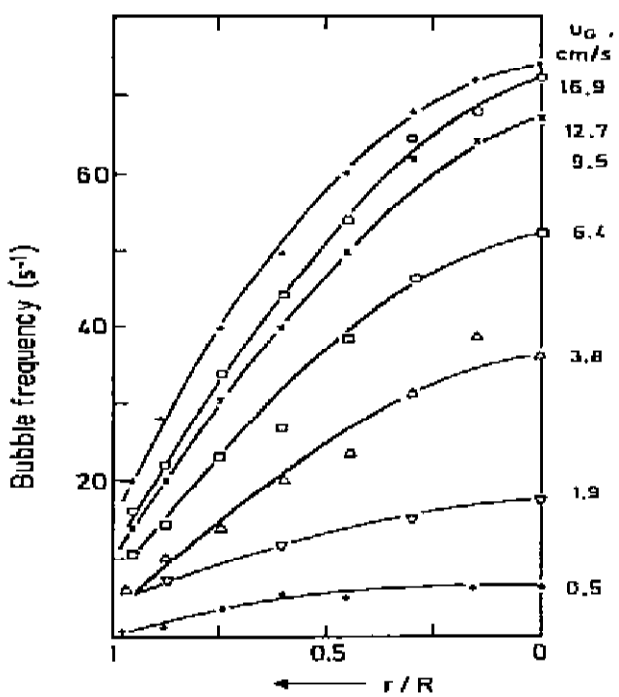

Fig. 2.8 – Radial bubble frequency profile (Hills, 1974)

Xue (2004) compared the bubble frequency with different spargers of different percentage open areas and numbers of holes. He found that all three spargers produced very similar bubble frequency behavior in the fully developed region. His results, shown in Figure 2.9, are in line with his findings for the gas holdup and specific interfacial area radial profiles.

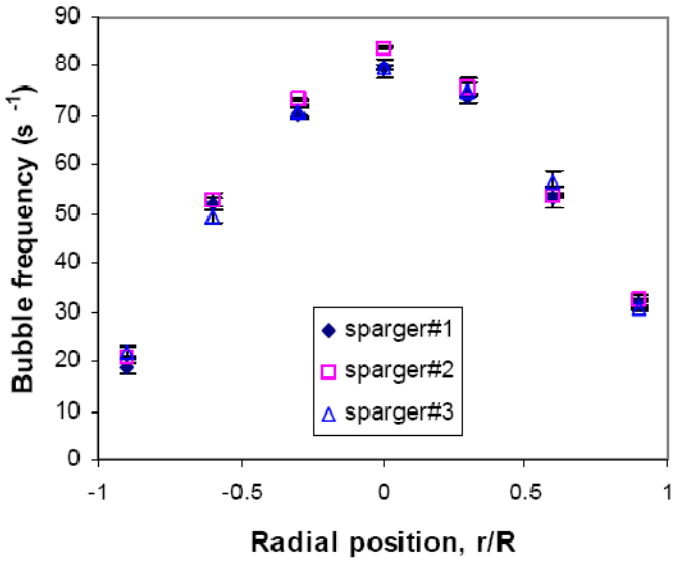

Fig. 2.9 – Bubble frequency for different spargers (Xue, 2004)

The above overview reveals a lack of studies involving the presence of internals in bubble column reactors. Thus, one of the main objectives of this study, as pointed out in Chapter 1, is obtaining insight into local bubble dynamics in bubble columns equipped with internals. Hence, this study focuses on the effect of vertical heat exchange tubes in units of 8" and 18" diameter, with an emphasis on internals typical for the Fischer-Tropsch process and Liquid Phase Methanol Synthesis.

2.3 – Scale-up

The development of bubble column scale up criteria has been attempted by a number of researchers, but considering the complex flow behavior and the interrelated parameters affecting the performance of these reactors, the quest remains elusive. Examples of past studies include Degaleesan (1997), Inga (1997), Safoniuk et al. (1999), Safoniuk (1999), Macchi et al. (2001) and Macchi (2002), Forret et al. (2006), and most recently, Shaikh (2007).

Although Nottenkämper et al. (1983) and others assert that the overall gas holdup is not function of a column's diameter (in columns of more than 15 cm diameter) for superficial gas velocities up to 20 cm/s, Degaleesan (1997) reports that gas holdup is scale dependent in the churn turbulent flow regime. Her developed scale-up methodology starts by deriving an empirical correlation for the overall gas holdup, using data from earlier studies. The scaling is based on obtaining the average recirculation velocity (knowing the axial liquid velocity radial profile) and the turbulent eddy diffusivities in a laboratory scale column and air-water system. Finally, by predicting (or measuring) the overall gas holdup in an industrial unit, an extrapolation of the simple air-water system to the specific conditions of interest is made, following the scheme shown in Figure 2.10.

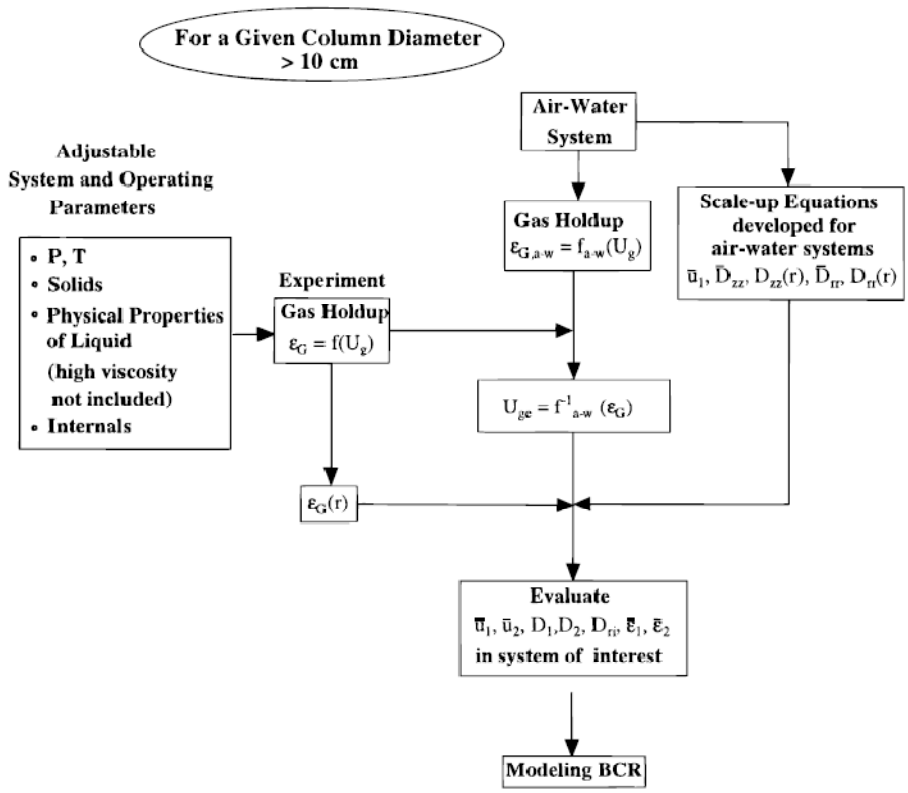

Fig. 2.10 – Scheme of characterization/scaling of churn turbulent bubble columns (Degaleesan, 1997)

Inga (1997) proposed a methodology for scaling up/down of slurry reactors. He claimed similarity between a 4 liter stirred tank reactor and a 0.3 m diameter slurry bubble column, based on maintaining constant gas/liquid mass transfer and reaction rates. He claimed a

balance between the supply and consumption of reactants in both reactors. The question remains whether the mass transfer coefficient alone can also account for the changes in the hydrodynamics and capture the variations in the transport phenomena of the fluid phases.

In the group of Prof. Grace at the University of British Columbia (UBC), Safoniuk (1999) utilized the pi Buckingham method with five dimensionless groups to dynamically match a 0.91 m diameter cold flow 3 phase fluidized bed of Syncrude Canada with a laboratory unit of 0.083 m diameter. Geometric similarity could not be achieved due to the different designs, and the predictive correlations were always limited to the range of conditions of that specific set of experiments. The bed expansion conditions could only be matched qualitatively, as the gas density was not taken into consideration within the matching. This is considered a shortcoming, given its significance when operating at high pressures. To assess the validation, further experimentation with variations in some of the identified dimensionless numbers was recommended.

Following in Safoniuk's footsteps, Macchi et al. (2001) tried to achieve dynamic similarity between two laboratory systems with different liquid and solids contents. Again, no match was achieved for bed expansion and gas holdup. As a result, the authors acknowledged the fact that more than five dimensionless numbers are required for dynamic similarity. Macchi (2002) proposed the utilization of the gas density to liquid density ratio to account for the pressure effect.

Forret et al. (2006) worked out a scale-up methodology based on phenomenological models that require the knowledge of overall gas holdup, center-line liquid velocity, and axial dispersion coefficient in columns up to 1 m diameter. They reconfirmed that the overall gas holdup is independent of the column's diameter for columns larger than 15 cm in diameter (Figure 2.11). They obtained the liquid phase velocity profile using a) an empirical correlation for the center-line liquid velocity as a function of gas velocity and column diameter, and b) the simplified one-dimensional two-fluid model accompanied by an adjustment of the turbulent viscosity as a function of column diameter and gas velocity.

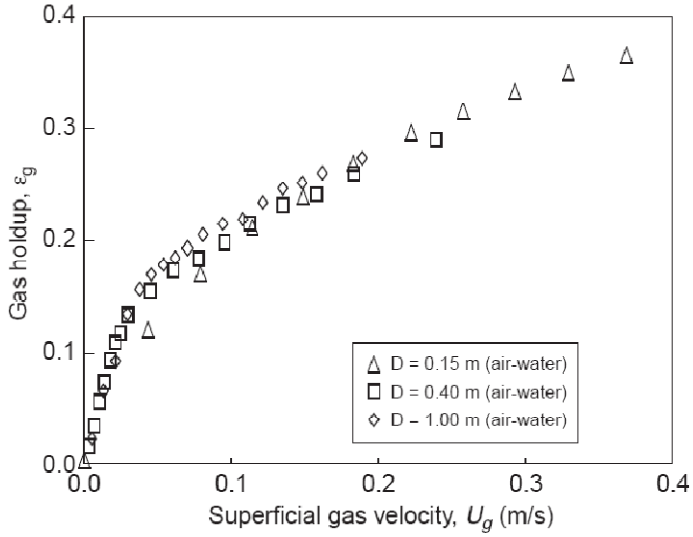

Fig. 2.11 – Overall gas holdup as a function of superficial gas velocity in different columns' scales (Forret et al., 2006).

Finally, a two-dimensional (2D) model was developed for the estimation of the dispersion coefficient in large columns, taking into account both the axial dispersion and the radial dispersion. It is noteworthy that their study also included some data in columns equipped with internals.

Shaikh (2007) proposed a dynamic similarity methodology which was validated in one size column at different conditions. The methodology needs to be evaluated for at least two different scales and with internals in order to qualify as a scaling method.

The above studies have one or more of the following drawbacks: (1) they examined only global parameters (overall gas holdup, mass transfer coefficient, etc.); (2) they are applicable only for the bubbly flow regime; (3) they do not account for the presence of internals; (4) they are based on dynamic similarity but with no actual scaling validation; (5) they are missing experimental validation in large scale units for CFD simulations studies.

Hence, there is no doubt that scale up bubble column reactors to an optimum design of industrial is a challenging task.

2.4 – Liquid Mixing

Liquid mixing in bubble columns has been extensively reviewed by many authors (e.g., Ong, 2003, and Rados, 2003). In addition, Han (2007) provided a tabulated summary of all experimental studies on liquid phase mixing. Moreover, Alvaré (2002) reviewed the associated models, their limitations, and applicability. However, most of the studies were performed in columns without internals. Very few studies were carried out in columns involving horizontal internals (multistage bubble columns), and even fewer included vertical internals.

In order to avoid redundancy, only the studies where columns were equipped with internals are tabulated (Tables 2.3 and 2.4). For details, the reader is referred to the published review paper (Youssef et al. (2010)).

Table 2.3 - Summary of liquid mixing studies in columns with horizontal internals

Research	System	Column and sparger features	Internals	Study
Sekizawa and Kubota (1974)	Gas phase: Air Liquid phase: ion-exchanged water, Glycerine aqueous solution (4 different properties variations), and 0.9 wt. % iso-amylalcohol aq. solution	5 cm diameter (100 cm height)/perforated plate distributor	Perforated plates: 10 and 20 cm spacing, 0.5 cm hole diameter, and plate thickness, with 0.07 free area fraction of the plate	Liquid mixing and backflow
		10 cm diameter (100 and 120 cm height)/perforated plate distributor	10, 20, and 40 cm spacing, 0.2, 0.3, 0.5, 1, 1.5, and 2 cm hole diameters; 0.3 cm 0.5, and 1 cm plate thickness; and 0.07 to 0.202 free area fraction of the plate	
		20 cm diameter (100 cm height)/perforated plate distributor	20 cm of plate spacing, 0.5 cm hole diameter and plate thickness, with 0.0775 to 0.202 free area fraction of the plate.	
Palaskar et. al. (2000)	Air-water	Acrylic: 6.2 cm diameter-77 cm height, and 20 cm diameter-90 cm height/	Acrylic perforated sieve plates with percentage free areas of 0.5%, 1.48%, 10.8%, and 100%	Liquid phase mixing
Dreher and Krishna (2001)	Air-water	Polyacrylic: 10, 15, 38 cm diameter – 6, 4, 4 m height/Brass perforated plate with 0.5 mm diameter holes and triangular pitch of 7 mm	Two perforated brass plates of 1 mm thickness and 10 mm diameter holes. Open areas of 18.6 and 30.7%	Liquid phase back mixing

Doshi and Pandit (2005)	Air-water	0.41 m diameter – 2.87 m height/spargers with 0.136% (25 holes of 3 mm diameter each) and 0.6% (251 holes of 2 mm diameter each) free area	3 or 4 sectionalizing plates with 61, 269, 537, 604, 607, or 617 holes of 10, 5, 5, 8, 6, and 7 mm diameters respectively. The % free area ranged between 4-23%.	Mixing behavior characteristics
Alvaré and Al-Dahhan (2006)	Air-water	19 cm diameter – 241 cm height/9.5 mm diameter single point nozzle	4 trays of three different configurations: a) 12 holes, 1.74 cm hole diameter, 10.2% open area; b) 52 holes, 0.6 cm hole diameter, 5.2% open area; and c) 105 holes, 0.6 cm hole diameter, 10.2% open area	Liquid phase mixing
Mecaial and Sadik (2007)	Air-water and air-NaCl solution	PVC: 10 cm diameter-207cm height/single point nozzle (10 mm diameter) and perforated plate (55 holes of 1 mm diameter each, giving 0.6% open area)	Two trays with five different configurations each (see Figure 21 for details)	Hydrodynamics and liquid mixing

Table 2.4 - Summary of liquid mixing studies in columns with vertical internals

Research	**System**	**Column and sparger features**	**Internals**	**Study**
Kölbel and Ralek, 1980	Syngas-catalyst slurry	Not Specified	Vertical honeycombed shafts with cooling pipes arranged centrally around or in corners	Liquid backmixing and catalyst efficiency
Forret et al., 2003	Air-water	1 m diameter/perforated plate: 312 holes of 2mm diameter and 50 mm pitch	56 tubes of 63 mm diameter each and a 10.8 cm square pitch	Liquid mixing-axial dispersion coefficient

Chapter 3

Bubble Dynamics in 8" Bubble Column with Vertical Internals

3.1 – Scope

Research on bubble columns has investigated their hydrodynamics, heat and mass transfer, liquid and gas phase mixing, and liquid entrainment. However, as highlighted in Chapter 2, most of the earlier studies have been performed in columns without heat exchanging internals. Because industrial applications of bubble and slurry bubble columns involve exothermic reactions (Table 2.1) and require heat transfer internals, bridging this gap in our knowledge is the focus of the current work. To begin, bubble dynamics are investigated in this Chapter.

As described below, a four point optical probe is utilized as the measuring device for the bubble dynamics and the local gas holdup. The overall gas holdup is also estimated from the bed expansion method. Since no study was reported for bubble dynamics in columns with internals, the current study has been the first to generate a database for future CFD modeling and scale-up studies of systems with internals. One of the distinct features of this work is that columns of different scales were utilized to assess the effect of column diameter with the presence of internals. Moreover, the investigations were focused on the operating conditions of interest for industrial applications. For example, high superficial gas velocities were applied to spotlight the impact of internals in the churn turbulent flow regime. Various configurations of internals bundles were investigated, although those typically needed for the Fischer-Tropsch (FT) conversion and the Liquid Phase Methanol (LPMeOH) Synthesis were placed at the center of attention, as discussed below. The insight gained from the bubble dynamics study, followed by that from the liquid mixing study (Chapter 5) underlines the development of the scale-up methodology presented in Chapter 6.

3.2 – Measurement Technique

The four-point optical probe was first developed by Frijlink (1987) at the Department for Multiscale Physics at the Technical University of Delft, and then was refined by Xue (2004), Xue et al. (2003), and Xue et al. (2008) in the Chemical Reaction Engineering Laboratory (CREL) at WUSTL, who developed and validated a new data processing algorithm in columns without internals.

The four-point optical probe is an excellent tool to use in systems including internals, for the following reasons:

- It can provide insight into the bubble characteristics (local gas holdup, bubble chord length, specific interfacial area, bubble velocity, and other properties) along the axial cooling tubes frequently used in industrial applications.
- It can provide local information on the effect of tube bundle design on bubble properties.
- It can generate a database for columns with internals in order to compare the validity of earlier developed correlations and results in empty columns

The probe has the following specifications (Figure 3.1):

- Three peripheral tips form an equilateral triangle.
- The fourth tip, around 2 mm longer, is situated at the center of the triangle.
- The overall probe diameter is 1.2 mm.
- All four fibers are glued together and inserted in a 3 mm (1/8") diameter stainless steel tube.
- A laser beam is sent into the optical fibers from a Light Emitting Diode (LED).

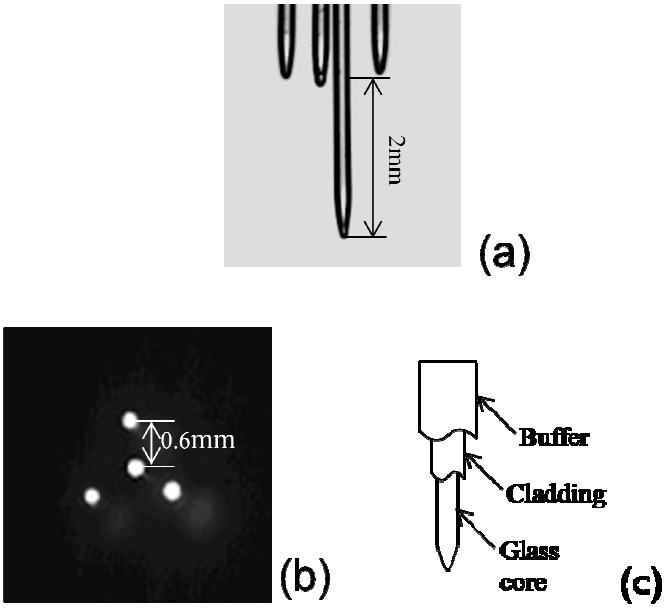

Fig. 3.1 - Configuration of the four-point optical probe (not to scale) (a) picture of the probe, (b) side view of probe tip, (c) bottom view of probe tip

When the tips are immersed in the liquid or in the bubbles, reflected light signals are collected by a data acquisition board and transformed into voltage (Figure 3.2). The signal processing, using the modified algorithm developed by Xue (2004) and Xue et al. (2003), directly results in the following parameters: local gas holdup, gas-liquid interfacial area, bubble frequency, bubble chord length, and bubble velocity. More details about the probe, the associated algorithm, and further applications can be found elsewhere (Xue, 2004, Xue et al. 2008, and Wu, 2007).

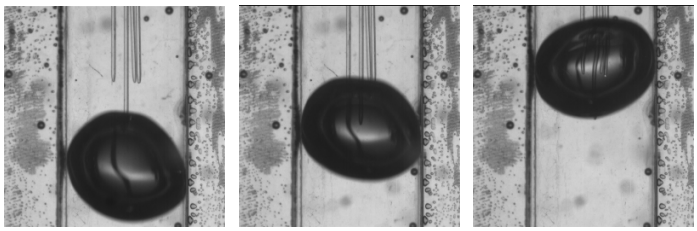

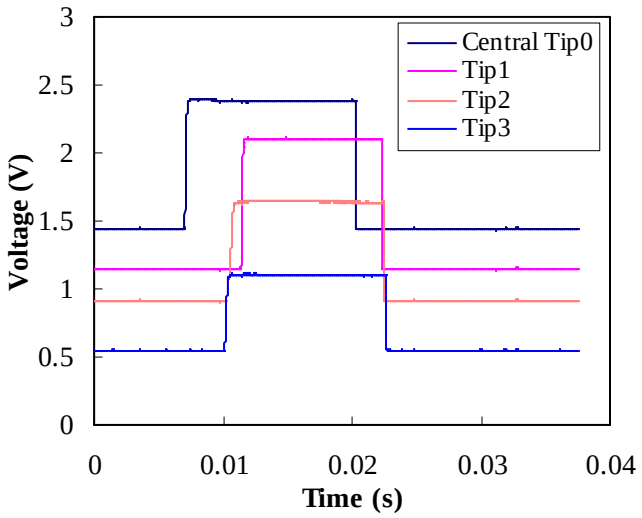

Fig. 3.2 - Response of a bubble passing by the four-point optical probe

3.3 – Selection of Heat Exchanger Bundle Configuration

Nishikawa et al. (1977) showed that internal cooling media is favored over an outside jacket even for small diameter columns (5 cm to 15 cm diameter). Moreover, Schlüter et al. (1995) specify that longitudinal (vertical) heat transfer internals are most suitable for producing high-pressure steam with highly exothermic reactions. No guidelines are reported in the open literature to assist in the design of the tube bundle. Therefore, one of the main objectives of this work is to provide a hypothetical picture of the structure of the heat exchanger in bubble columns for both the Fischer-Tropsch and the LPMeOH syntheses.

As pointed out in Chapter 1, the Fischer-Tropsch reaction has been known since German scientists first obtained a large amount of oxygenated products via the hydrogenation of carbon monoxide in the presence of alkalized iron as catalyst (Wender, 1996). In the same year, 1923, the same researchers used nickel and cobalt used to obtain higher hydrocarbons. Nowadays, the catalysts used are the same; however, the scale of the operation is much larger, with Sasol and Shell leading among commercial technologies. Kölbel and Ralek (1980) state that, two main technical challenges of the FT process are rapidly removing the heat of reaction and avoiding local overheating of the catalyst. Due to the exothermicity of the reaction (heat of reaction= -170 to -210 kj/mol) the use of an internal heat exchanging bundle is inevitable. In order to approach an optimal design for the internals, some basic calculations and considerations are shown below:

Assume an industrial reactor of 7m diameter and 30m in height, used for the catalytic hydrogenation of carbon monoxide to produce liquid fuels. The reactor temperature and pressure are 240°C and 30 bar, respectively. The syngas is flowing at a superficial gas velocity of 35cm/s and enters the reactor in a H_2:CO ratio of 2:1.

From the above example, the total volumetric flow rate to the column is:

$$\dot{V} = 0.35 \times \frac{\pi \times 7^2}{4} = 13.46\, m^3/s$$

In molar units and assuming ideal gas behavior:

$$P\dot{V} = nRT,$$

where $n = \frac{30 \times 13.46}{8.314 \times 10^{-5} \times (240+273)} = 9467 mol/s$

Hence, 1/3 of this total amount is CO reactant, or moles (CO)=3156mol/s.

The heat of reaction for the primary FT chemical reaction is -170kj/mol CO.

Therefore, the total heat generated from the reactor (Q) is 536,496kj/s.

Now, Q=U.A.ΔT.

Assuming an overall heat transfer coefficient of U=0.4 kcal/m^2.s.K or 1.674 kj/m^2.s.K, with a temperature difference between the coolant and the reactor conditions of 10° (i.e., the coolant enters the heat exchanger at 230°C), we can calculate A (the total surface area of the tube bundle) as follows:

$$A = \frac{536{,}496}{1.674 \times 10} = 32347m^2$$

But $A=N_{tubes} * 2\pi r_{tube} * h_{tube/reactor}$.

Assume that each tube has a diameter of 4 cm (following Casanave et al., 1999). The total number of tubes in the reactor is then: (N)=8585 tubes.

The percentage of the cross sectional area (CSA) covered with internals can be calculated as follows:

$$\% = \frac{N \times \pi (0.04)^2/4}{\pi \times 7^2/4} \times 100 = 28\%$$

The above is in line with a FT process patented by Maretto and Piccolo (1998) who reported, in a reactor of the same dimensions and assuming the same heat exchange tube diameter, a specific exchange surface area per unit volume of the reactor of 30.5 m^2/m^3, which results in a similar value of the CSA percentage occupied by internals.

In order to mimic the tube bundle used in a FT reactor and lack in information on the design, the CSA percentage is matched for the columns used in this work. In addition the TEMA (Tubular Exchanger Manufacturer Association) standards for the tube pitch are well maintained in the bundles, as will be further discussed in Chapter 4.

The Liquid Phase Methanol Synthesis (LPMeOH)

Methanol, one of the main chemicals in today's world, is involved in the production of a wide variety of chemicals and fuels. Recent developments by Air Products and Chemicals in the production process of methanol included the utilization of a slurry bubble column reactor for the conversion of syngas in order to reduce the capital costs and pressure drop, to minimize catalyst deactivation, and to allow better control of the reactor's temperature (Brown et al., 1991 and Wender, 1996). A major difference with respect to the FT reaction is

that copper based catalysts are preferred for methanol synthesis. The primary chemical reaction for methanol production is:

$$CO + 2H_2 \rightarrow CH_3OH$$

The heat of reaction is -91 kj/mol. Typically, the reactor's temperature and pressure range from 220-270°C and 50-100 bar, respectively. For a H_2/CO ratio=0.69, an overall heat transfer coefficient U=0.63 kcal/m^2.s.K (Lee, 1990), and a superficial gas velocity of 15 cm/s, similar calculations to the FT case can be made for the LPMeOH synthesis. The resulting percent covered cross sectional area is CSA=7.9%.

The current study used a bundle of heat exchanger tubes copied from the Alternative Fuels Development Unit (AFDU) in LaPorte, Texas (Kumar et al., 1998), as will be described below.

3.4 – Impact of Internals on Gas Holdup and Bubble Properties in an 8" Bubble Column

3.4.1 – Experimental setup

The experiments were carried out in a Plexiglas column of 8 inch (19 cm) diameter with a height of 2 m, as shown in Figure 3.3. As the gas phase, compressed air, was introduced from the bottom of the column, while tap water was used as the liquid phase.

In all experiments, the dynamic height of the bed was maintained constant at a level of 160 cm above the gas distributor. The gas distributor had 225 holes of 1.32 mm diameter, arranged in a triangular pitch, with a total free area of 1.09% and yielding an intermediate flow condition (dimensionless capacitance number characterizing the bubble formation ($N_c=4V_{ch}g\varrho_l/\pi d_o^2 p_h=1.57$), since a capacitance less than 1 yields constant flow and that higher than 9 yields constant pressure (Ong, 2003).

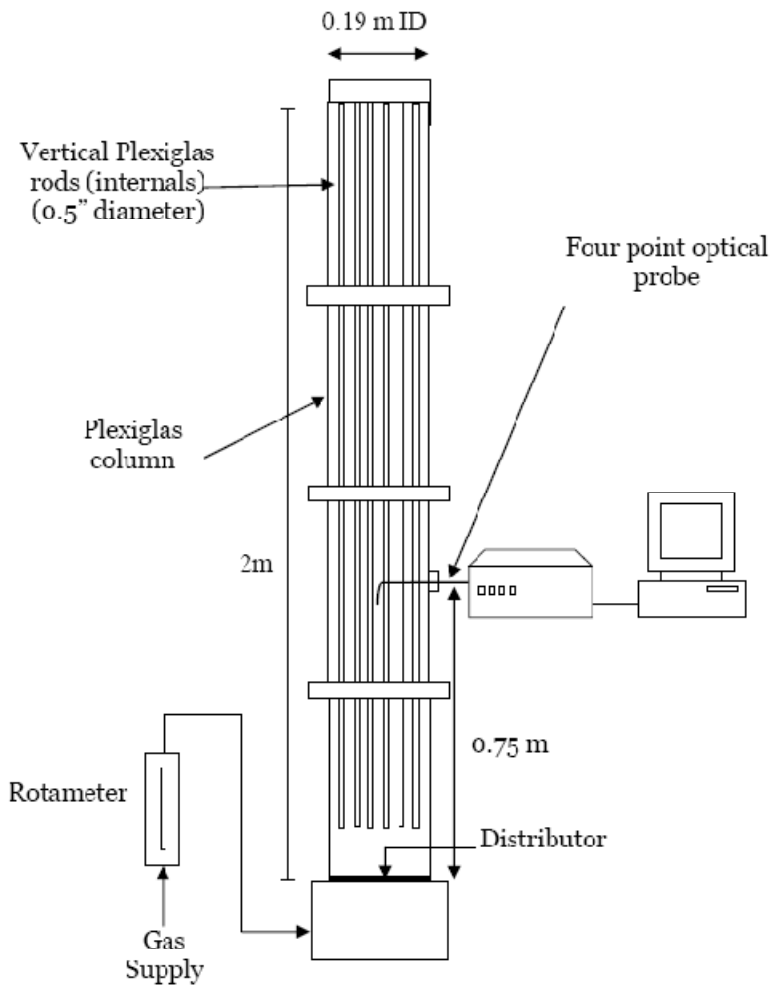

Fig. 3.3 - Schematic diagram of the bubble column setup

The experiments were carried out over a range of superficial gas velocities from 3 to 20 cm/s and at three percentages of covered cross-sectional area: 0 (no internals), 5% (typical for methanol synthesis), and 22% (typical for FT synthesis).

Local probe measurements were taken at seven dimensionless radial positions: ±0.9, ±0.65, ±0.3, and 0 (center of the column). The ±0.65 locations were included because in the bubble column without internals they are around the inversion point between the time averaged liquid upward flow in the central region of the column and the time averaged liquid downward flow in the wall region of the column. Rados (2003) reported the value for inversion to be ±0.65-0.7, while Sannaes (1997) found it to be ±0.60-0.65 (both in 3-phase systems). From their investigations in 2-phase units of different diameters and at varying

superficial gas velocity, Degaleesan et al. (2001) assert that ~r/R=0.65 as the inversion locus is the common and distinct feature of all systems. In this study, the probe tips were pointing downwards, yielding bubble property measurements for bubbles moving upwards. In addition, the probe was rotated 180º to be facing upward to account for the bubbles moving downwards with what we refer to as negative velocity. Hence, upward and downward velocities are both reported.

The internals were vertical Plexiglas rods of 1.27 cm (0.5") outer diameter. Two different configurations of the internals geometry were investigated: 1) Two circles of six rods each covered 5% of the total cross section of the column. The two concentric circles were of 8 and 14 cm diameter, and 2) 48 rods placed in a triangular (equilateral) pitch of 2.4 cm that covered 22% of the total cross-sectional area (Figure 3.4).

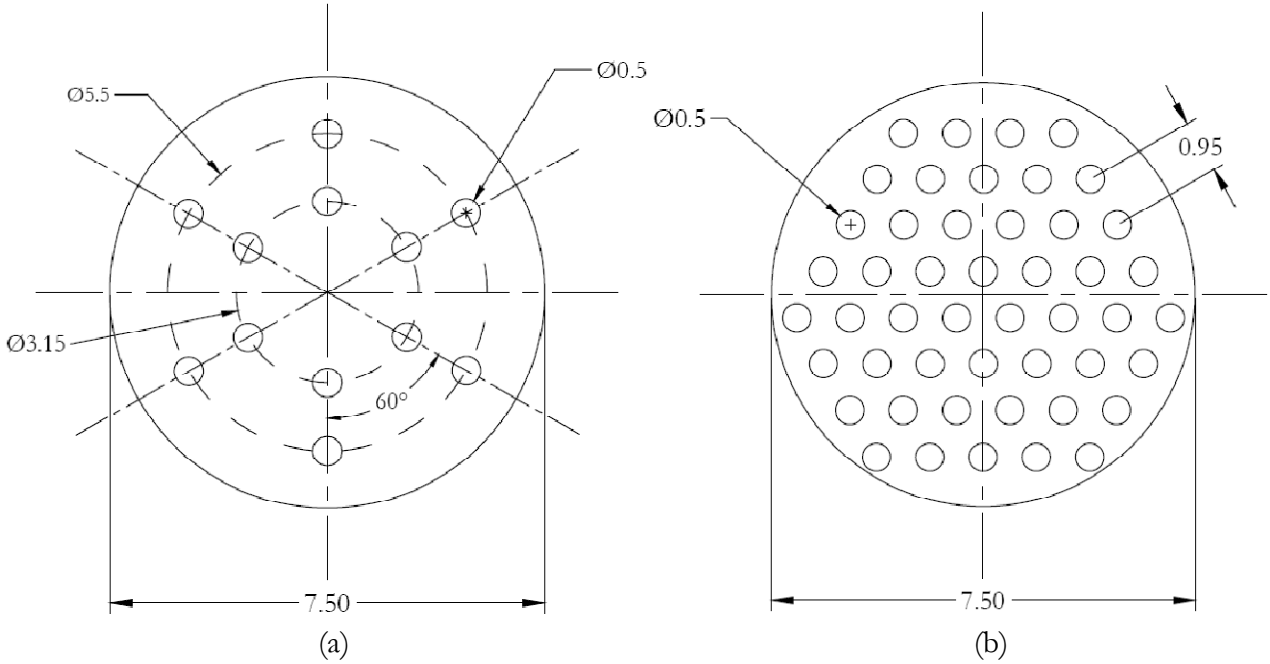

Fig. 3.4 - Internals configuration: (a) 5% covered cross-sectional area and (b) 22% covered CSA (dimensions in inches).

As discussed before (§3.3), the first step in proposing these designs relates to the heat removal requirements for each reaction. The heat exchanging tubes transport the cooling fluid longitudinally from a supply point to be discharged as steam at an exit point. Thus boiling is expected in the tubes. For internals structures of low density (such as (a)), circular bundles are chosen so that a feeding header at the reactor's bottom and a steam collecting header at the top are used for each. Rentech, Inc. has patented a similar idea (Hawthorne et al., 2006). It is believed that such a structure would ease the removal and installation for repair and maintenance. As mentioned above, a similar design was also adopted by Air Products and Chemicals in the AFDU. On the other hand, for dense internals (covering ~25% of the CSA) (such as (b)), the utilization of the above headers results in a very cumbersome design (Soraker et al., 2005). Typically, Sasol utilizes serpentine coils for the heat exchanging tubes (Espinoza et al., 1999). Hence, a triangular and a square pitch are the only options considered. A triangular pitch was selected to provide flexibility for the entry of the optical probe to the column through various ports from several angles.

3.4.2 – Results and discussion

3.4.2.1 – Overall gas holdup

The overall gas holdup was measured by the change in dynamic liquid height compared to the static liquid height:

$$\epsilon_g = \frac{H_{dyn} - H_{st}}{H_{dyn}},$$

where H_{dyn} is the dynamic height of the bed and H_{st} is the static height, reported from visual observations. For an empty column, the overall gas holdup was found to be 0.23 at a superficial gas velocity of 20 cm/s. Figure 3.5 shows the overall gas holdup as a function of superficial gas velocity with and without internals. No significant effect was observed with internals covering 5% of the total CSA (average difference 8%). For the case where internals occupied 22% of the column's cross sectional area, an average increase of 21% was obtained in the overall gas holdup. These findings are in line with Yamashita (1987) and Bernemann (1989). Two reasons lead to the above result: first, the area available for the flow decreases with internals insertion yielding a higher 'actual' or interstitial superficial gas velocity; second, the internals effect on the bubble characteristics, as will be discussed below.

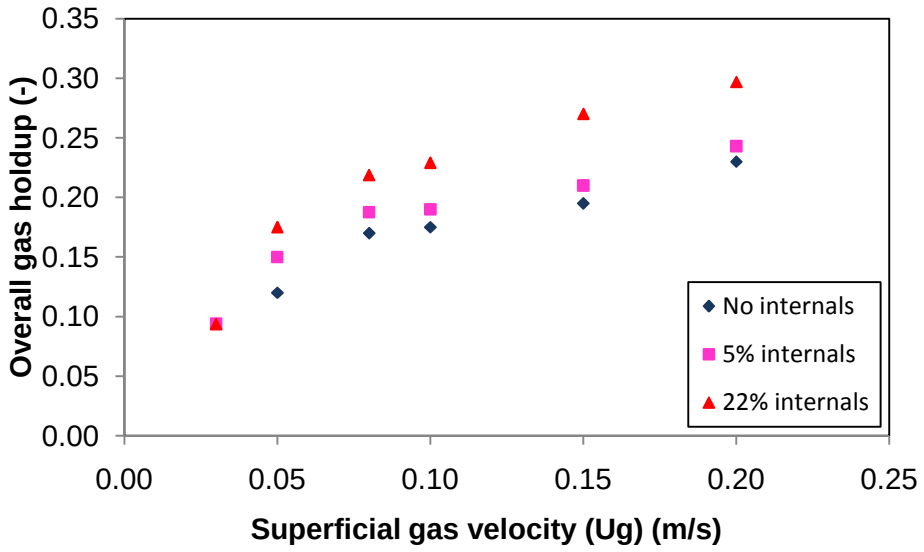

Fig. 3.5 – Effect of internals on overall gas holdup (Courtesy of Hamed and Al-Dahhan (2010) - experiments performed by Mohamed Hamed)

3.4.2.2 – Local gas holdup

As shown in Chapter 2, local gas holdup profiles are parabolic as a function of radial position in columns without internals (with the exception of very low superficial gas velocities, where an almost flat distribution prevails), (Hills, 1974). All radial holdup profiles shown in this study were measured within the fully developed region where the gas holdup is not a factor in the axial position, especially at higher gas velocities. This assumption was previously, confirmed from CT experiments (Ong et al., 2009) and from probe experiments (Xue, 2004). As a first check, these trends needed to be investigated with the presence of internals. Figure 3.6 presents the radial gas holdup profiles with internals covering 5% of the column's CSA at 3, 8, and 20 cm/s. It is obvious that these internals do not impact the shape of the radial distributions considering typical trends observed in columns without internals.

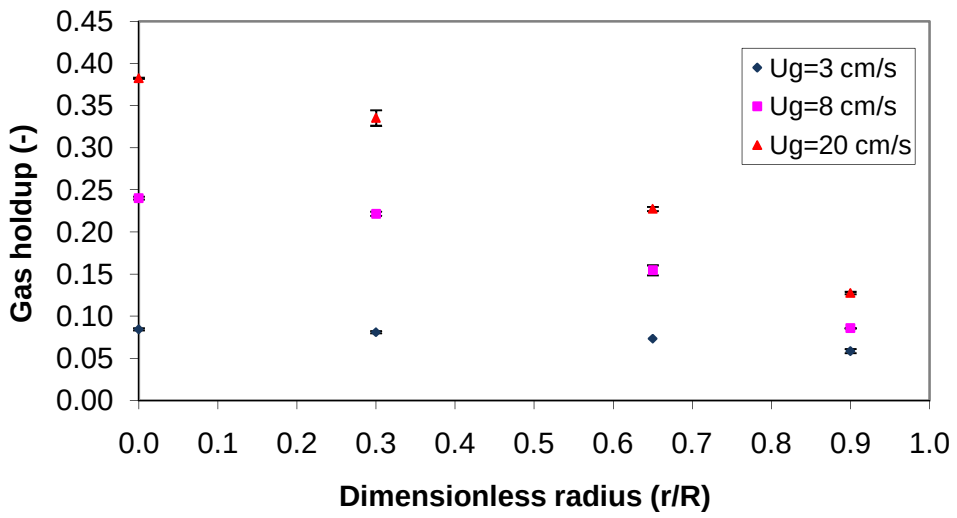

Fig. 3.6 – Radial gas holdup profiles at different superficial gas velocities (5% internals)

Similar trends were observed for 22% covered CSA. However, it is noteworthy that the full radial profile could not be obtained in the case of 22% internals at low superficial gas velocities. It is common at low velocities to have a maldistribution of the gas flow through the sparger holes, with some inactive zones, if the sparger was not designed for low velocities as in our case (Degaleesan, 1997 and Pandit and Doshi, 2005). In such cases, bubble swarms flow upwards from the various active bubbling zones on the distributor, which have been found to shift circumferentially. Earlier studies in empty columns showed that the recovery from the above mentioned maldistribution, yielding a radially well-distributed gas plume, occurred at higher axial locations or at higher gas velocities. Visual observations from the current study showed that the presence of dense vertical internal structures (22% covered cross sectional area) prevented the full development of the flow at such a low superficial gas velocity (8 cm/s and 3 cm/s). The internals trap the maldistributed gas flow and prevent the bubbles from dispersing radially as the gas flows upwards. As a consequence, at certain radial locations the optical probe did not encounter bubbles, and hence no measurement was recorded. This observation highlights the importance of sparger design for the desired range of gas velocity to ensure gas uniformity at the sparger region, especially when internals are present. In other words, use a sparger with a capacitance number (N_C) less than 1 for a constant flow of bubbles through the holes. Another solution is to extend the column to have a larger L/D ratio (which was not feasible here).

Figure 3.7 shows the effect of internals on the gas holdup radial profile for the studied air-water system at a superficial gas velocity of 20 cm/s, calculated based on the empty column's cross-sectional area. Similar to trends seen with the overall gas holdup, an increase in the local values of gas holdup occurred when 5% of the column's cross sectional area was covered. Chen et al. (1999) reached analogous conclusions using CT in an 18" column. However, when the internals covered 22% of the cross-sectional area, a significant increase in the gas holdup was observed. Statistically, a 2^3 factorial design shows that internals covering 5% (and by default 22% as well) of the CSA have a significant effect on the gas holdup, based on a 95% confidence interval. For example, at r/R=0, the gas holdup increased from 0.34 to 0.43, an increase of ~26% that can be explained as follows. In columns without internals, it is natural to find large bubbles due to coalescence at the column's core region, while the physical presence of internals impedes such bubble coalescence and rather enhances the break-up rate of the bubbles. The bubbles are forced to a maximum size dictated by the tube pitch. Bubbles of small size rise with lower velocities that extend the residence time of the gas phase in the system, hence, they elevate the gas holdup. These phenomena will be further discussed below.

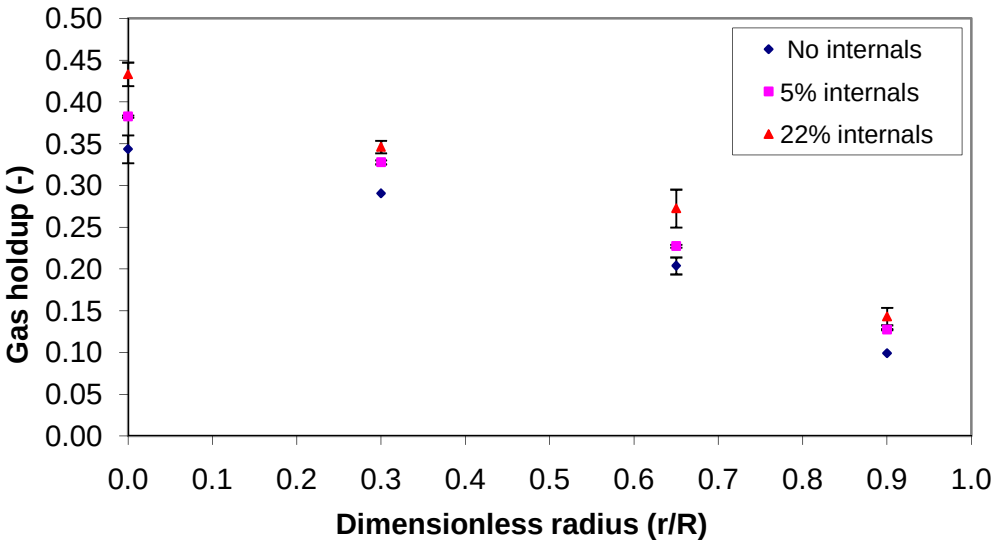

Fig. 3.7 – Effect of internals on local gas holdup at Ug=20cm/s

3.4.2.3 – Specific interfacial area

Xue (2004) and Wu (2007) showed that the specific interfacial area increases with an increase in the superficial gas velocity. Figure 3.8 shows that this finding holds with the presence of internals (5% internals shown). Note that the case of no internals is also provided for reference.

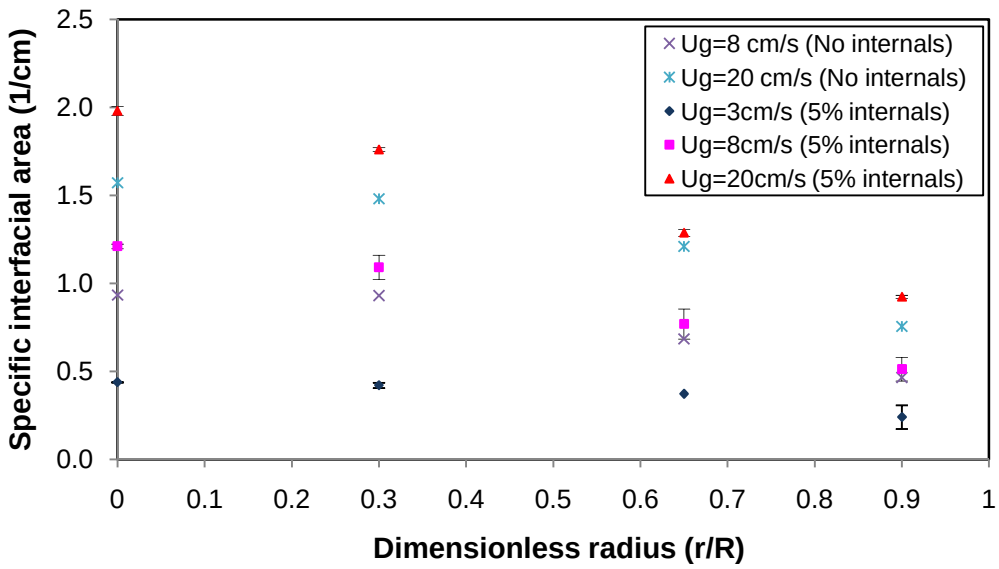

Fig. 3.8 – Effect of superficial gas velocity on interfacial area with 5% internals

Figure 3.9 shows how the radial profile of the interfacial area was affected by the presence of internals at a superficial gas velocity of 20 cm/s. As shown in Figure 3.8, trends similar to those illustrated in this figure were also found at superficial gas velocities lower than 20 cm/s.

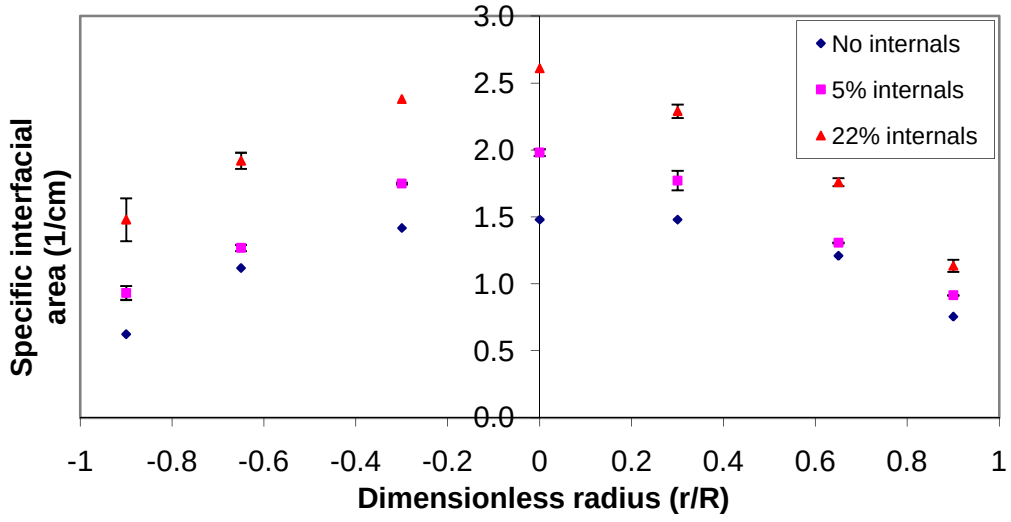

Fig. 3.9 – Effect of internals on specific interfacial area at Ug=20cm/s

Figure 3.10 illustrates the effect of the less dense internals structure (5% internals) on the specific interfacial area at a superficial gas velocity of 8 cm/s. It is clear that there is an increase in the specific interfacial area upon insertion of the internals. There is also a qualitative and quantitative agreement between the current data and that generated by Wu (2007), taking into consideration the differences between the setups used in both studies.

From Figure 3.9, one can see that the more internals cover the column's cross sectional area, the more interfacial area is generated. Furthermore, the increases in bubble frequency and interfacial area are due to rapid bubble breakup and coalescence, as will be explained later.

It was found that a larger interfacial area existed at the column's center than in the region near the wall, which is similar to the findings of Xue (2004) and Xue et al. (2008). This difference is due to enhanced rates of breakup and coalescence among bubbles in the central region of the column in the churn turbulent flow regime, which was confirmed by the bubble frequency measured by the probe. An increase in bubble frequency leads to an increase in specific interfacial area. The same trend was observed and explained by Wu (2007) for the case of empty bubble columns. At low velocity, small bubbles uniformly distribute across the column in low numbers, which causes low local gas holdup both in the center and wall region of the column. With an increase in superficial gas velocity, bubbles, including the newly coalesced large bubbles from coalescence that move towards the center

of the column, move in greater numbers, causing an increase in gas holdup. Most small bubbles still stay in the wall region and move across the probe at a relatively low frequency. Hence, the gas holdup, the specific interfacial area, and the bubble frequency in the center all become larger than those in the wall region (see Figure 3.11).

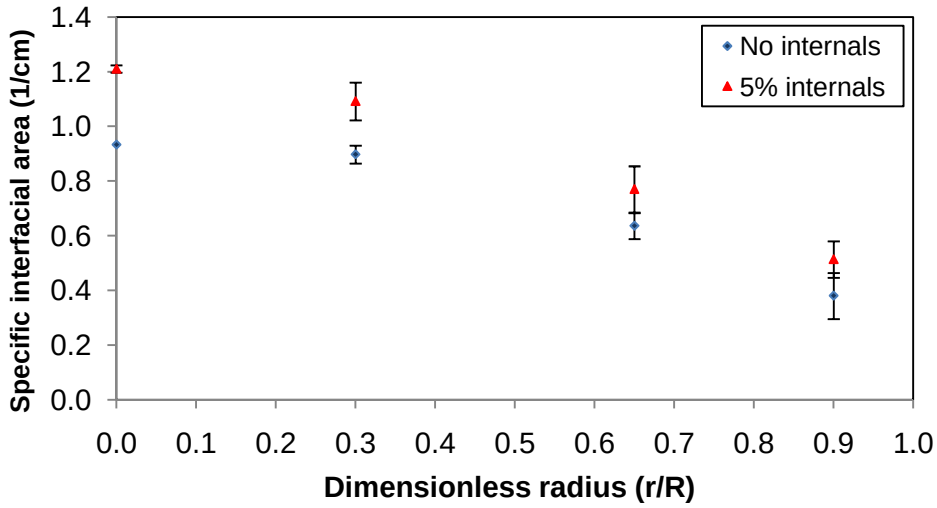

Fig. 3.10 - Effect of internals on interfacial area radial profile (Ug= 8 cm/s).

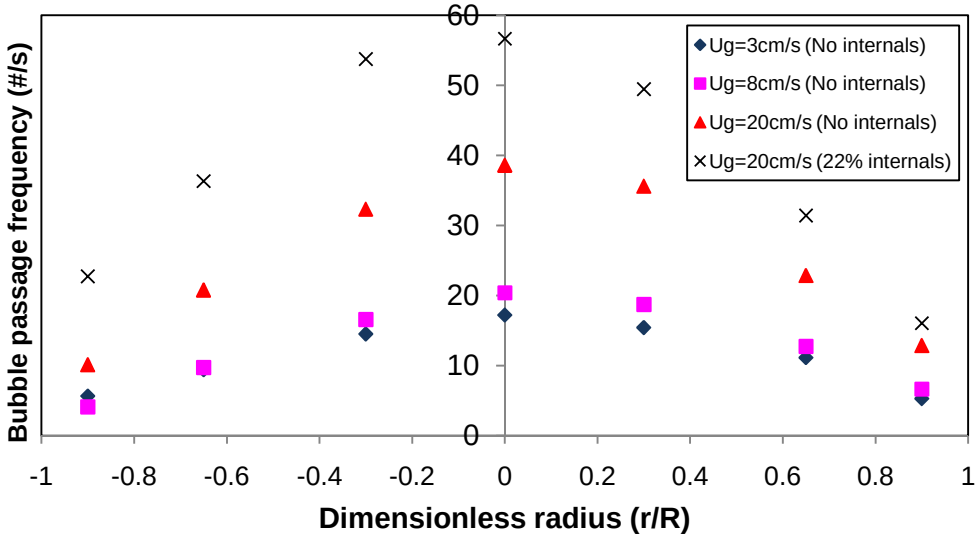

Fig. 3.11 – Bubble passage frequency as a function of radial position at various conditions

3.4.2.4 – Bubble chord length

As shown in Figure 3.12, the bubble chord length distribution consistently follows a lognormal distribution. The results clearly show a decrease in the bubble chord length as the

internals density increases, which confirms the findings of increased specific interfacial area and local gas holdup with internals.

The bubble chord length distributions have been analyzed statistically by providing the mean and the variance, as shown in Table 3.1. The variance of the distribution is defined as

$var(x) = \frac{1}{n-1}\sum_{i=1}^{n}(x_i - \bar{x})^2$, where n is the number of data points and $\bar{x}$ is the mean.

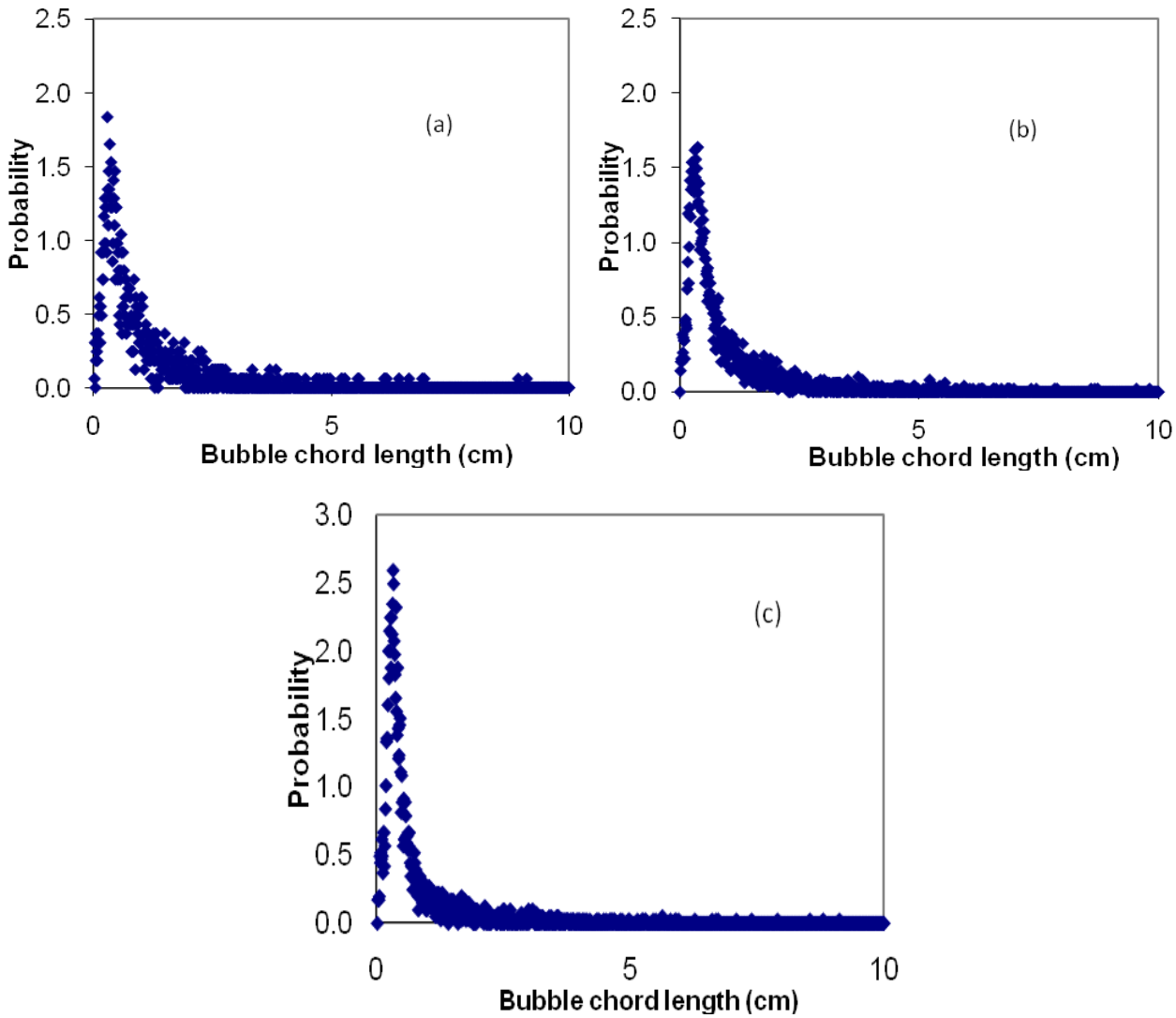

Fig. 3.12 - Bubble chord length distribution at the column's center at Ug=20 cm/s and different percentages of internals: (a) no internals, (b) 5% internals, and (c) 22% internals.

Table 3.1 - Statistical measures of the chord length distribution for different internals arrangements at Ug=20 cm/s

Internals	Mean (cm)	Variance (cm^2)
No	0.91	0.94
5%	0.87	0.96
22%	0.68	0.67

The chord length distribution with 22% internals exhibits a mean value of 0.68 cm, compared to 0.88 cm and 0.91 cm for the cases of 5% internals and an empty column, respectively. This finding suggests that the bubble size gets smaller when high density internals are used. Moreover, the mean chord lengths for the 5% internals and empty column cases are close to each other, implying that the effect of low density internals is nearly negligible. It is noteworthy that the variance was lower for the 22% internals case than for the empty column and 5% internals cases, revealing that a narrower range of bubble chord lengths exists with the dense internals configuration. Also, Figure 3.12 shows larger chord length bubbles in the cases of the empty column and 5% internals.

The observed fact that internals density directly impacts the hydrodynamics is supported by the results presented earlier, showing that smaller bubbles are generated in the 22% internals system due to enhanced bubble breakup. In summary, it has been experimentally as well as statistically proven that high density internals substantially affect the bubble characteristics.

3.4.2.5 – Bubble velocity

Figure 3.13 shows the mean upward bubble rise velocity probability distribution (the probability is defined here as # bubbles with a specific velocity/ total # bubbles) at a superficial gas velocity of 20 cm/s, in the column's center, and with different percentages of the cross sectional area of the column covered with internals. In this case, the probe was pointing downwards, so that only bubbles moving upwards (given positive velocities) were measured. The mean value of the upward bubble rise velocity with 22% internals is 77 cm/s, which is lower than those for the cases of an empty column and 5% internals (86 cm/s and 91 cm/s, respectively).

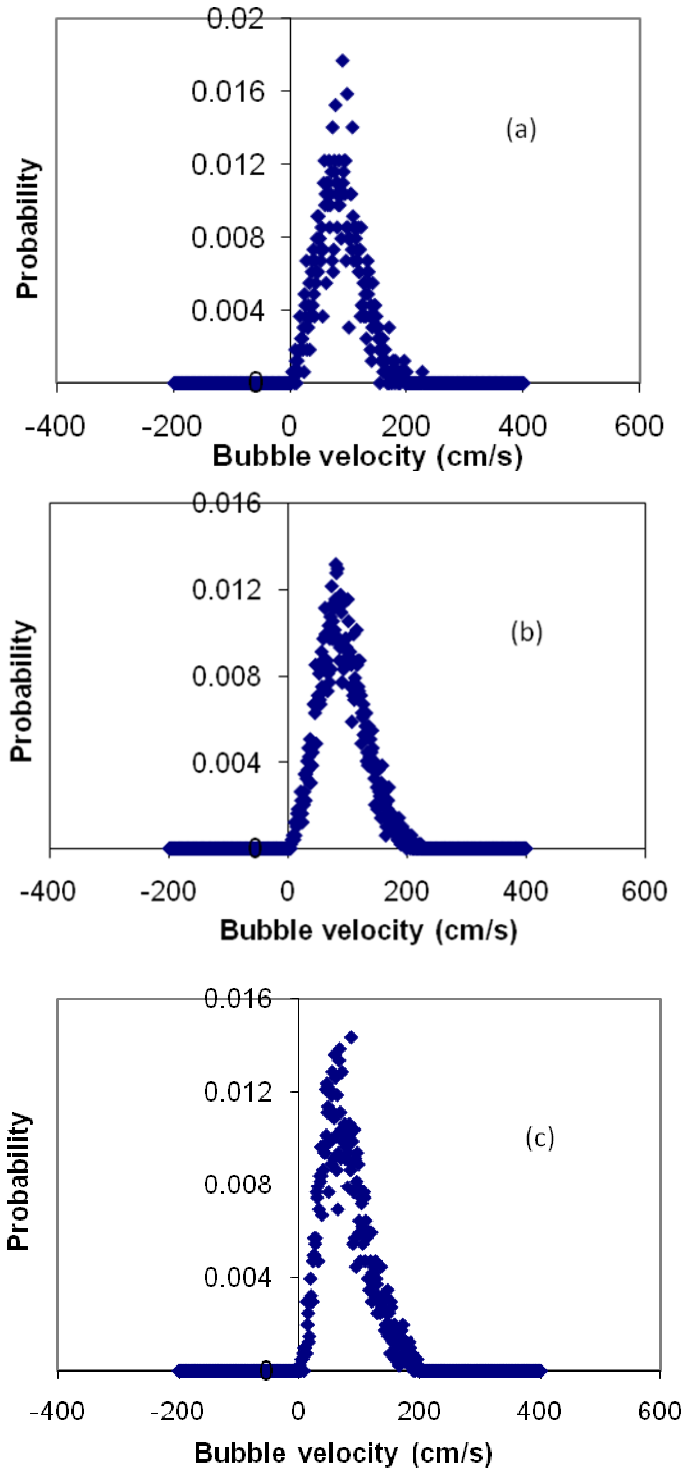

Fig. 3.13 - Bubble velocity distribution at the column's center at Ug= 20 cm/s and different percentages of internals: (a) no internals, (b) 5% internals, and (c) 22% internals.

One explanation for the slightly higher upward velocity with 5% internals than in the empty column might be as follows. As was detected by the probe, the 5% internals geometry arrangement tends to stabilize large bubbles inside the inner circular tube bundle. On the other hand, the dense internals led to a smaller bubble size, for which not only the viscous forces and surface tension forces were more pronounced but also the spectrum of eddies having sufficient energy to break or carry these bubbles changed dramatically, resulting in a lower upward bubble velocity and a longer residence time, an effect similar to that due to increased pressure (Yang et al., 2007). The variance is lower for the upward bubble velocity distribution of 22% internals, as seen in Figure 3.13.

Figure 3.14 shows the upward bubble velocity distribution at the column's center for 5% internals at a superficial gas velocity of 3 cm/s. Comparing the results of Figure 3.14 to the velocity distribution in Figure 3.13(b), it is clear that as the superficial gas velocity decreases, the velocity distribution gets narrower, with a higher fraction of bubbles at lower upward velocities. This is confirmed by the variance, which decreases by ~62% to a value of 2026 $(cm/s)^2$ for Ug=3 cm/s, compared to 5288 at 20 cm/s. The same comparison shows that the mean upward bubble velocity decreases to a value of 57.5 cm/s as the superficial gas velocity decreases to 3 cm/s, as compared to 91 cm/s at Ug= 20 cm/s. These values are summarized in Table 3.2.

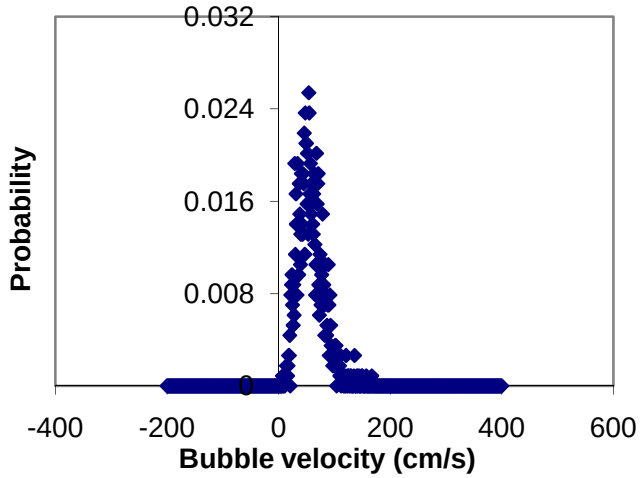

Fig. 3.14 - Bubble upward velocity distribution at the column's center at Ug=3 cm/s and 5% internals

Table 3.2 - Statistical measures of the upward velocity at 5% internals for different superficial gas velocities

Superficial gas velocity	Mean (cm/s)	Variance $(cm/s)^2$
3 cm/s	57.5	2026
20 cm/s	91	5288

Note that the later mean values for the bubble velocity and bubble chord length result in Re~7900, Eo~10, and Mo~2.6 x 10^{-11}.

To account for the downward bubble velocity, a separate measurement was conducted where the probe was oriented with the tips pointing upwards at the same point where it had previously been oriented downwards. The downward and upward bubble velocity distributions with and without 22% internals at the column's center and the wall region for 20 cm/s gas velocity are shown in Figure 3.15. In the cases of with and without internals, at the column center it is clear that small bubbles that were dragged downward with the liquid phase resulted in a downward velocity distribution (represented in terms of negative velocity). The latter observation becomes of greater significance with the presence of internals.

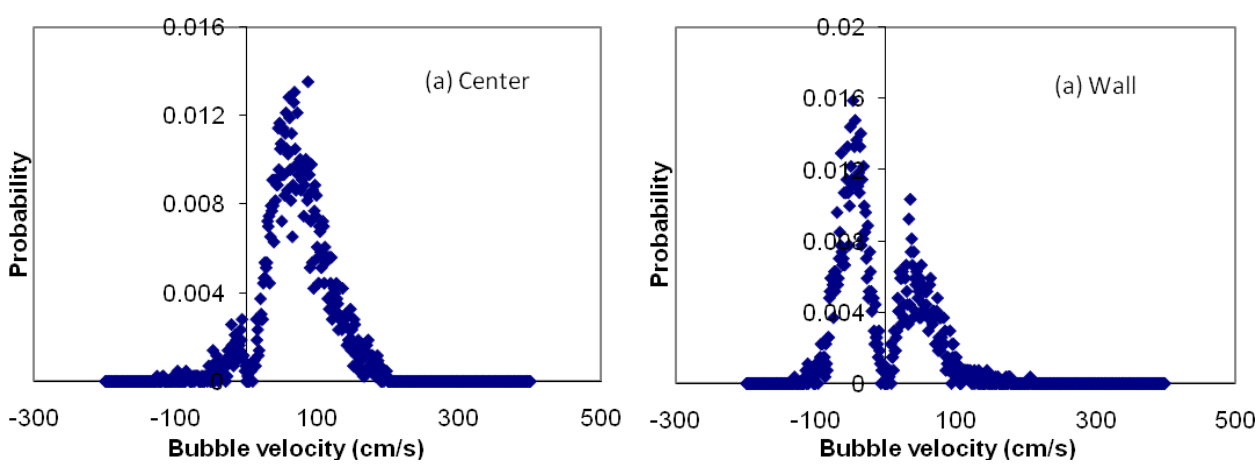

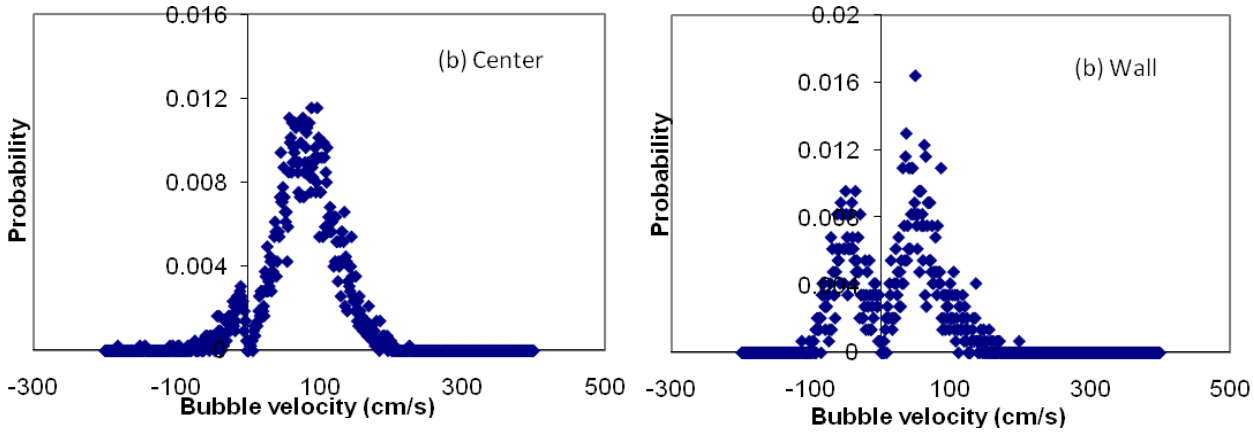

Fig. 3.15 - Bubble velocity distribution at 20 cm/s in the wall region and the column's center with different percentage of internals; (a) 22% internals, (b) no internals

Furthermore, the figure qualitatively indicates a slightly larger fraction of bubbles moving downwards without internals which indicates that less gas recirculation occurs with the dense internals structure. However, at r/R=0.9 (the wall region), a greater fraction of bubbles moving downwards ("negative" velocity) was observed, which was due to the overall flow pattern of the bubble column, where the liquid moves downward in the wall region, dragging along the small bubbles. Figures 3.15 (a) and (b) show that the downward bubble velocity without internals has a wider range of negative velocities than that with 22% internals. In addition, a greater fraction of smaller bubbles with downward bubble velocity was obtained with 22% internals. This could be attributed to the reduction in small scale-liquid recirculation intensity with 22% internals, in which small bubbles are dragged downwards at a lower velocity compared to those without internals. In other words, this finding implies the reduction of local small eddies and the manifestation of a greater global recirculation scheme, which is also confirmed by the wide range of upward bubble velocity in empty columns compared to that with 22% internals. The observation is supported by the experimental and numerical results of Chen et al. (1999) and Larachi et al. (2006), respectively, who found decreased radial eddy diffusivities and enhanced advective liquid flow as a result of funneling behavior due to internals presence. Such findings necessitate the need for detailed studies in bubble columns with high intensity internals.

Chapter 4

Impact of Internals on Gas Holdup and Bubble Properties in a Pilot Plant Scale Bubble Column

The same measurement technique described in Chapter 3 is utilized here, and the previously discussed guidelines governing the internals choice still apply as well.

4.1 – Experimental Setup

The experiments were performed in a 45 cm (18") diameter Plexiglas unit, shown in Figure 4.1, using the four-point optical probe, the details of which were outlined above (§3.2). While the compressed filtered air entered the column through a perforated plate distributor of 1.09% open area with 241 holes of 3 mm diameter each, distributed in a square pitch; the liquid phase (water) was kept in batch mode. The dynamic height of the bed was fixed at 2.66 m (105") above the sparger for experimental runs involving the optical probe, while the quiescent liquid height varied with the operating conditions.

Local probe measurements were taken at seven dimensionless radial positions: ±0.9, ±0.65, ±0.3, and 0 (center of the column) and with two orientations: 1) with the tips facing downwards and 2) with the tips facing upwards. Thus, it was possible to account for both bubbles moving upwards and those moving downwards. Hence, both upward and downward (negative sign) velocities are reported. It is to be noted that the probe measurements were carried out at L/D=3.1 in the fully developed region, within which the gas holdup is not a function of axial location (Xue, 2004).

In most experimental runs, two configurations of internals were examined. The first arrangement was the same as that used by Chen et al. (1999), who copied the design from the previously operated Alternate Fuels Development Unit (AFDU) in La Porte, TX for LPMeOH synthesis. The second design was used to provide insight as to what happens when a larger number of cooling tubes are used (i.e., a larger fraction of CSA is occupied by internals) as required in Fischer-Tropsch synthesis. Both configurations are shown in Figures 4.2 (a) and (b), and they have the following specifications:

- 16 rods in two concentric circular bundles of 17 cm (6.7”) and 27 cm (10.63”) diameter, to cover 5% of the total column’s CSA
- 75 rods in 1.75” equilateral triangular pitch, to cover about 25% of the total column’s CSA

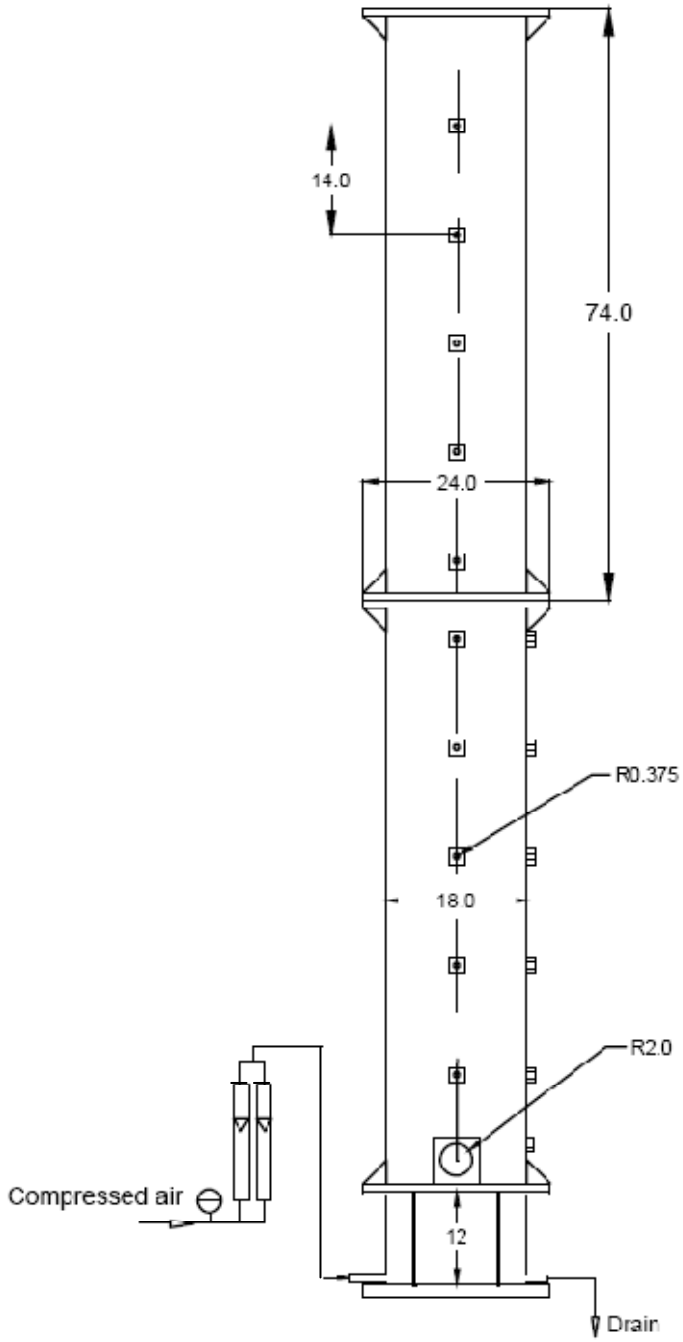

Fig. 4.1 – Schematic diagram of the pilot plant experimental setup (dimensions in inches)

The internals are solid PVC rods of 1" diameter each. To assure stability of the structure, three spacers/supports were used in addition to a top plate. The bundle of rods was hung 5" above the sparger, and this height could be modified by lifting the top plate.

The triangular pitch also allowed flexibility in generating different configurations with internals covering less CSA (specifically 10%, 15% and 20%), simply by removing some of the rods and rearranging the geometry accordingly (see Appendix B for the details on the internals installation procedure). These designs are shown in the next section, where more discussion is provided thereof.

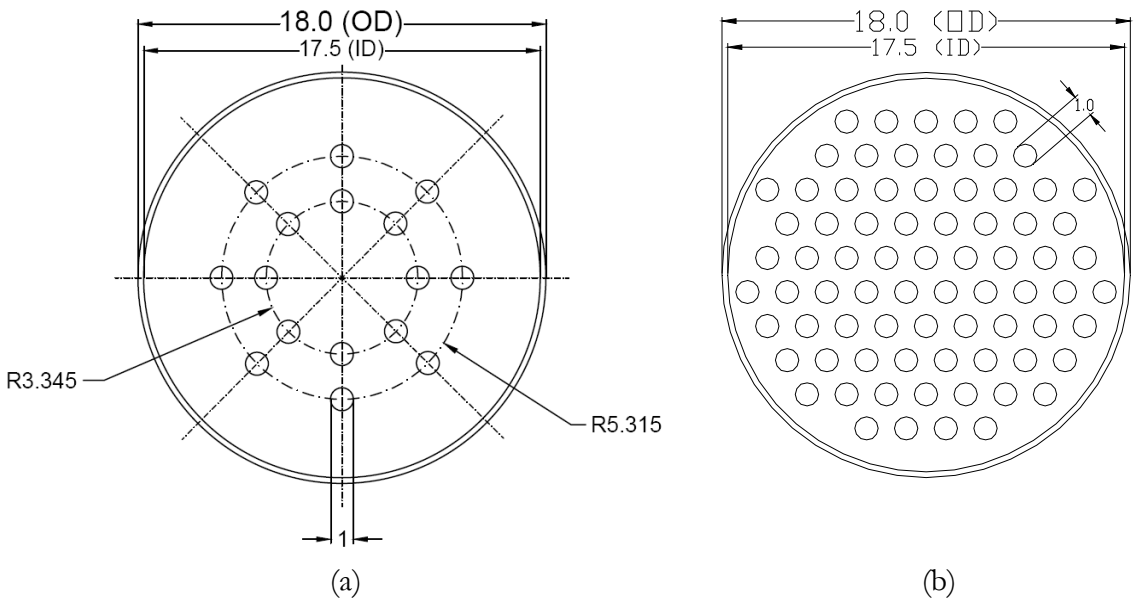

Fig. 4.2 - Design of internals bundle; (a) 5% coverage and (b) 25% coverage (dimensions in inches)

The experiments were carried out over a range of superficial gas velocities, from 5 to 55 cm/s, and at six percentages of covered cross-sectional area: 0 (no internals), 5% (simulating conditions for methanol synthesis), 10%, 15%, 20%, and 25% (simulating conditions for FT synthesis) (see Figures 4.2 and 4.3). The gas velocity values were chosen to reflect industrial interest by focusing on the churn-turbulent flow regime. At a superficial gas velocity of 20 cm/s, comparison with data generated in the previous section in an 8" diameter column was possible and is used here to assess the effect of the column diameter.

4.2 – Results and Discussion

4.2.1 – Overall gas holdup

The column was filled with a liquid volume producing a dynamic height of 105" at the highest applied gas velocity. Afterwards, the dynamic height of the bed varied in the experiments according to the conditions. The quiescent liquid height was visually observed after shutting off compressed air and after gas disengagement, at each of the operating conditions. The overall gas holdup was, thus, calculated based on the change in the bubbling liquid level compared to the quiescent liquid level following the simple relation:

$$\varepsilon_g = {(H_{dyn.} - H_{st.})}/{H_{dyn.}},$$

where $H_{dyn.}$ is the dynamic height of the bed and $H_{st.}$ is the static height.

Overall gas holdup measurements by visual observation of the bed expansion exhibit, generally, an uncertainty arising from strongly fluctuating dynamic height and from the fact that the observation is usually limited to the Plexiglas wall region which is easiest to record. In order to minimize the error associated with the measurement, both the maximum and minimum dynamic heights are noted, and the average is used for the dynamic bed height.

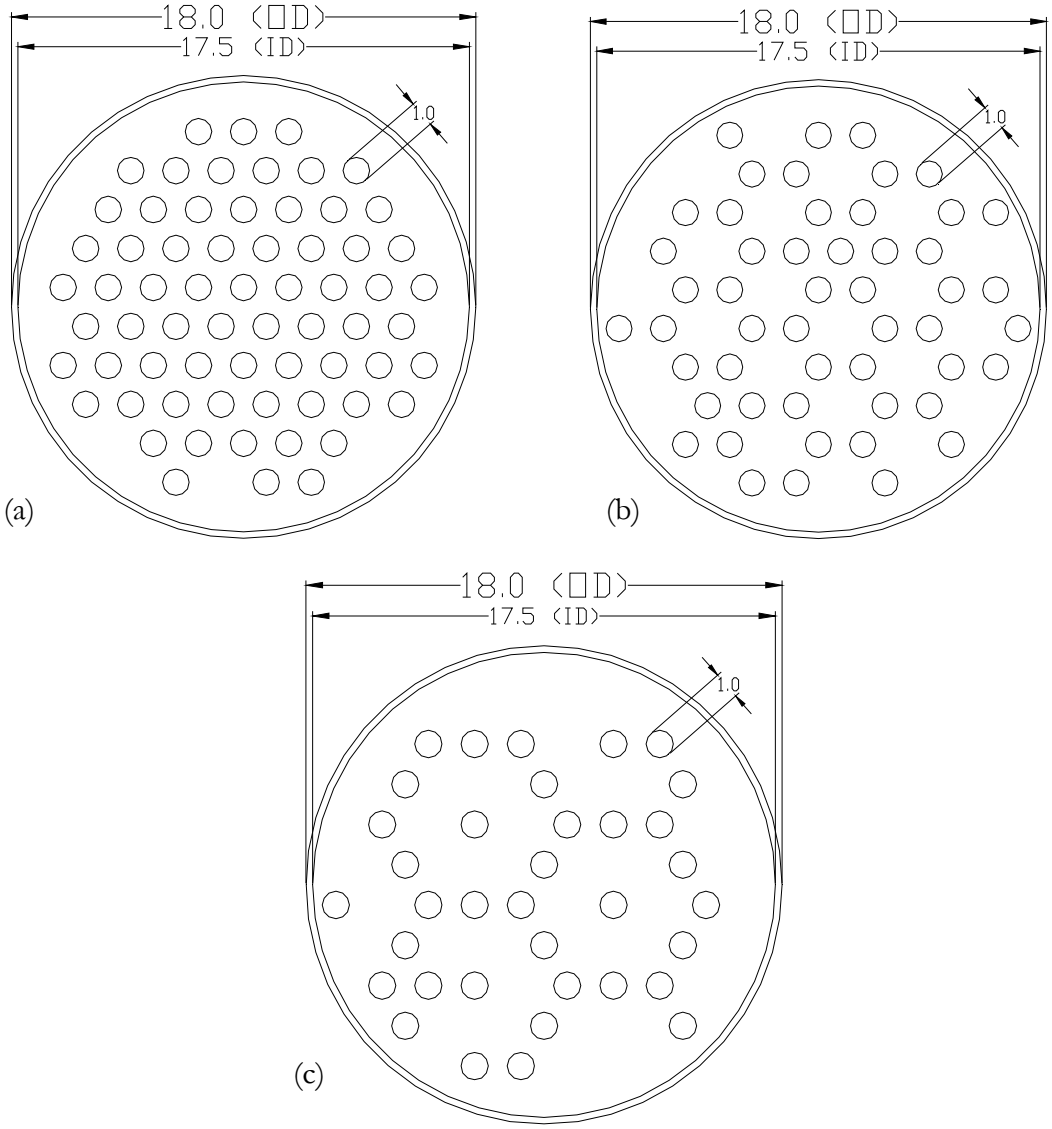

Fig. 4.3 – Configurations of internals bundles covering (a) 20%, (b) 15%, and (c) 10% of the total column's CSA.

The overall gas holdup profiles at a range of superficial gas velocities are shown in Figure 4.4. It is clear that a significant increase in the gas holdup occurs as 10% of the column's CSA is occluded as compared to the no internals case, while the overall gas holdup becomes a weak function of the percentage covered area from 10% to 15%. Finally, negligible impact is exhibited in the range 15% to 25% covered CSA.

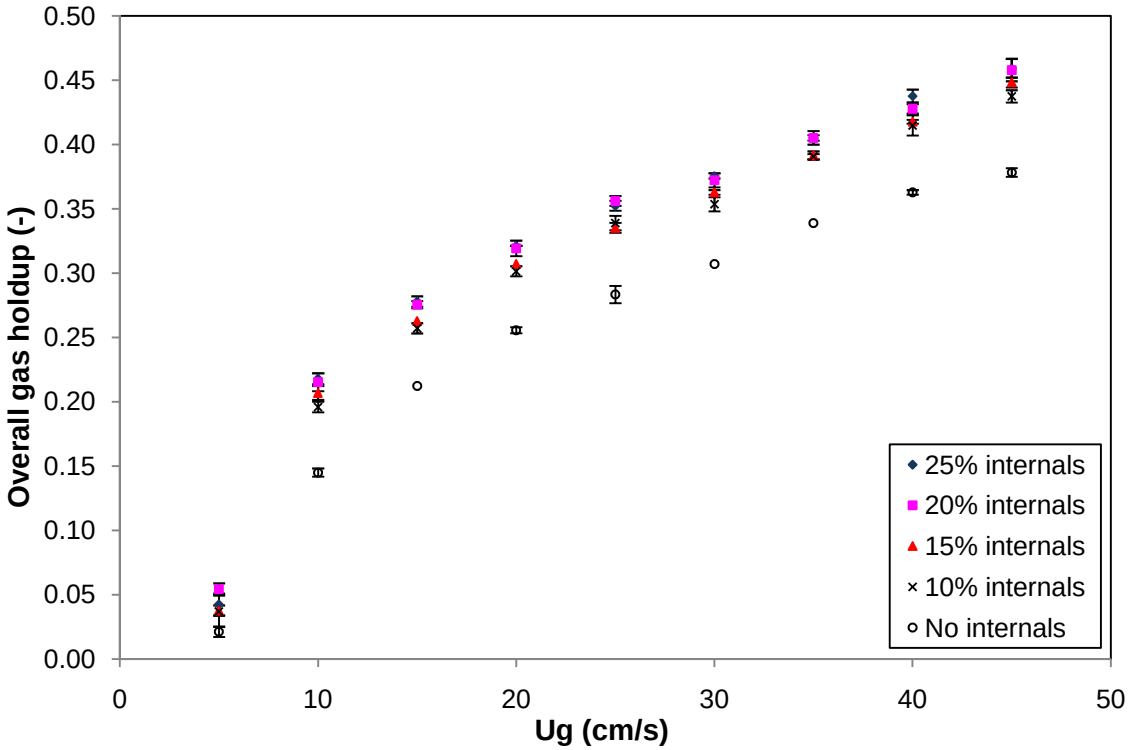

Fig. 4.4 – Overall gas holdup profiles with various internals coverage

Figure 4.5 shows the data of Bernemann (1989) in a 45 cm diameter column with an air-water system and 11% covered CSA with internals plotted with data from the present work, using the internals configuration shown in Figure 4.3 (c). The two profiles are in agreement despite the different geometry of internals while the covered CSA is almost constant. This implies that the effect of internals on gas holdup is not configuration dependent, which is in line with Yamashita (1987). Note that slightly lower values are obtained by Bernemann (1989), which can be attributed to applying a continuous liquid phase with low superficial velocity. At 5cm/s, a larger discrepancy is exhibited since a maldistribution of air through the sparger (Capacitance number (N_C)=2.68, yielding an intermediate flow) in our study resulted in the weeping of some liquid into the plenum chamber in our studies, which reduced the gas holdup. The superficial gas velocity for open area only replaces the superficial gas velocity in Figures 4.5 and 4.6. The two can be related by the following simple equation:

$$A_{tot} \text{ x } U_{sup} = (1\text{-fraction covered CSA}) \text{ x } A_{tot} \text{ x } U_{O.A.}.$$

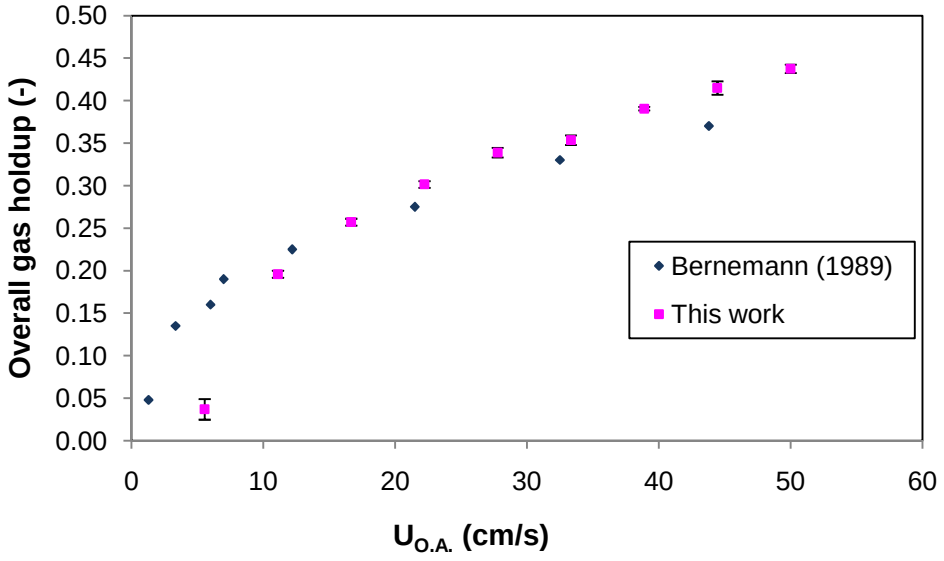

Fig. 4.5 – Overall gas holdup profile comparison with literature data at 10% covered CSA.

The superficial gas velocity for open area can be defined as the volumetric flow rate of the gas divided by only the free CSA of the column (i.e., the total CSA minus the area obstructed by the rods). As a matter of fact, utilizing the superficial gas velocity for open area can be useful to better evaluate the factors affecting the overall gas holdup.

Figure 4.6 shows similar profiles to those illustrated in Figure 4.4 although interstitial gas velocities are utilized on the abscissa axis. It is obvious that the small differences between the gas holdup profiles with internals covering 10% to 25% disappear in this representation. Lower gas holdup values are observed for the case of no internals, however. This finding is highlighted in Figure 4.7, the 25% internals case. The gas holdup increases as a result of the internals' impact on bubble characteristics (expressed in the difference between the no internals data series (hollow circles) and superficial velocity for open area with 25% internals data series (magenta squares)). In addition, the increase in the actual gas velocity in the column due to the decrease in available flow surface area causes another boost in the gas holdup values (expressed in the difference between the superficial velocity for open area with 25% internals data series (squares) and that of the superficial gas velocity data series (diamonds))

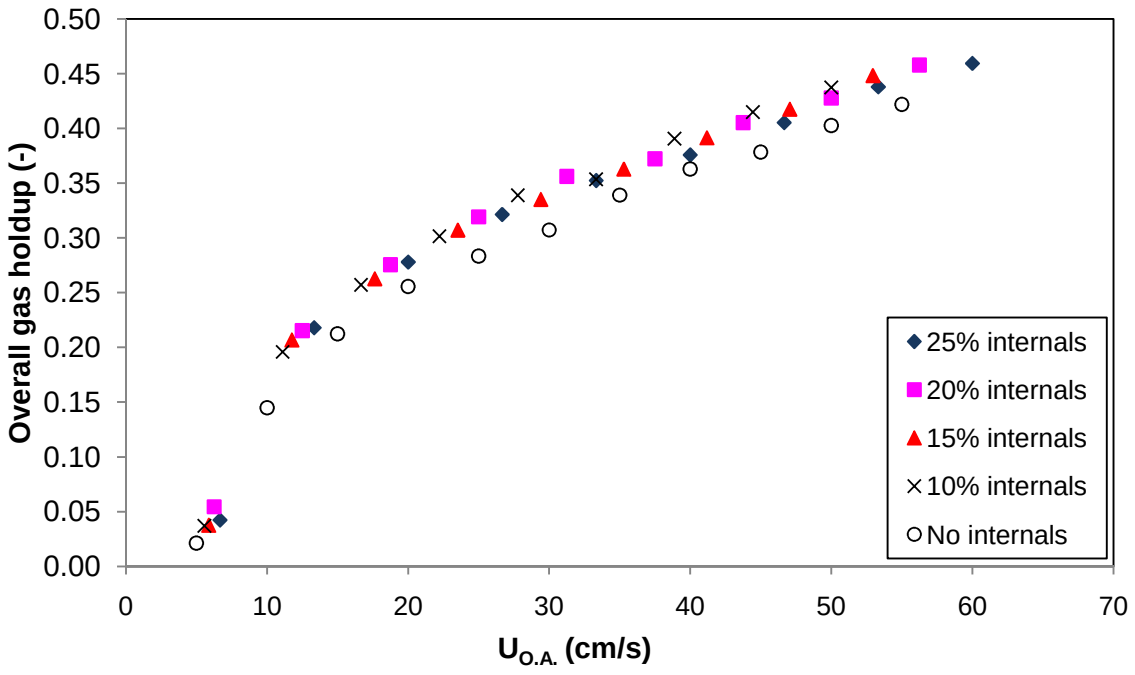

Fig. 4.6 – Effect of superficial gas velocity for open area on overall gas holdup at different internals arrangements

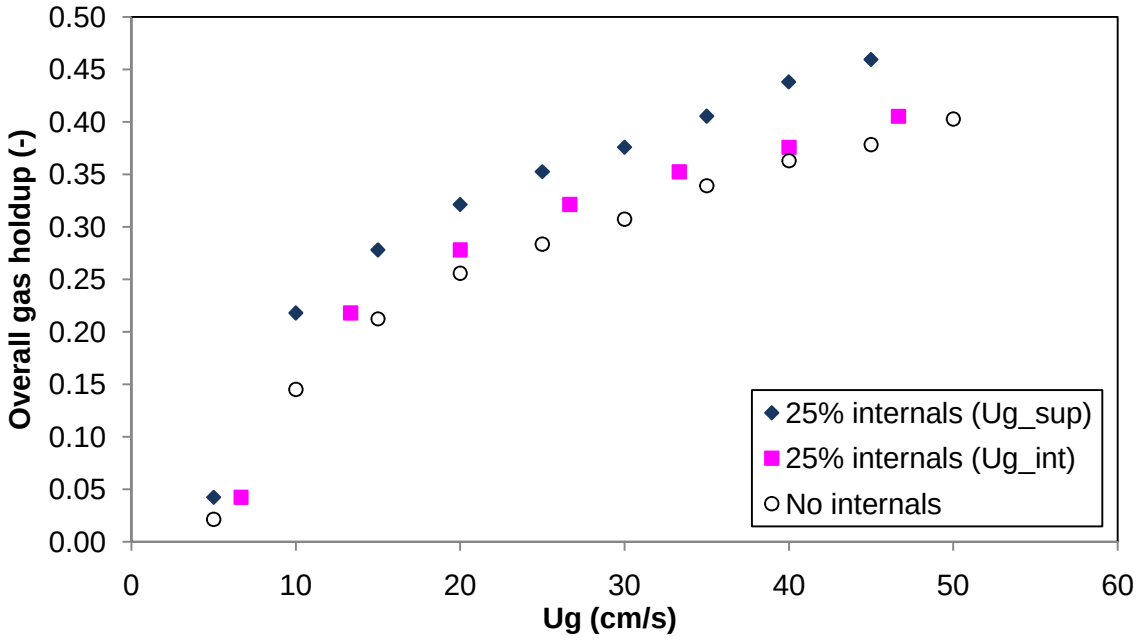

Fig. 4.7 – Effect of gas velocity on overall gas holdup at different internals arrangements

As pointed out before, the main focus of this study is to investigate the effects of internals typically used in the FT and LPMeOH syntheses. Accordingly, internals covering 5% and 25% of the column's CSA are tested thoroughly, noting that the effect of 10%, 15%, and 20% internals is close to that of 25% in general. Table 4.1 summarizes the overall gas holdup at selected conditions and highlights the effects of both the superficial gas velocity and the internals.

Table 4.1 – Effect of internals and gas velocity on the overall gas holdup (%)

	No internals	**5% internals**	**25% internals**
20 cm/s	25.6% (±1.9%)	25.7%	32.3% (±0.06%)
30 cm/s	30.7%	34.7% (±1.3%)	39.5% (±1.2%)
45 cm/s	37.8% (±1.8%)	41.4% (±1.1%)	46.2% (±3.2%)

From Table 4.1, it is evident that gas holdup increases in presence of internals, but that such increase is hardly noticeable at the lowest superficial gas velocity (20 cm/s) and at low percentage occluded open area (5%). No difference in holdup at 20cm/s gas velocity between 0% and 5% coverage by internals of the CSA was also reported by Youssef and Al-Dahhan (2009) in 8" diameter column. On the other hand, as internals become more densely packed, occupying 25% of the CSA, a considerable boost is noticed in the overall gas holdup, as compared to the empty column. Quantitatively, an average increase in holdup of about 27% results with addition of internals that block 25% of the column's CSA. Considering the entire data series at all investigated gas velocities, the Average Absolute Relative Difference (AARD) (defined as $AARD = \frac{1}{N}\sum_1^N \left|\frac{x-y}{x}\right|$) between the no internals case and that of the 25% internals is computed to be 26%.

Although the overall gas holdup, as a global parameter, gives an idea on the impact of the internal structures on the flow field, it does not provide insight on the associated flow pattern, bubble dynamics, and transport parameters. Hence, the information available from the optical probe experiments is discussed in the coming sections.

4.2.2 – Local gas holdup

Gas holdup radial distributions were investigated as a function of percentage covered CSA at different superficial gas velocities based on the total CSA of the column.

As expected from the visual observation of the dynamic and static bed heights, the addition of internals enhances the gas holdup, with a considerable increase in the local values along the radial profile when 25% internals are used. This can be explained by the inhibition of large bubble formation due to the presence of the PVC rods. Large bubbles are known to ascend faster, yielding a lower gas holdup. Figures 4.8 and 4.9 show the effect of the internals on the gas holdup radial distribution at both Ug= 20 cm/s and Ug= 30 cm/s.

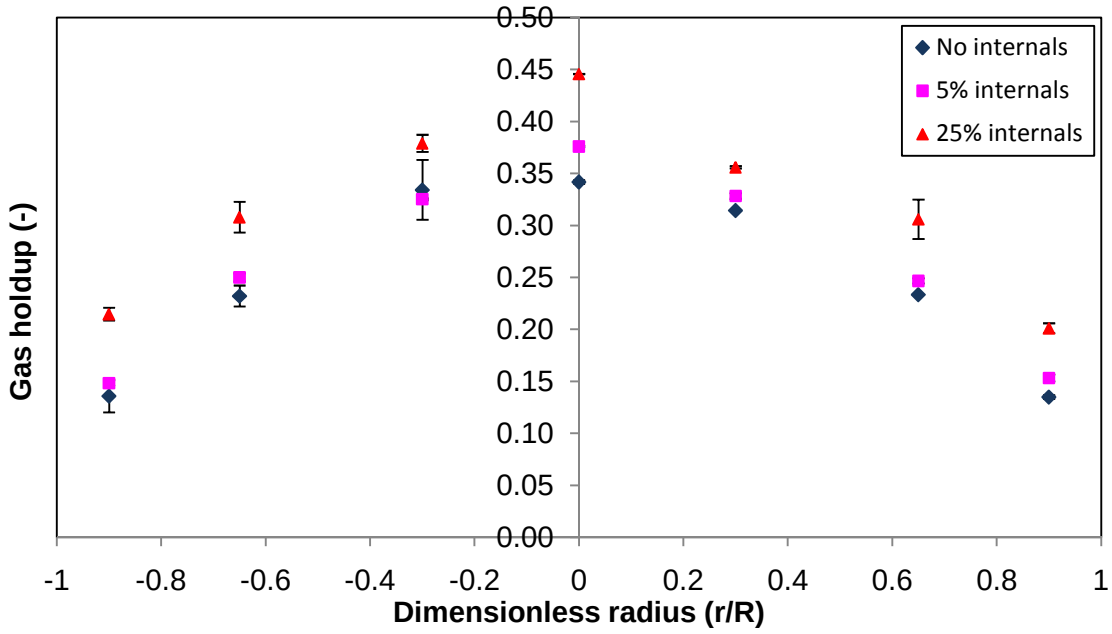

Fig. 4.8 - Effect of internals on gas holdup at Ug=20 cm/s

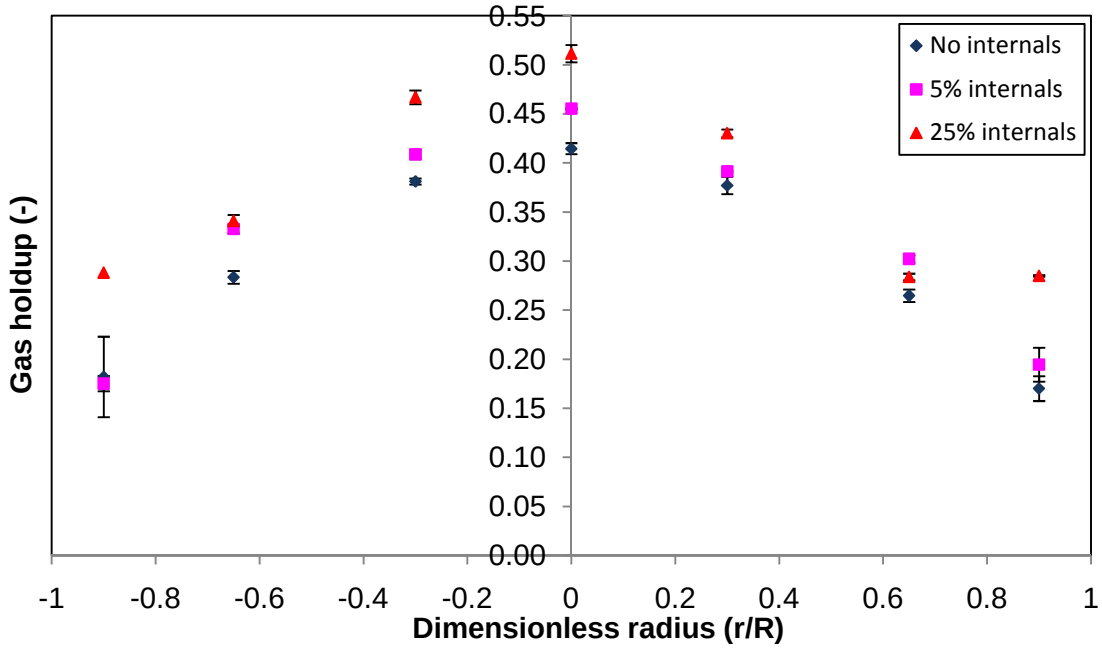

Fig. 4.9 - Effect of internals on gas holdup at Ug=30 cm/s

Figure 4.9 indicates that at the higher superficial gas velocity, in case of 25% internals, there exists a dip in the radial holdup profile at dimensionless radii r/R=±0.65. In an empty column this is the locus of the inversion point of the time averaged profile of the axial component of the liquid phase velocity. The study of Chen et al. (1999) showed that the inversion point is not affected much by the presence of internals occupying 5% of the CSA by internals. The same finding as in Figure 4.9 was observed for the case of Ug=45 cm/s, indicating that a change in the mixing phenomena and flow field is occurring at gas velocities higher than 20 cm/s in presence of 25% internals. Shaikh (2007) reports, using Computed Automated Radioactive Particle Tracking (CARPT), that at the inversion point, the contribution of both positive and negative slurry velocities are equal, which results in an enhancement in the fluctuations in the vortical region (the region near and around the flow reversal). In addition, Degaleesan (1997) found the Reynolds shear stress radial profile to exhibit a maximum around the same position. No similar data is available in the literature for systems including dense internals. However, possible explanations are discussed here as the specific interfacial area radial profiles are reported.

In order to assess the effect of scale in the presence of internals, Figure 4.10 displays the gas holdup radial distribution in two different columns equipped with dense internals covering

22% (for the 8" diameter column) and 25% (for the 18" diameter pilot-plant unit) at Ug= 20 cm/s. Both systems were operated with air-water. From Figure 4.10, it is evident that the effect of column diameter is within the experimental error range (taking into consideration the slight difference in the covered CSA). This finding is in agreement with the conclusion of Forret et al. (2006), who asserted that the gas holdup and its radial profile are independent of the column diameter (for columns larger than 15 cm in diameter (Wilkinson, 1991)) as they studied columns up to 1m in diameter. In order to affirm the above conclusion, a 2^3 factorial design was performed to test the effects of the three factors (internals "0% and 22-25%", radial position "r/R=0 and 0.9", and column diameter "8 in. and 18 in."). The results show that only the radial position and the internals have significant effects, based on a 95% confidence interval.

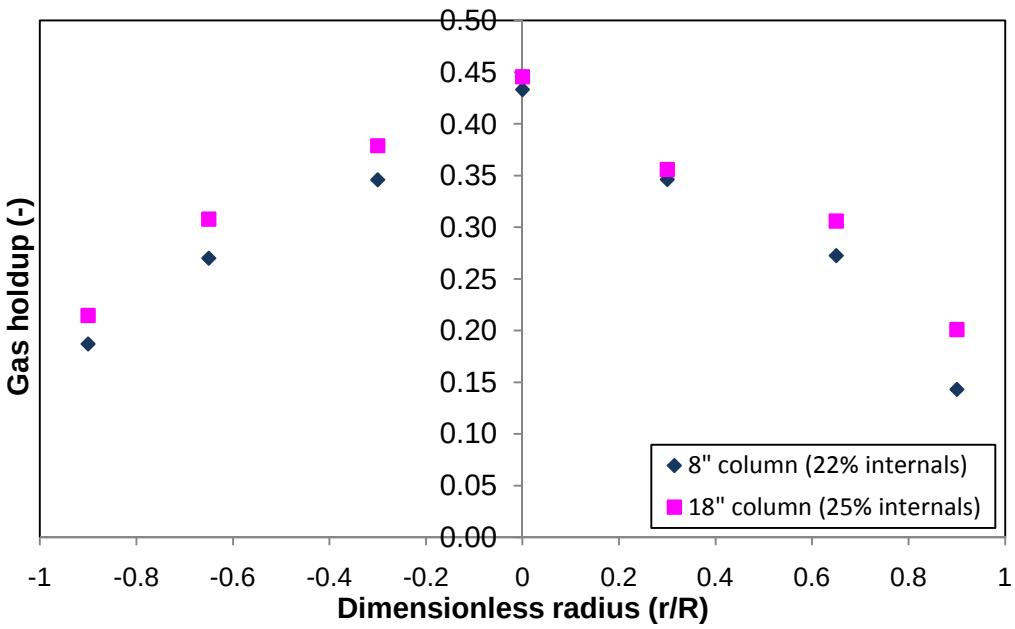

Fig. 4.10 - Effect of column diameter on the gas holdup radial profile at Ug=20 cm/s and with dense internal structures

4.2.3 – Specific interfacial area

Figure 4.11 shows the radial distribution of the specific gas- liquid interfacial area as measured by the four-point optical probe at superficial gas velocities of 20 cm/s, 30 cm/s, and 45 cm/s. Clearly, a higher interfacial area is available for mass transfer as the superficial gas velocity increases, due to increased turbulence, bubble break up, and frequency, (Xue, 2004) resulting in a large number of smaller bubbles in the column. The investigations spanning the diameter of the column show that higher interfacial area exists in the center of the column, with a gradual decrease as one approaches the wall region in case of no and 5% internals and at all operating superficial gas velocities. Figure 4.11(a) shows that the 5% internals arrangement did not affect the interfacial area values as compared to the case of no internals. This finding was expected, since few rods (16 only) were inserted in the column; not enough to disrupt the bubble characteristics or affect the flow field. Thus, the radial profile of the specific interfacial area remains almost unchanged. However, for the 25% internals configuration, a remarkable change in the values of interfacial area is observed close to the column wall (for dimensionless radii larger than the usual inversion point for time averaged liquid velocity). The dense internals are likely to augment the bubbles' break up rate, leading to a larger number of small bubbles, which ultimately should result in an increase in the specific interfacial area. On the other hand, as evident from Figure 4.11, interfacial area values close to those in the empty column (and with 5% internals) are observed in the core region (r/R=0 to 0.65). Despite of the presence of internals, the specific interfacial area did not exhibit an increase in this region of liquid upflow, while the values of the specific interfacial area at the wall region (r/R=0.9) were found to be significantly higher than the measured values in both the empty column and that filled with 5% internals. The value at the wall region was even higher than that reported in the column's center, which is contrary to the findings of earlier studies (Wu, 2007 and Wu et al., 2008) for columns without internals. The data were satisfactorily reproducible (mean relative error = -0.5%), and similar trends of the specific interfacial area profiles were also obtained at higher superficial gas velocities (Ug= 30 cm/s and Ug= 45 cm/s), as can be seen in Figure 4.11 (b and c). As a result of the unanticipated interfacial area profile in case of 25% internals, more data points were investigated in the annular region (r/R=0.65-0.9), as shown in Figure 4.12. This figure confirms that the radial distribution of the interfacial area exhibits a minimum at

the inversion point of the axial liquid velocity radial profile and reaches a maximum in the vicinity of the wall.

The above can be explained by the intensified large-scale liquid phase recirculation enforced by the structured configuration of the internals covering 25% of the column's CSA. The internals magnify the single cell recirculation loop (Deen et al., 2010), driving a vigorous ascending liquid flow in the column's core region which is balanced by an equivalently enhanced down-flow at the wall region. This vigorous large scale recirculation causes an increase in the axial liquid velocity as shown in the radial profiles reported by Bernemann (1989). Now, a closer look at bubble break-up is necessary. It is well known that a bubble will maintain its shape as long as that the forces acting upon its surface are in equilibrium. Wilkinson (1991) concluded that the break-up of small bubbles occurs due to shear stresses in the liquid generated by velocity differences. More detailed analysis of this phenomenon was provided by Hinze (1955), who postulated that bubbles may deform following interaction with fluctuating eddies and that break-up occurs when local shear stress generated from an eddy exceeds the surface tension force maintaining the bubble. This can be represented in a dimensionless form via the Weber number.

If $We > We_C$, break-up occurs with $We = (\tau\, d_{b.max})/\sigma$.

Here, $\tau = \frac{1}{2}\rho_l \overline{u_e}^2$ and the average value of the fluctuating velocity ($\overline{u_e}$) is expressed using:

$$\overline{u_e}^2 = 2(l_e.\rho_l.\frac{P}{V})^{2/3}.$$

Hinze classifies three cases where 1) eddies of smaller size than the bubble size do not deform the bubble surface, 2) eddies of larger size transport the bubble, and 3) eddies of the same scale as the bubble size ($l_e = d_b$) cause break-up. This classification is supported by Luo and Svendsen (1996), who suggested that any eddy larger than the bubble would just give the bubble a translational velocity, while those eddies of comparable length can cause breakup. Typically, the maximum bubble size, used to evaluate the critical Weber number, is obtained from correlations. However, in the case of internals, the bubble size is governed by the system's specific pitch. From the above theoretical overview, it seems that the flow field is altered significantly due to the internals by a change in the scale of the turbulent eddies (l_e)

(which may be followed by a change in the Prandtl mixing length). Hence, we propose new bounds for the characteristic eddy scale (l_e): Internals Pitch $>l_e \geq d_b$. In the middle of the column, the eddy scale is larger than the bubble size but bubbles are carried away for only short distances before they "bombard" a tube, causing higher break-up rates than in columns with no internals. The larger bubbles stay in the central region, thus giving similar values of interfacial area as in columns with no internals. However, the small bubbles, due to enhanced liquid recirculation, accumulate in the wall region. Only small bubbles can survive in the wall region due to enhanced values of shear stress there. Thus, an increase in interfacial area is observed at the wall. Finally, the aforementioned robust recirculation phenomenon drags almost all the small bubbles towards the wall region. The increased population/frequency of these small bubbles results in the increase in the interfacial area observed in the wall region of the column. In order to fundamentally represent flow behavior altered by internals, and following Bernemann's (1989) study, the enhancement of the axial component of the liquid velocity is demonstrated, starting with the equation of motion in cylindrical coordinates as follows:

$$-\frac{1}{r}\cdot\frac{\partial}{\partial r}[r\cdot\tau] = \frac{\partial p}{\partial z} + \left(1-\varepsilon_g(r)\right)\cdot\rho_l\cdot g$$

where $\tau = -\nu_t(r)\cdot\rho_l\cdot\frac{\partial V_l}{\partial r}$

Note that this simplified version assumes 1-Dimensional, steady, fully developed, axisymmetric, negligible end effects and 2-phase flow (Gupta, 2002).

In order to obtain the expression of the pressure gradient (dp/dz), one typically follows Ueyama and Miyauchi's (1979) approach by multiplying above equation by $2\pi r$ then integrating between r=0 and r=R then dividing the result by πR^2.

However, in the case of columns with internals, a slight modification is needed since the column's cross-section is equipped with tubes and as a result of a force balance from center to wall results in the extra term $\frac{1+n_R\cdot\varphi'}{1-n_R\cdot\varphi'^2}$

The pressure term in the equation can be expressed in terms of the wall shear stress (τ_w) and by accounting for the presence of internals as follows:

$$\frac{\partial p}{\partial z} = -\frac{2\cdot\tau_w}{R}\cdot\frac{1+n_R\cdot\varphi'}{1-n_R\cdot\varphi'^2} - \rho_l\cdot g\cdot\left(1-\varepsilon_g(r)\right),$$

where $\varphi' = {d_R}/{D_R}$

d_R is the diameter of an internal tube, and n_R is the number of tubes.

Substitution of the pressure term within the equation of motion, followed by integration with the following boundary conditions (Bernemann, 1989):

$\left.\frac{\partial V_l}{\partial\varphi}\right|_{\varphi=0}$ $and\ V_l(\varphi=0) = V_{LZ}$, yields:

$$V_{LZ}(\varphi) = A\cdot ln\left\{1-\frac{a_2}{a_1}\cdot\varphi^2\right\} + B\cdot\varphi^2 + V_{LZ}.$$

$A = \frac{R}{2\cdot a_2\cdot v_{t,Z}}\cdot\left[\frac{\tau_W}{\rho_l}\cdot\frac{1+n_R\cdot\varphi'}{1+n_R\cdot\varphi'^2} - \frac{g\cdot\varepsilon_g(r)\cdot R}{2}\cdot(1-1{,}647\cdot\frac{a_1}{a_2})\right]$, and

$B = \frac{1{,}647.g.\varepsilon_g(r).R^2}{2\cdot v_{t,Z}\cdot(b+2)}$,

where a_1=1, a_2=0.75, and b=2.

Where A is proportional to the number of internals (increases with an increase of n_R). Moreover, Bernemann reports A/v_{LZ} to be a constant value [v_{LZ} is the centerline velocity]. This simply means that the last term on the right hand side of the expression for A also increases as a result of the increase in internals density.

As a matter of fact, and based on physical reasoning, the presence of internals decreases the fluctuating velocity and leads to the increase of the axial liquid velocity in the column's central region as found by Forret et al. (2003) from Pitot tube measurements. From experimental investigation using CARPT, Chen et al., 1999 found the internals to decrease the eddy diffusivities and turbulent stresses since the internals reduce the turbulent eddies length scales.

These justifications will be confirmed by the velocity distributions reported later at both the center and wall regions showing higher probabilities of finding slower downwardly moving bubbles (i.e., of small size) at the wall region.

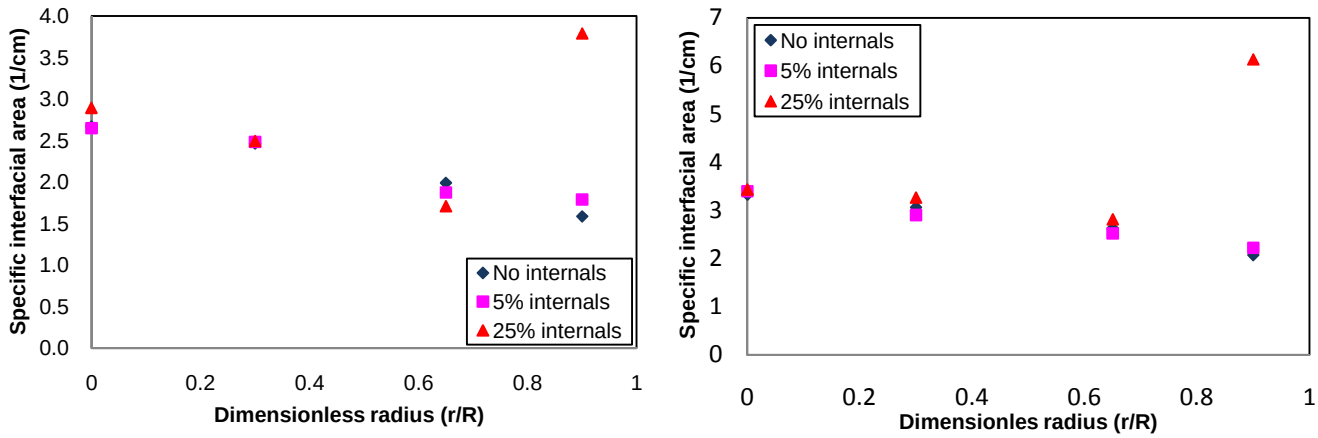

(a) (b)

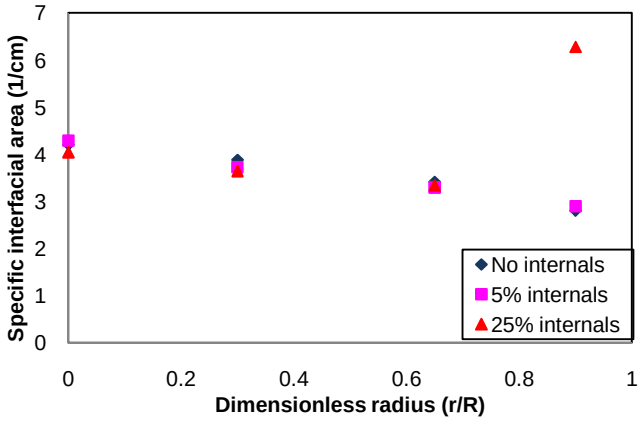

(c)

Fig. 4.11 – Effect of internals on the specific interfacial area at different superficial gas velocities (a) Ug= 20 cm/s, (b) Ug= 30 cm/s, and (c) Ug= 45 cm/s

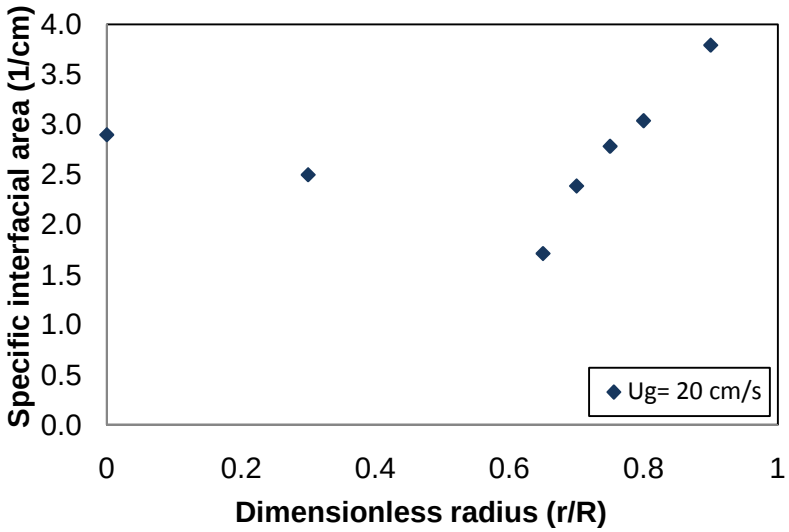

Fig. 4.12 – Radial interfacial area profile at Ug= 20 cm/s and 25% internals

4.2.4 – Bubble chord length

As noted above, bubble size is an important parameter that affects the bubble velocity and, hence, the residence time of the gas phase (i.e., the gas holdup). However, due to the various shapes (spherical, ellipsoidal, etc.) that bubbles may have in the bubble column media, it becomes more complicated to measure the size of dynamic bubbles moving at high velocities. Here, as an estimation of bubble size, bubble chord length probability distributions are reported with the presence and absence of dense internals structures.

As shown in Figures 4.13 and 4.14, at Ug= 20 cm/s, comparing the bubble chord length distributions at the center and wall (r/R=0.9) regions, reveals that smaller bubbles exist at the wall. This is true for the empty column and when 25% internals are inserted. As confirmation, the mean values of the distributions are 0.616 and 0.618 cm for the center with no internals and 25% internals, respectively. For the wall region, the corresponding values are 0.464 and 0.363. These values, along with the variance of the distributions, are provided in Table 4.2. In addition, although the mean bubble chord length at the column's center is comparable with and without 25% internals, the mean bubble chord length at the wall region is about 28% smaller when the dense internals are inserted. This can be explained by the enhancement of the break-up phenomenon enforced by the presence of these solid barriers within the flow field, which prevents the formation of larger bubbles. Corroborating this finding with the remarks resulting from the analysis of the specific interfacial area

measurements, it is confirmed that more of the smaller bubbles are present at the wall region as the internals are introduced to the system.

As the highest superficial gas velocity (Ug= 45 cm/s) is applied, the mean bubble chord length of the distribution in the column's center, with presence of 25% internals, becomes higher than that in a column with no internals (Table 4.2), as highlighted in Figure 4.15. This can be elucidated by observing the probability distribution of the chord length at Ug= 45 cm/s and 25% internals for the wall region, shown in Figure 4.16. It is obvious that there is a much higher probability for smaller bubbles, caused by the dragging of most of the small bubbles from the core region of the column towards the wall region. Further validation will be provided in the next section via the bubble velocity distribution analysis.

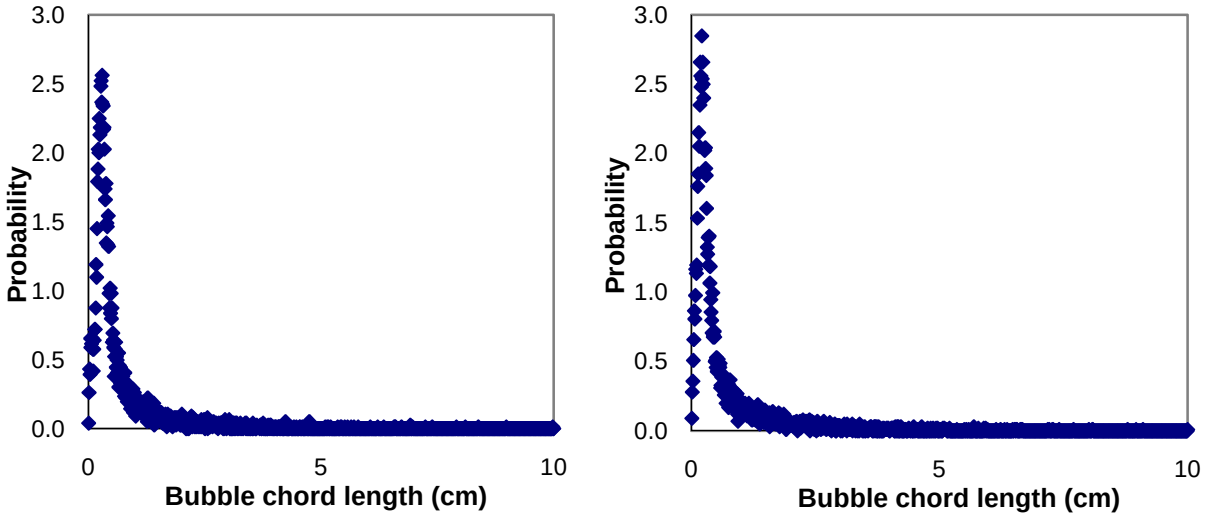

(a) (b)

Fig. 4.13 – Bubble chord length probability distribution at Ug= 20 cm/s and column's center with (a) No internals, (b) 25% internals

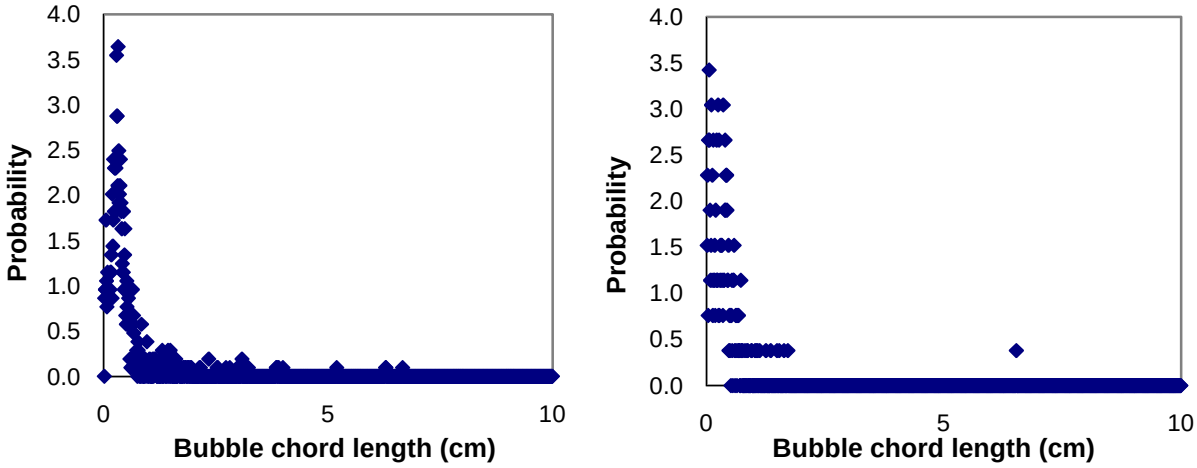

(a) (b)

Fig. 4.14 - Bubble chord length probability distribution at Ug= 20 cm/s and r/R= 0.9 with (a) No internals, (b) 25% internals

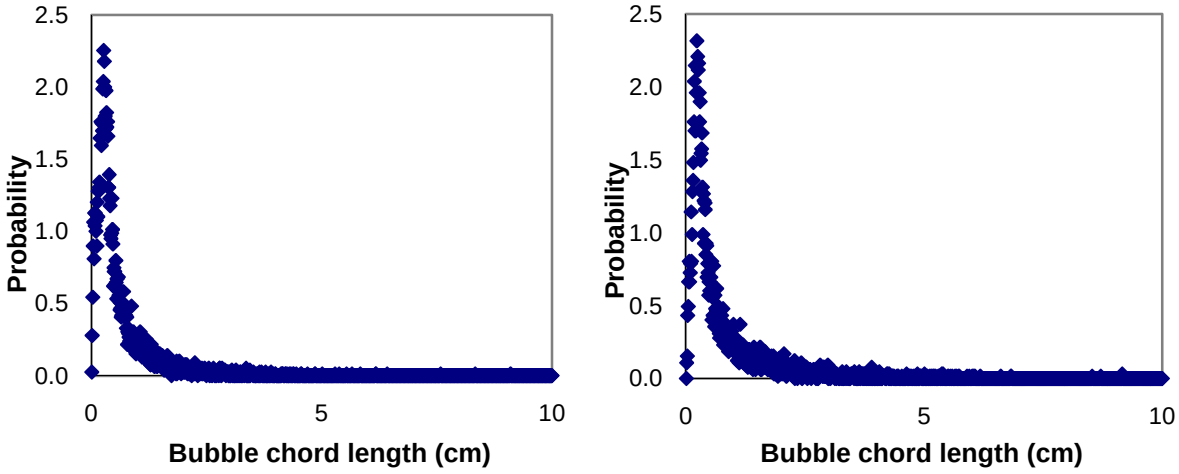

(a) (b)

Fig. 4.15 - Bubble chord length probability distribution at Ug= 45 cm/s and column's center with (a) No internals, (b) 25% internals

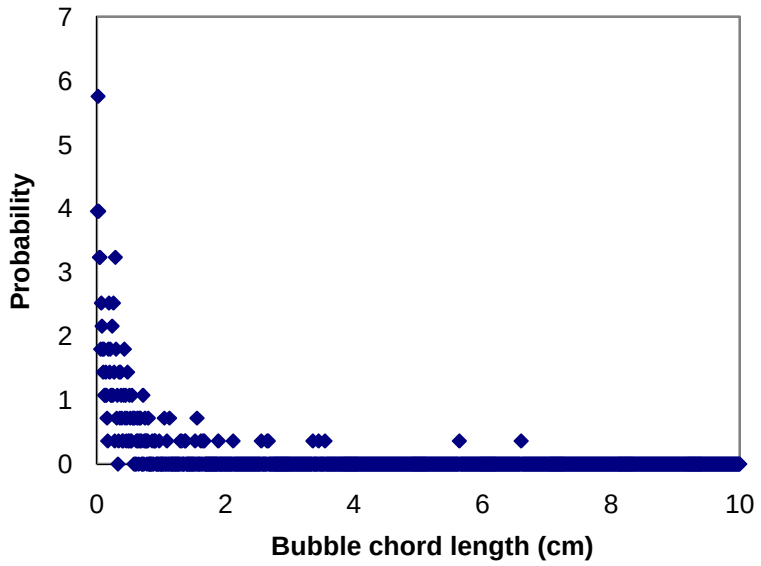

Fig. 4.16 - Bubble chord length probability distribution at Ug= 45 cm/s and 25% internals (wall region)

Table 4.2 - Statistical measures of the chord length distribution for different investigated conditions

	Mean (cm)	**Variance (cm^2)**
Ug=20cm/s – No internals – Center	0.62	0.55
Ug=20cm/s – 25% internals – Center	0.62	0.71
Ug=20cm/s – No internals – Wall	0.46	0.35
Ug=20cm/s – 25% internals - Wall	0.36	0.22
Ug=45cm/s – No internals - Center	0.58	0.40
Ug=45cm/s – 25% internals - Center	0.70	0.71

4.2.5 – Bubble velocity

The four point optical probe, with varying tips orientation, is utilized to investigate the bubble upward and downward velocities. As shown in Chapter 3, accounting for the bubbles moving upwards is achieved via the regular probe direction with the tips facing downwards; while the fraction of the bubbles which are moving downwards (represented with a negative

velocity in the distributions) is obtained by introducing the probe tips facing upwards. The bubble velocity probability distributions provide insight not only on the residence time of the gas phase in the column, but also on the liquid phase flow structure.

Figure 4.17 shows the velocity distributions at 30 cm/s without internals.

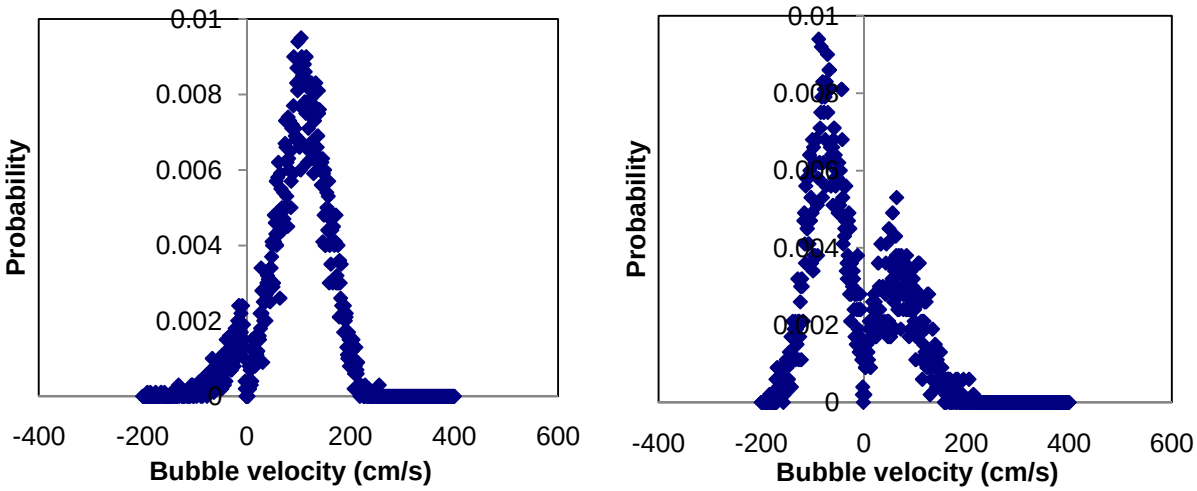

(a) (b)

Fig. 4.17 – Bubble velocity probability distribution at Ug= 30 cm/s and no internals for (a) Column's center, (b) Wall region

Figure 4.17 shows a higher probability of bubbles possessing a negative velocity (i.e. moving downwards) at the wall region. This well known behavior is caused by the flow structure forcing the bubbles to move upwards in the column's center and to travel downwards along the reactor's walls in order to ensure the conservation of mass in the system. Similar results have been reported in the literature (Xue et al., 2008 and Wu et al., 2008).

Figure 4.18 (a) presents the velocity distribution with 25% internals and at the column's center. Comparing Figures 4.17 (a) and 4.18 (a) reveals no significant differences between both distributions. Qualitatively, a slight shift of the upwards rise velocity (positive velocity) towards the left with a small increase in the probability is observed for the case of 25% internals, which can be caused by bubble breakup occurring because the PVC rods yield smaller bubbles with lower rise velocities.

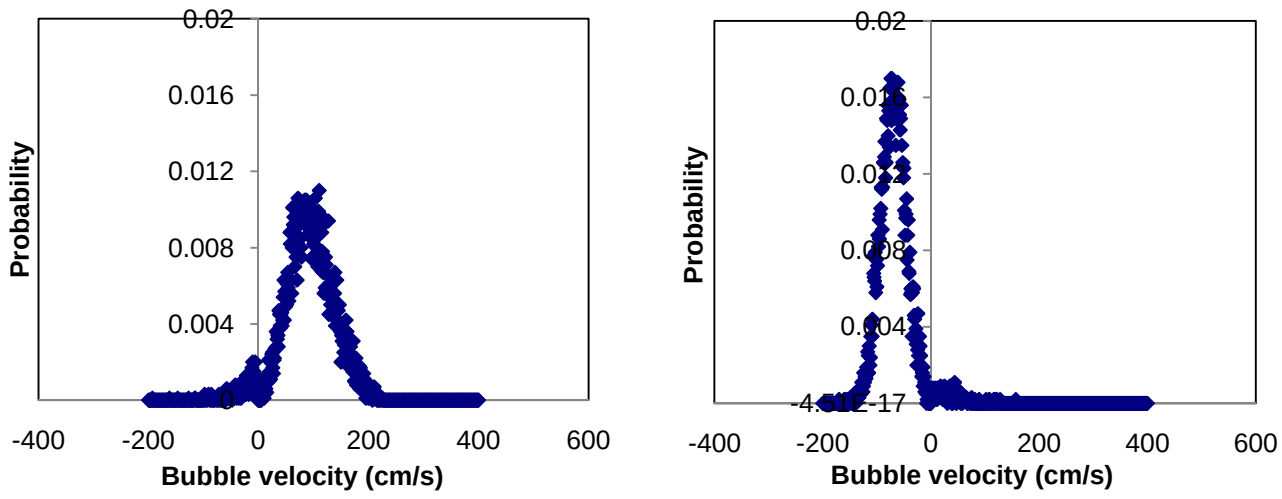

(a) (b)

Fig. 4.18 - Bubble velocity probability distribution at Ug= 30 cm/s and 25% internals for (a) Column's center, (b) Wall region

With dense internals, the velocity distributions at the column's center and the wall region vary widely, as shown in Figure 4.18. There is a negligible probability for bubbles moving upwards at the column's wall, and bubbles with negative velocity dominate the region. No similar trends have been reported in the literature before. This indicates that, at 25% CSA occupied by internals, the flow structure is largely affected by the presence of internals for both the dispersed and the continuous phases. This finding supports the previously mentioned remarks with regard to the bubble chord length distributions as well as the gas-liquid specific interfacial area radial profiles. It also implies that the intensity of the large scale recirculation is increased when heat exchanging tubes are placed vertically inside the reactor.

For better understanding of the phenomenon described above, Figure 4.19 shows the obtained bubble direction angle distribution by the probe pointing upwards at the wall region for the cases of (a) no internals and (b) 25% internals. Note that the negative sign is assigned to denote bubbles moving downward.

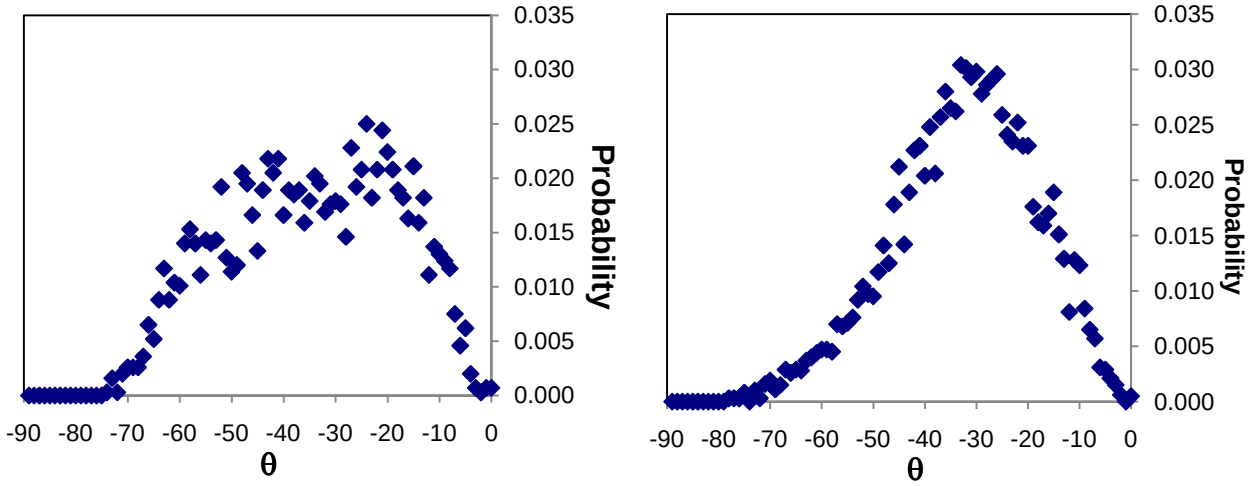

(a) (b)

Fig. 4.19 - Bubble direction angle probability distribution at Ug=30cm/s in the wall region for (a) No internals, and (b) 25% internals

It is clear that a scattered distribution exists for the case of no internals, as the bubbles are moving in a multiplicity of directions attacking the probe tips. However, the probability distribution for the case of 25% internals shows a more structured profile. The distribution is right skewed (possesses positive skewness), and a distinctive peak at a smaller angle is observed with a higher probability. This indicates that the tubes are forming a path for the bubbles in this region to move more vertically downwards, decreasing the tumbling motion that would result from small eddies generated in columns with no internals. This finding confirms earlier results of Bernemann (1989) who investigated liquid velocity profiles with longitudinal internals.

The effect of the bubble column scale on the velocity distribution was also investigated. Optical probe measurements were performed in the 18" diameter column, as well as in an 8" diameter column with the same air-water system. Degaleesan (1997) found the liquid recirculation velocity to be a function of the column's diameter for empty columns. As the column's diameter increased, the mean upflow liquid velocity increased accordingly. These findings were limited to columns with no internals.

Figures 4.20 and 3.14(a) show the velocity distributions at Ug= 20cm/s in 18" and 8" diameter columns.

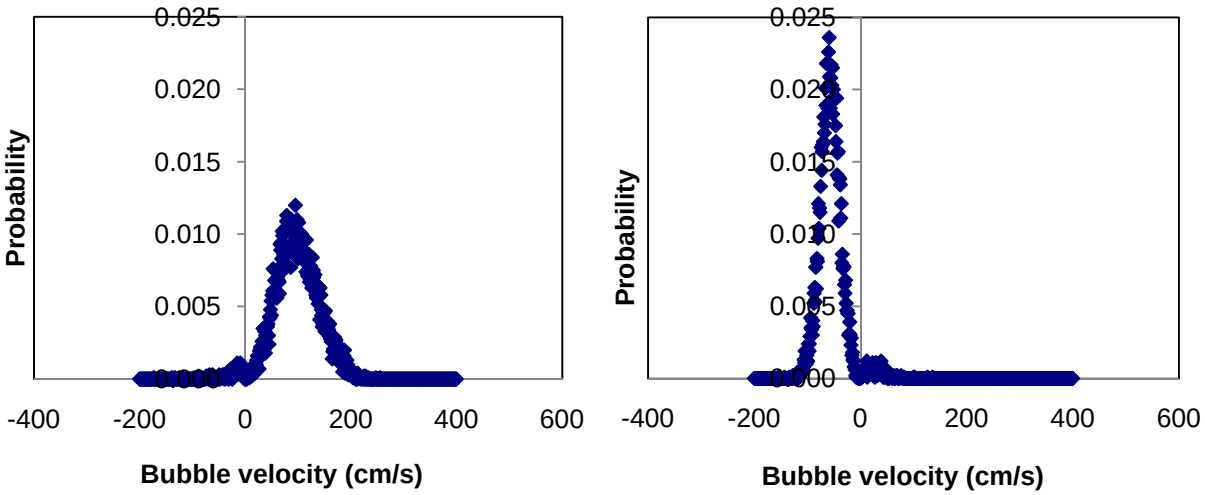

(a) (b)

Fig. 4.20 – Bubble velocity probability distribution at Ug= 20 cm/s and 25% internals in 18" diameter column for (a) Column's center, (b) Wall region

In the larger column, the liquid global recirculation is enhanced, which is reflected in the probability distribution of the bubbles in the system, as shown in Figures 4.20 and 3.14 (a). In both the large and small columns and at the center location, almost all of the bubbles are moving upwards. However, for the small column in the wall region, while a considerable fraction of the bubbles are moving upwards, most bubbles have a negative velocity. Interestingly, this observation does not hold as one examines the velocity distribution in the wall region of the larger scale column. In the 18" diameter column, a minor fraction of the bubbles moves upwards in the wall region. Although this can be expected from earlier findings in empty column studies, the presence of internals magnifies these differences. Such behavior has not been clearly reported in the literature before.

4.3 – Guidelines for the Design of Heat Exchangers for Fischer-Tropsch Slurry Reactors

Based on the above findings and following a thorough scrutiny of available literature on heat removal equipment in a bubble column, a summary of the main considerations is provided below:

Internal longitudinal heat exchanging tube internals are advisable to 1) obtain a more uniform temperature distribution radially and axially and avoid overheating, 2) prolong the lifetime of the catalyst, 3) maintain reaction stability and prevent excessive formation of methane, 4) produce high pressure steam (as opposed to cross-flow tube bundles), 5) yield low pressure drop (as opposed to cooling coils), and 6) preclude an external heat exchanger requiring a large/expensive slurry pump (Schlüter et al., 1995).

Design features

The internal tube bundle details can be described by a ratio (heat exchanger area (m^2)/reactor volume (m^3)) or by tube diameter and tube pitch. The former would typically be around 30 m^2/m^3, while the latter depends on many factors. An internal tube in a commercial reactor can be 2" to 5" in diameter (Maretto and Piccolo, 1998, Hawthoorne et al., 2006, Korte, 1987). The tube pitch is governed by well documented information from heat exchanger literature, and a minimum of 1.25 times the outer diameter of the tube is required for a triangular pitch. For a square pitch, this becomes 1.25 times the diameter or 1.25 times the outer diameter plus 6 mm (whichever is larger). The geometry of the tube pitch (triangular vs. square) can be a matter of convenience, since it is proven above (see Figure 4.5) and from the work of Yamashita (1987) that the configuration of the tubes (as long as it is uniform and the total covered CSA is constant) does not affect the gas holdup and the heat transfer coefficients. It is to be noted that for large numbers of tubes in the reactor, horizontal supports stiffening the structure are mandatory to provide mechanical strength and to eliminate vigorous vibrations when large gas velocities are employed. For a triangular tube pitch, three-direction fixation is required for a rigid bundle, while only two direction fixation is needed for square pitch.

It is important to note that since the bubble size and the height of the liquid circulation eddies depend largely on the pitch (Saxena, 1995), and although the heat transfer coefficient radial profiles are independent of the pitch (Korte, 1987), practical experience remains the best guide in choosing the head-to-head tube distance.

Based on their heat transfer studies, Li and Prakash (2001) recommend not placing tubes in the wall region (r/R=0.75-1). In light of the findings from the current work, decreasing the density of the tube internals in the annular region (for r/R larger than the inversion point) might be beneficial to allow some bubble agglomeration, yielding a more uniform radial profile of the specific interfacial area. Moreover, this may also yield a narrower distribution of small bubble size (referring to Table 4.2), which is very advantageous in bubble columns from a practical and theoretical (modeling) viewpoint.

Thus, bundling the heat exchanging internal tubes in groups of 4-12 tubes each is useful. Such bundles give better control of the density of the internals locally and provide improved means of removal and installation of the tubes in an industrial reactor. Although the use of serpentine cooling tube is adopted in Sasol's reactors, simple header designs for the boiler feed water input and the steam collection can be sought and coupled with the bundling criteria mentioned above.

Along these lines, Chapter 6 discusses a scale-up methodology making use of the internals' compartmentalization.

Chapter 5

Liquid Phase Mixing in Bubble Columns with Internals

5.1 – Scope

The typical hydrodynamic phenomena observed in bubble columns were summarized in Chapter 1. These included the liquid phase velocity profile which involved a central plume of upward flow compensated by a downwardly moving liquid in the wall region to ensure continuity. Such flow pattern has been reported in the time averaged sense using a number of measuring techniques such as CARPT. Ueyama and Miyauchi (1979) presented one of the earliest models to describe this profile as shown in Figure 5.1.

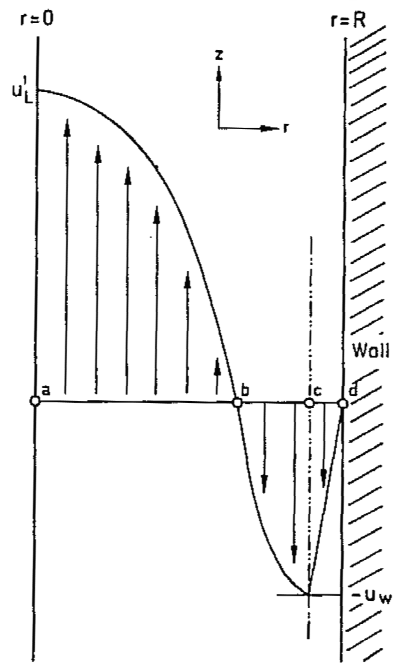

Fig. 5.1 – Flow profile of the liquid phase in a bubble column (Ueyama and Miyauchi, 1979)

In the simplest, and most commonly used slurry bubble column reactors models, the gas phase is assumed in plug flow while the pseudo-homogenous liquid–solids suspension is

considered fully backmixed. The assumption for the gas phase can be justified in the bubbly flow regime. The liquid phase assumption is more appropriate for churn turbulent flow in which liquid recirculation is strong and turbulent liquid movement is induced by bubble swarms (Millies and Mewes, 1995). However, such an ideal picture of the flow is not typically the case in bubble columns. Consequently, more complex models were developed involving two classes (or a population balance) of bubbles and accounting for liquid and gas recirculation. The latter type gives a better representation of the flow behavior (e.g., Degaleesan's (1997) 2D convection-diffusion model).

As pointed out in Chapter 2, there are scarce studies of liquid mixing in columns with vertical internals. This lack in the database hinders the validation of models and is a challenge.

In this Chapter, the effect of heat exchanging vertical internals on the liquid mixing behavior is investigated via the analysis of the liquid Residence Time Distribution (RTD) curves of the system using a standard tracer/conductivity probe technique.

5.2 – Experimental Setup

The experimental work has been carried out in the 18" diameter column described in Chapter 4 (Figure 4.1). Several modifications were applied to the system as shown in the schematic diagram of the new system in Figure 5.2. Two 2" diameter outlet ports were manufactured on the sides of the column at a height of 105" to accommodate a continuously flowing liquid phase during the experiments. The latter ensured that the dynamic height was maintained at 105" for all experimental runs. The liquid flows outwardly through 2" hoses to the drain with no recycle. Superficial liquid velocities of 0.5, 1, and 1.5 cm/s were applied via a 1" diameter inlet located at the bottom of the column just above the gas sparger. Both the empty column and that equipped with internals covering 25% internals (Figure 4.2 (b)) were utilized for the experiments in order to assess the impact of the tubes bundle on the liquid mixing characteristics. Superficial gas velocities of 20, 30, and 45 cm/s were employed.

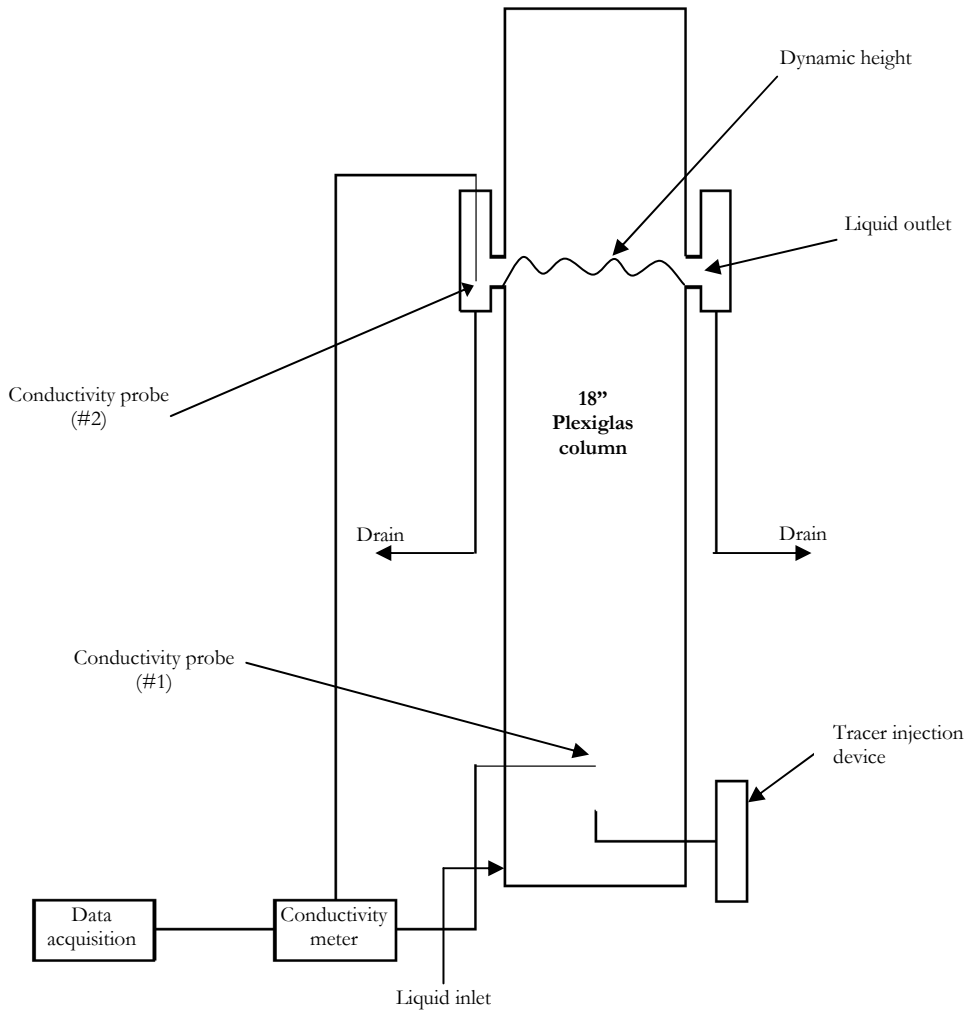

Figure 5.2 – Schematic diagram of the bubble column for the tracer experimental setup

5.3 – Measurement Technique

The liquid mixing characteristics are measured by means of a standard liquid tracer/conductivity probe technique. The conductivity probes (MI-900 Series conductivity electrodes) are obtained from Microlelectrodes Inc. Each probe is linked to a data acquisition board (AT-MIO-16E-10 having a 12-bit resolution and capable of sampling at a rate of 100 kilo-samples/sec) from National Instruments. The probes consist of two electrodes (platinum black coated) approximately 3 mm apart, which are encased in plastic tubing approximately 6 mm in diameter and 30 cm in length. The probes are connected to conductance meters (YSI Model 35), and the output from the meters is sent to the data acquisition board.

Impulse tracer injections are made in the system. Considering the large volume of the system and the relevant operating conditions, a special injection device is used for the introduction of tracer into the column (Figure 5.3). The tracer solution is contained in a compartment that is pressurized and then the tracer pulse input is achieved with a solenoid valve to ensure that an equal quantity of the tracer solution is injected in each run.

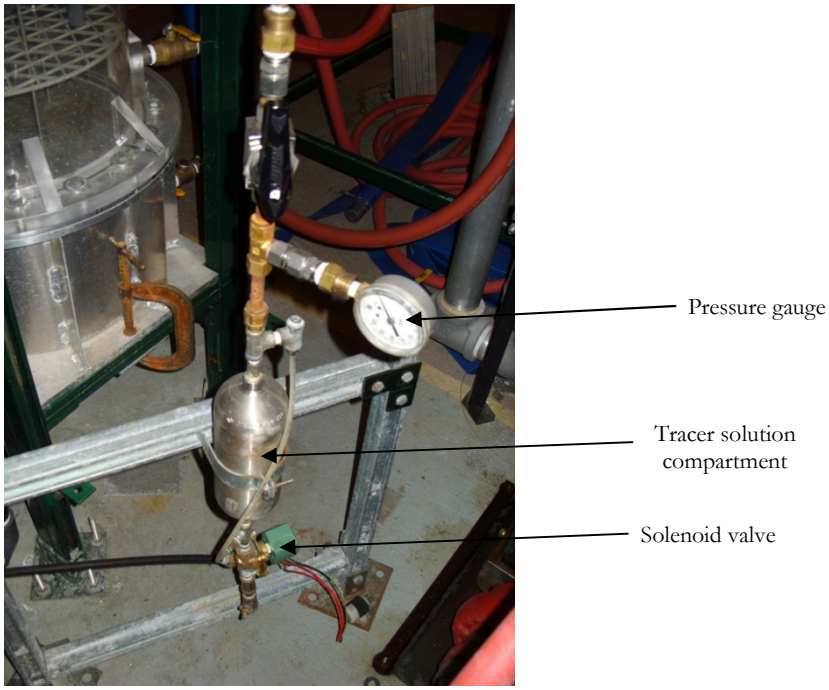

Fig. 5.3 – Tracer injection device

One of the two conductivity probes (#1) is mounted 14" above the sparger and just above the tracer injection point. The second probe (#2) was placed at the liquid outlet to capture the system's response as shown in Figure 5.4.

Fig. 5.4 – Conductivity probe (#2) inside a PVC tube at the liquid outlet

KCl was chosen as a tracer since it satisfies two important constraints: 1) It is non-volatile and miscible in the liquid phase (water), and 2) the conductivity of the (tracer+solvent) mixture is much higher than that of solvent (water) only. This enables one to record and distinguish the resulting signal from base lines. By trial and error, the concentration of the tracer solution utilized in the current study was chosen to be 0.1g/ml of KCl which (considering the volume of the column) did not result in any change in the hydrodynamic behavior of the system as monitored by bed expansion/gas holdup visual observations. Further details on the ideal pulse assumption, probe characteristic response time and calibration procedure can be found elsewhere (Alvaré, 2002 and Gupta, 2002).

5.4 – Experimental Procedure

1. The KCl solution is prepared and the compartment in the injection device is filled and pressurized by means of an inert gas.

2. The flow rates of the gas and liquid are adjusted and the system is allowed few minutes to reach steady state.

3. Once a constant flow is exiting from Drain outlets, data acquisition starts for 30 s. prior to the tracer injection by means of the solenoid valve in order to establish a base line of the signal.

4. Following the injection, 9 min 30 s. are allowed for the tracer to be completely washed out of the system. The data acquisition is then stopped. Five more minutes are allowed before the start of the first reproduced run.

5. The generated data is analyzed carefully after the utilization of the filtering algorithm (Gupta, 2002) to minimize the noise that is typically encountered in 2-phase systems.

5.5 – Results and Discussion

5.5.1 – Preview

When an ideal tracer pulse is introduced/injected with an entering fluid to a vessel, the spreading of the pulse within the system can be caused by velocity profiles or mixing. The collection of the tracer at the exit point of the system and the analysis of the shape of the resulting response curve can provide information about the system's behavior (Levenspiel, 1999). Along these lines, a number of measures are quantified in the current work to evaluate the effect of internals on liquid mixing in bubble columns. These can be summarized as follows:

$\bar{t}$ =the mean time of passage or the mean residence time of the tracer.

σ^2=the variance or the measure of the curve's spread.

$$\bar{t} = \frac{\int_0^\infty t\ C\ dt}{\int_0^\infty C\ dt} = \frac{\sum t_i C_i \Delta t_i}{\sum C_i \Delta t_i}$$

$$\sigma^2 = \frac{\int_0^\infty (t-\bar{t})^2\ C\ dt}{\int_0^\infty C\ dt} = \frac{\int_0^\infty t^2\ C\ dt}{\int_0^\infty C\ dt} - \bar{t}^2$$

$$Or, \qquad \sigma^2 \cong \frac{\sum (t_i - \bar{t})^2\ C_i\ \Delta t_i}{\sum C_i\ \Delta t_i} = \frac{\sum t_i^2 C_i\ \Delta t_i}{\sum C_i\ \Delta t_i} - \bar{t}^2$$

The dimensionless variance (σ_D^2) is a convenient way of describing the backmixing of a system with values ranging from 0 (Plug Flow) to 1 (perfectly mixed), where:

$$\sigma_D^2 = \frac{\sigma^2}{\bar{t}^2}.$$

5.5.2 – Notes on the data analysis procedure

a) As pointed above, the data acquisition started 30 s. prior to the tracer injection. Therefore, the signal from the probe located at the injection point (#1) was used to determine the time of initiation of the data series (t=0).

b) The filtering algorithm developed by Gupta et al. (2000) was utilized to smooth the resulting tracer signals. By trial and error, a cut-off frequency of 0.5 Hz and a tolerance no larger than O (10^{-3}) were found appropriate.

A word of caution is that the utilization of the filtering algorithm in case of such high superficial gas velocities deep in the churn turbulent flow regimes is expected to be associated with uncertainty due to large resulting noise. This explains the difficulties in assessing some of the output curves as will be shown later.

c) The response curves were normalized during the analysis taking into account the maximum and minimum values of resulting curves and the output plots are expressed by:

$$R_{norm.} = \frac{R - R_{min}}{R_{max} - R_{min}}.$$

Two examples of typical response curves are shown in Figures 5.5 and 5.6. Clearly, the first peak results from the probe at the injection point (#1) which was found to satisfy the assumption of an ideal pulse given by Prenosil et al. (1968) stating that:

$\Delta t/\bar{t} < 0.05$ is the criterion to check the validity of the pulse, where Δt is the injection time.

For instance, this ratio for the example cases shown in Figures 5.5 and 5.6 is 0.016 and 0.015, respectively.

It should be noted that several probes have been utilized during the experiments which explains the different range of output signal between the two figures.

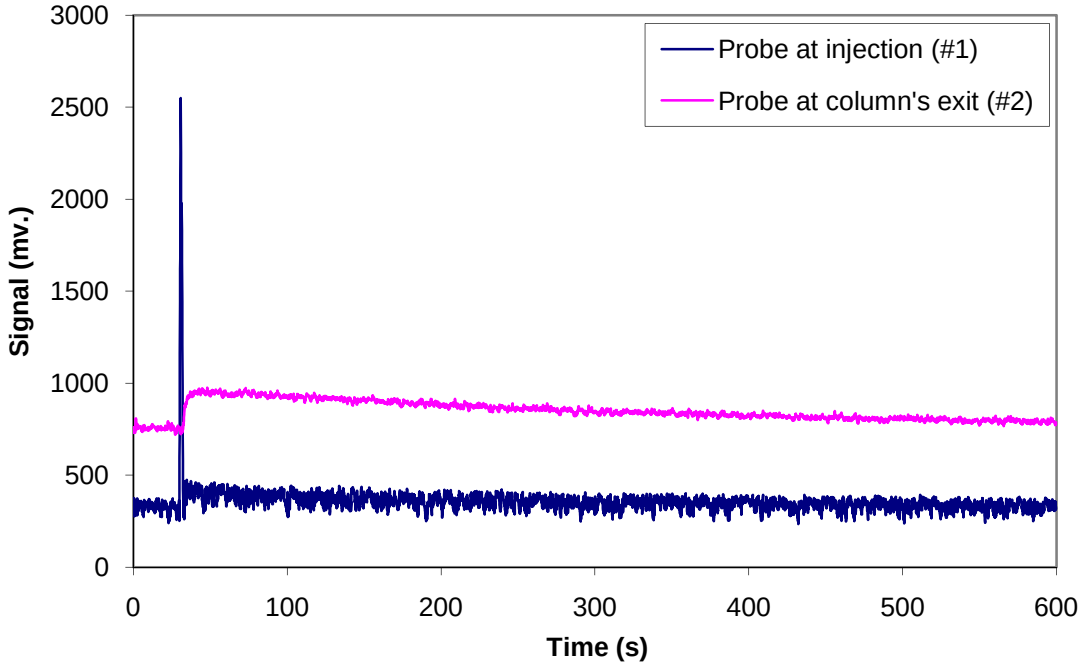

Fig. 5.5 – Filtered output signal from conductivity probes at Ug=45 cm/s and U_l=0.5 cm/s in a column with no internals

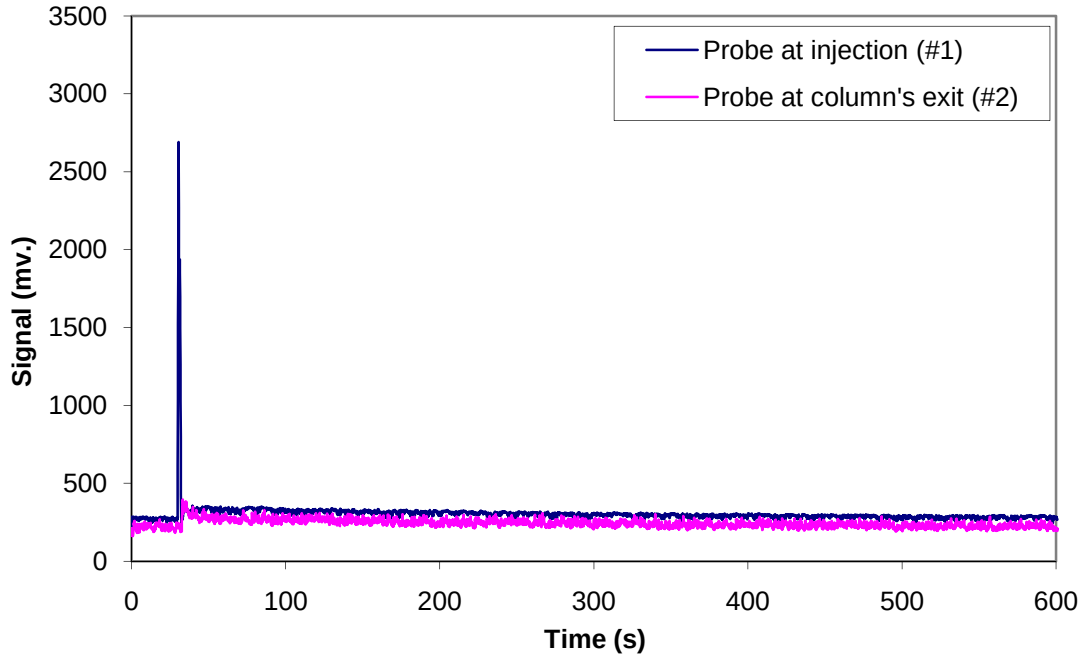

Fig. 5.6 – Filtered output signal from conductivity probes at Ug=20 cm/s and U_l=0.5 cm/s in a column with 25% internals

As mentioned above, the main objective of the current study is to qualitatively examine the impact of dense internals on the liquid phase mixing characteristics. This is accomplished by discussing the effect of internals (and operating conditions) on the shape and magnitude of the response curves obtained from probe #2. The investigation of the relevant measures (i.e., mean residence time and dimensionless variance) will provide insight on the liquid backmixing with presence of internals.

Figure 5.7 shows the normalized response curves at Ug=20 cm/s and U_l=1 cm/s with and without internals.

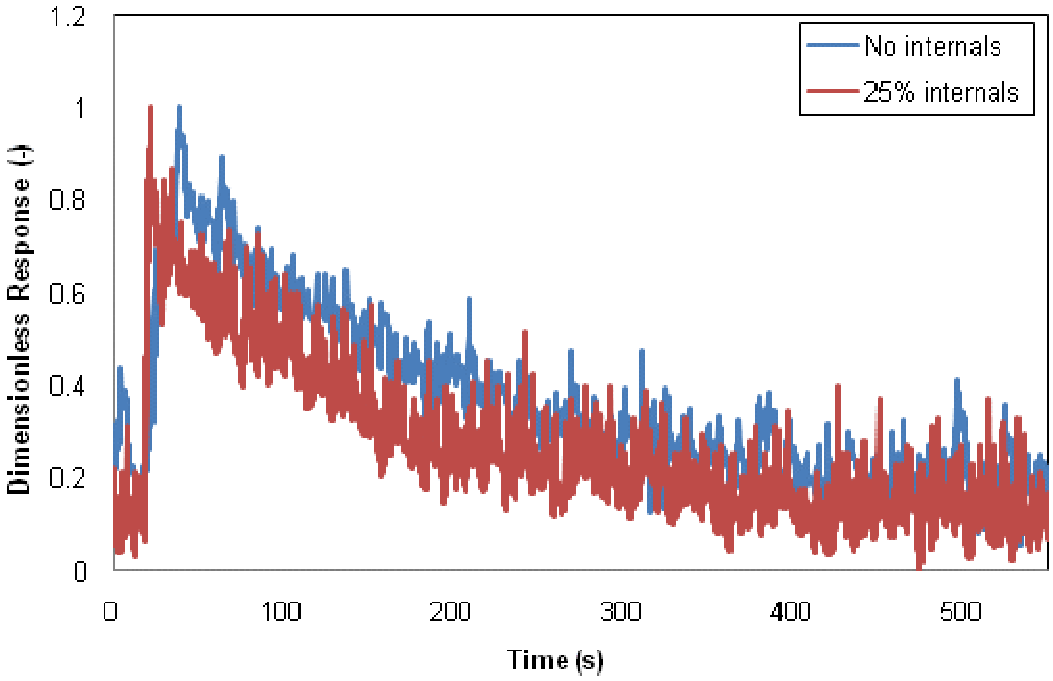

Fig. 5.7 – System response curves with and without internals (Ug=20 cm/s and U_l=1 cm/s)

Although the data is presented after filtration, it is obvious that the noise contribution is large. However, the analysis via the evaluation of the corresponding first moments and variances allows for better understanding of the associated phenomena. Table 5.1 lists these values for the above case. In addition, the axial dispersion coefficient of the liquid phase (lumped with the liquid holdup), back-calculated from the dimensionless variance, is computed assuming open-open boundary conditions and utilizing the Axial Dispersion Model (ADM) for simplicity and for lack of better knowledge on systems with internals.

Dimensionless variance = 2/Pe + 8/Pe^2 (Thyn, et al., 2000)

where, $Pe = \frac{U_l L}{D_{ax}(1-\varepsilon_g)}$

Table 5.1 – Measures of response curves from Figure 5.7

	Ug=20 cm/s - U_l=1 cm/s	
	No internals	**25% internals**
Mean residence time (s)	217.4	200.1
Variance (s^2)	24453	23377
Dimensionless variance (-)	0.52	0.58
$D_{ax}(1-\varepsilon_g)$ (cm^2/s)	42.4	45.8

Similarly, Figure 5.8 shows the results for the case of Ug=30 cm/s and U_l=1 cm/s.

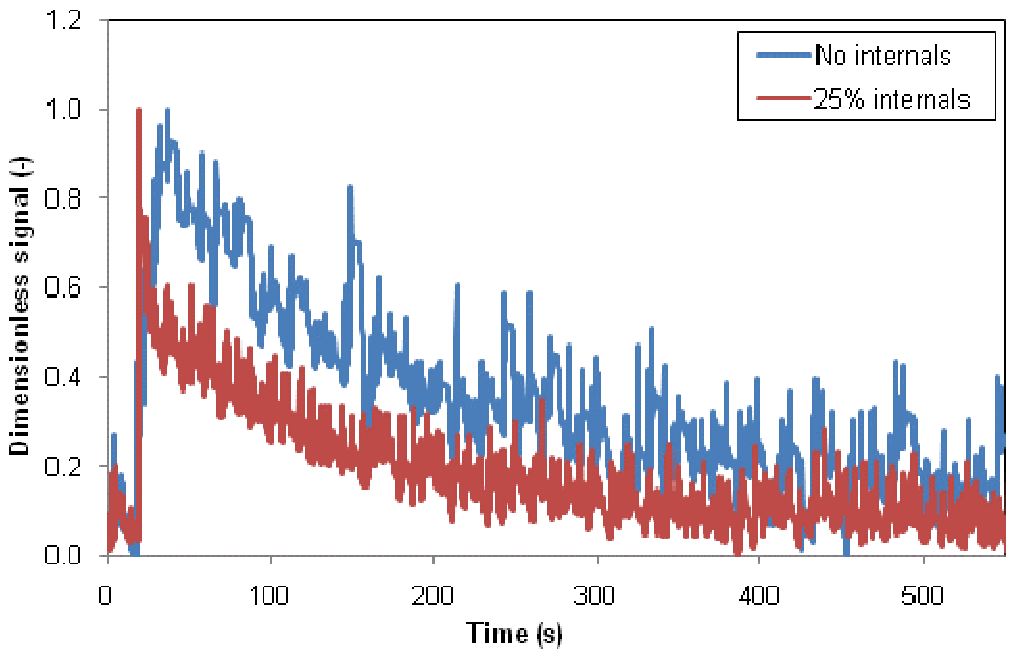

Fig. 5.8 - System response curves with and without internals (Ug=30 cm/s and U_l=1 cm/s)

The quantification of curves' characteristics is shown in Table 5.2. So far, it can be concluded that the insertion of internals yields a higher dimensionless variance. Thus, the system shifts towards more mixed behavior, as is also the case when the superficial gas velocity increases from 20 cm/s to 30 cm/s. Due to the internals, an increase in the

dimensionless variance of 10% at Ug=20 cm/s and of 17% at Ug=30 cm/s occurs compared with the column with no internals. This increase is accompanied by a corresponding decrease in the residence time of the tracer in the system.

Table 5.2 - Measures of response curves from Figure 5.8

	Ug=30 cm/s - U_l=1 cm/s	
	No internals	**25% internals**
Mean residence time (s)	215.9	194.7
Variance (s^2)	24358	23997
Dimensionless variance (-)	0.52	0.63
$D_{ax}(1-\varepsilon_g)$ (cm^2/s)	42.4	48.6

Similarly, at higher superficial liquid velocity (U_l=1.5 cm/s), the residence time decreases and the dimensionless variance increases as a result of the increase of internals density (Figures 5.9 and 5.10).

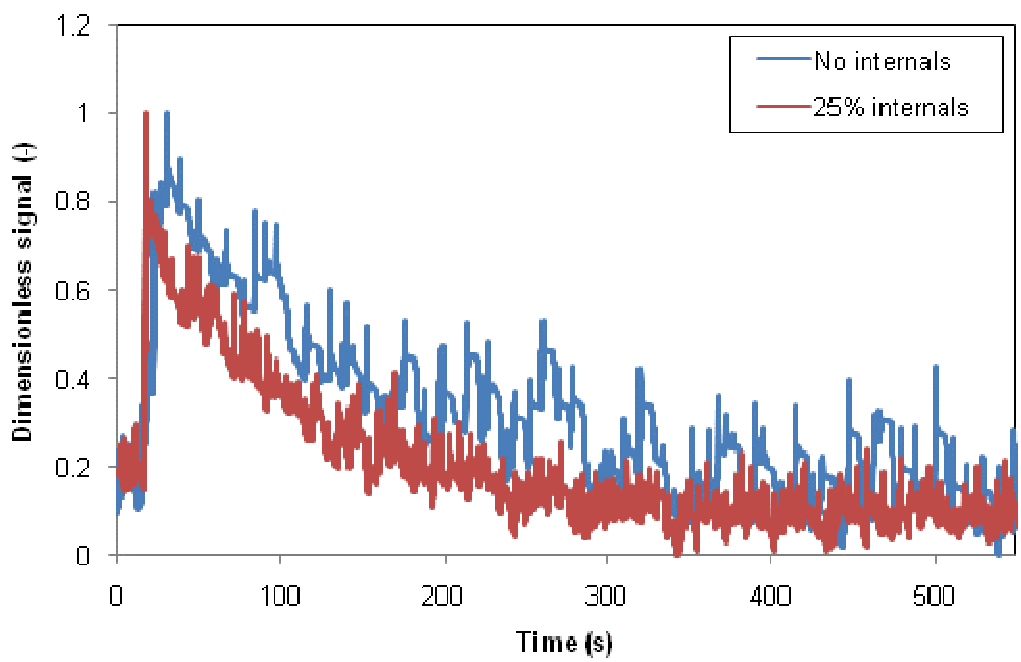

Fig. 5.9 - System response curves with and without internals (Ug=30 cm/s and U_l=1.5 cm/s)

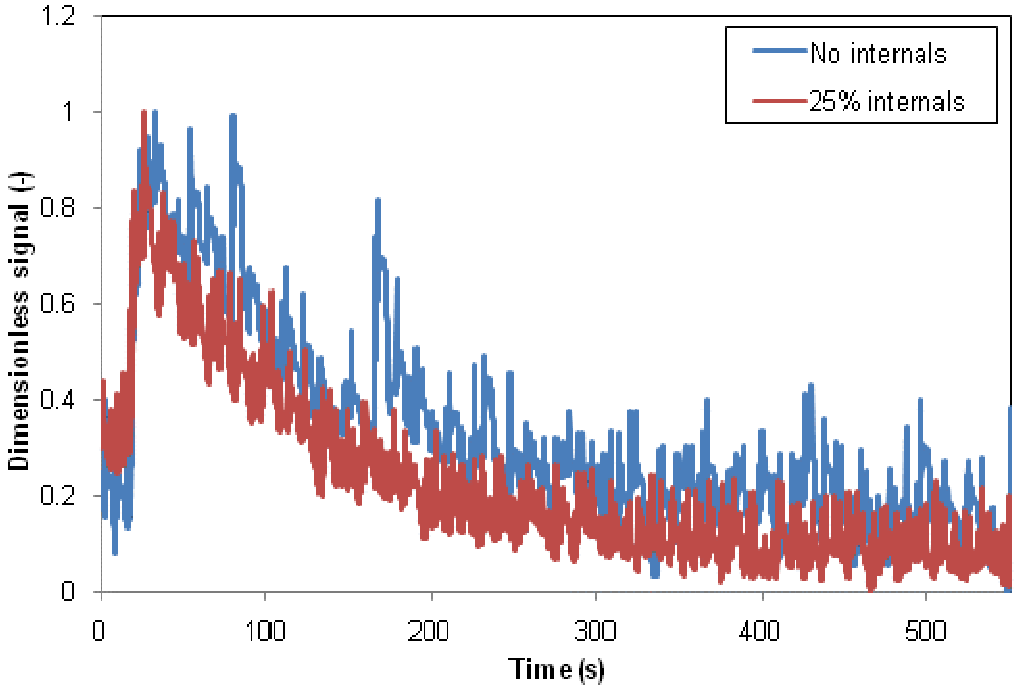

Fig. 5.10 – System response curves with and without internals (Ug=45 cm/s and U_l=1.5 cm/s)

Finally, Table 5.3 summarizes the effect of internals and superficial gas velocity for the above two cases.

Table 5.3 - Measures of response curves from Figures 5.9 and 5.10

	Ug=30 cm/s - U_l=1.5 cm/s		**Ug=45 cm/s - U_l=1.5 cm/s**	
	No internals	**25% internals**	**No internals**	**25% internals**
Mean residence time (s)	206.6	176.2	202.9	167.2
Variance (s^2)	23338	23405	24378	21768
Dimensionless variance (-)	0.55	0.75	0.59	0.78
$D_{ax}(1-\varepsilon_g)$ (cm^2/s)	44.2	54.9	46.4	56.4

A clear trend can be deduced from the above results since there is a consistent increase in the extent of liquid mixing as a result of vertical internals covering 25% of the column's CSA. This increase reaches its maximum (24%) at the extreme conditions applied in this work (Ug=45 cm/s and U_l=1.5 cm/s).

It is noteworthy that the above findings are in line with earlier studies since Bernemann (1989) observed an increase in the effective dispersion coefficient as a result of the addition of vertical internals in columns of different diameters. He agreed with Shah et al. (1978) and Kafarov (1975) that the increase in the dispersion coefficient was not due to the increase in the actual gas velocity resulting from the decrease in the free (open) CSA but was caused by the physical effect that the tubes themselves imposed on the flow and mixing behavior through their effect on the bubbles rising motion. The longitudinal internals tend to damp the undisturbed tumbling motion of the rising large bubbles and impose a more linear rising motion as confirmed from the findings presented in Chapter 4. Moreover, 25% internals result in an interstitial gas velocity (i.e., actual gas velocity based on open CSA only) of 26 cm/s and 40 cm/s for corresponding superficial gas velocities of 20 cm/s and 30 cm/s. One wouldn't expect the boost in the dimensionless variance reported above to be solely caused by this increase in the gas velocity. However, further experimentations with internals covering different CSA (more and less than 25%) at a wider range of gas velocities are recommended to confirm this finding.

5.6 – Conclusions

The main conclusions from this Chapter can be listed as follows:

1) It is confirmed that the increase in the superficial gas velocity leads to an increase in the liquid mixing for columns with internals, as was proved before for columns without internals (e.g., Yang and Fan, 2003)

2) The insertion of internals covering 25% of the total column's CSA results in an increase in the dimensionless variance. In other words, the dense internals structure causes an enhancement in the liquid phase mixing which drives the system's behavior farther than that of a plug flow reactor.

3) The effect of internals on liquid mixing is most pronounced at the extreme conditions involving the highest superficial gas velocity (Ug=45 cm/s) and the highest superficial liquid velocity (U_l=1.5 cm/s).

The latter point is worth investigating at higher superficial gas and liquid velocities which could not be achieved with the current facilities.

Finally, it is important to point out that limited information could be drawn from the RTD curves presented above and that the dimensionless variance is only an overall measure of the liquid phase mixing behavior. Moreover, more rigorous parameters (Péclet number and/or the backmixing coefficient) obtained from adequate models.

It is recommended to make use of available mechanistic models to describe the systems with internals. Based on the data obtained in Chapters 4 and 5, it is obvious that models compartmentalizing the reactor in several zones might be a good approach to follow. Specifically, Gupta's (2002) phenomenological models need to be implemented for the columns with internals and to be modified accordingly. This need stems from the fact that the flow behavior changes dramatically with presence of internals showing a clear central plume of the gas phase that is flowing upwards and another plume flowing downwards at the annular region.

It is, however, a fact that with incomplete database in systems equipped with internals, the development of a suitable model for the estimation of the liquid phase mixing in bubble columns with internals needs to be further addressed.

Chapter 6

Scale-up of Bubble Column Reactors

6.1 - Scope

The scaling of bubble column reactors is a challenging task. Dudukovic (2007) summarizes the scale-up issue as follows: "Once the reaction system is successfully run in the laboratory to produce the desired conversion, yield, and selectivity, reproducing these results at a commercial scale is next". For this to be achieved, Euzen et al. (1993) list three types of experiments that need to complement each other: laboratory studies, pilot-plant studies, and mock-up (cold flow models) studies. The first category includes the thermodynamics and kinetics assessments and their experimental verification in lab scale units; the second involves the simultaneous analysis of physical and chemical mechanisms and implies mathematical models that are transposable to industrial units; and the last category typically includes the utilization of dimensional similarity and the utilization of RTD measurements via tracer studies for example.

Deckwer and Schumpe (1993) differentiate between two types of scale-up based approaches, namely 'know-how' and 'know-why'. In the first, conventional scaling rules and dimensional analysis guidelines are followed as clarified above, while for the second, an estimation of the rates and limiting steps of the entire process are normally considered as a starting point. Along these lines, Dudukovic (2009) classifies scaling into 'vertical scale-up' where an increase in size is implied and 'horizontal scale-up' or scale out (scale-in-parallel). In the latter, a multiplication of the small units is adopted keeping geometry, flow pattern and regime the same.

With a diameter of 5 m and a height of 22 m, Sasol is operating its slurry bubble column reactor for Fischer Tropsch synthesis (Krishna, 2000). Laboratory scale bubble column units have diameters of about 25 cm (Krishna et al., 2001). Such huge difference between the two scales indicates that scale-up calculations are essential for approaching industrial applications.

It is noteworthy that anticipated scale-up problems of a slurry bubble column for the Fischer-Tropsch synthesis were among the main reasons Shell decided to implement the

multi-tubular trickle bed technology in their plant in Malaysia, for a quicker and safer route (de Swart, 1996).

6.2 - Preview

As highlighted in Chapter 2, few researchers have attempted to derive the scaling relations for bubble columns. Earlier studies only met with limited success. These, mostly, followed the conventional scaling rules as derived from mass and momentum balances resulting in dimensionless hydrodynamic numbers like Reynolds (Re) and Froude (Fr). For example, van den Bleek and Schouten (1993) suggested that for proper scaling these numbers should be kept constant, together with dimensionless geometric numbers, such as L/D, in order to ensure both dynamic and geometrical similarity.

Based on careful literature review and analysis of three-phase systems, Safoniuk et al. (1999) identified eight variables they believed to affect the bed hydrodynamics significantly. These are the superficial liquid velocity (U_L), the superficial gas velocity (U_g), the liquid viscosity (μ_L), the interfacial surface tension (σ), a buoyancy term ($\Delta\rho g$), the catalyst particle diameter (d_p), the liquid density (ρ_L), and the solids density (ρ_p). They utilized the pi Buckingham theorem to group these variables into five dimensionless groups, namely:

$$M = \frac{g\Delta\rho\mu_L^4}{\rho_L^2\sigma^3}, Eo = \frac{g\Delta\rho d_p^2}{\sigma}, Re_L = \frac{\rho_L d_p U_L}{\mu_L},$$

$$\beta_d = \frac{\rho_p}{\rho_L}, and\ \beta_U = \frac{U_g}{U_L}.$$

For their experiments at atmospheric pressure, no inclusion of the gas density is present (except within the $\Delta\rho$ term). Also, no geometric similarity constraints were added, with the assumption that d_p<<D and d_b<<D would suffice to guarantee insignificant wall effects. Matching the dimensionless numbers between a laboratory column and an industrial unit yielded an acceptable simliraty in behavior. However, the differential pressure measurements of hold-up showed discrepancies with the industrial data for the covered range of operating conditions. The authors concluded that the bed expansion (gas holdup) is a strong function of the liquid flow rate and, hence, Re_L and the gas holdup is also highly dependent on the gas velocity and, hence, Re_g (=Re_L*β_U).

To investigate further this methodology, Macchi et al. (2001) tested 2 systems involving phases of different physical properties but could not obtain dynamic similarity. Although the above five dimensionless numbers were matched for the two systems, neither the gas holdup nor the minimum fluidization velocity were the same. Differences were attributed to the complex coalescence behavior of the liquid mixtures and as a result, the authors recommended the utilization of more than five dimensionless numbers to characterize the hydrodynamics of such multiphase systems.

Obviously, adopting such scaling mechanisms is difficult in such complex systems and the process becomes overly cumbersome. Therefore, novel methodologies need to be proposed. Hence, it is not surprising that Deckwer and Schumpe (1993) concluded that 'know-how' based scale-up should be replaced by 'know-why' based models.

Two examples are highlighted below due to their relevance to the proposed scale-up methodology hereafter.

In 1958, Kölbel and Ackermann patented a slurry reactor design for carrying out the Fischer-Tropsch process. Their design was meant to decrease the disadvantageous recirculating effect well-known to occur in large, commercial-scale columns. Kölbel and Ackermann proposed a way to subdivide the reactor space using similar vertical shafts which were open at both the top and the bottom. The design was meant to suppress the strong liquid recirculation that results from the large difference in buoyancy forces between the center of the column and the walls. The gas supply to the shafts was equalized, and the reaction results were similar to what one would obtain in a reactor of the same size as one shaft with its own gas distributor. The configurations of the shafts presented by the authors are shown in Figure 6.1 with 'a' denoting the vertical shafts and 'b' indicating the heat exchanger tubes. Figures 6.1 (a), (b), (c) and (d) illustrate the heat exchange pipes positioned inside the shafts, while Figures 6.1 (e) and (f) show the heat exchange pipes located in part or entirely through the intermediate spaces between the shafts, respectively. To eliminate the dead spaces between the shafts caused by circular geometry (Figures 6.1 (a, e and f)), hexagonal geometry was suggested (Figures 6.1 (b, c and d)). The ultimate result of the Kölbel and Ackermann work was the elimination of the large vertical recirculation loops and

the formation of a stable liquid (slurry)-gas suspension system in each shaft with uniformly sized gas bubbles and a uniform rate of rise.

The latter study is significant since it not only shows a thorough understanding of the needs in practice but also offers a methodical solution to one of the major drawbacks of bubble columns (backmixing). It provides as well insight on scale-up related issues. Compartmentalizing the bubble column can serve as the basis of a novel design for scaling up bubble column reactors in parallel.

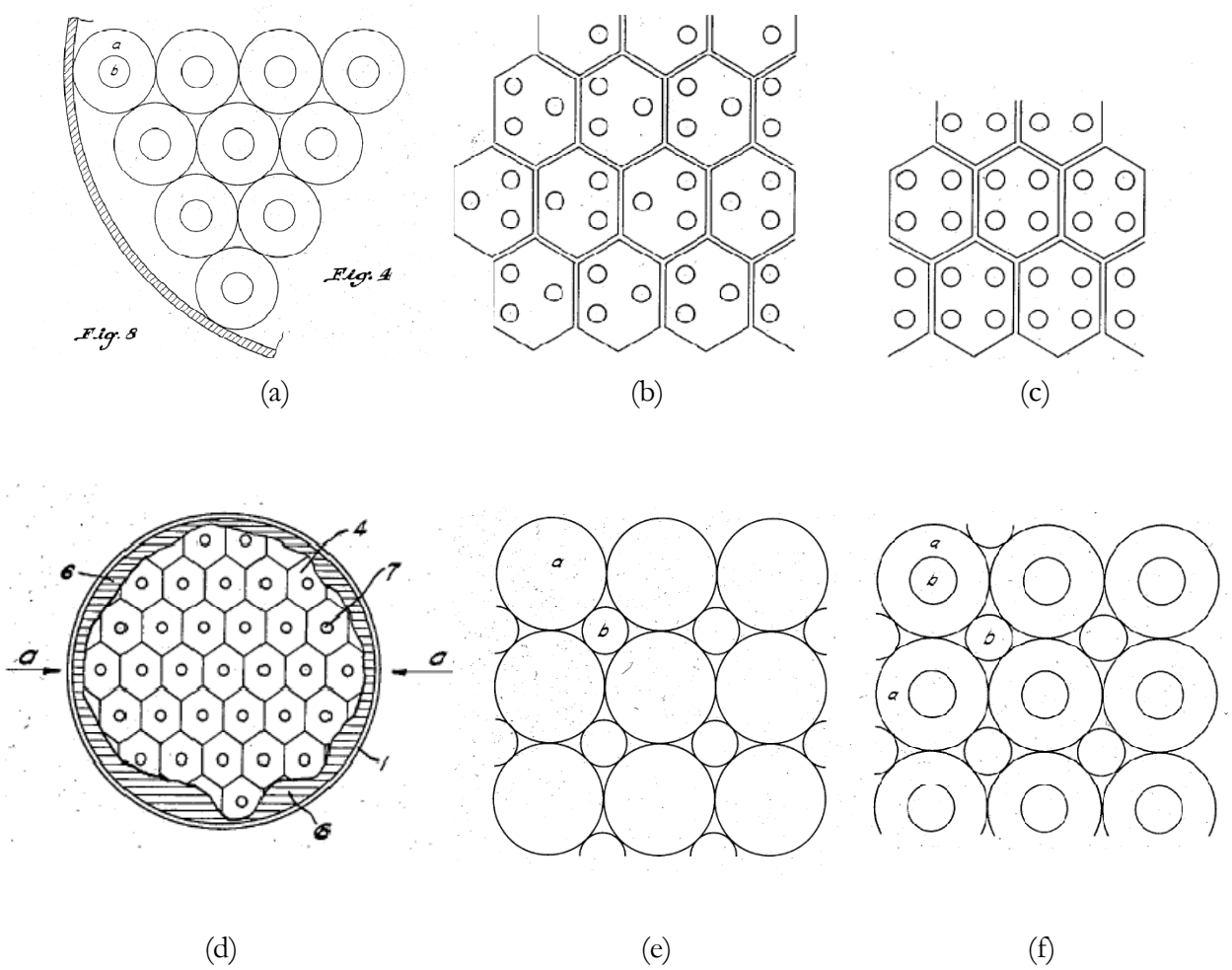

Fig. 6.1 – Various designs of slurry phase bubble column compartmentalized by means of shafts and with the presence of internal heat exchanging tubes (Kölbel and Ackermann, 1958)

The second example is presented in Sasol's recently published patent (Steynberg et al., 2009) on the design of Fischer-Tropsch slurry reactor. They have addressed the scale-up risks by developing a solution based on the creation of zones in the reactor that effectively mimic the behavior of a reactor with a smaller characteristic diameter. The reactor involves a plurality of vertically extending horizontally spaced channels inside the outer shell of the reactor. These discrete channels are separated by heat transfer medium flow spaces. They claimed that the design and testing of each of these channels on a pilot plant scale is feasible rendering the scaling process easier. In addition, such design allows preventing the formation of macro-scale mixing patterns. Finally, the presence of heat exchanging surfaces surrounding the slurry channels leads to improved heat transfer since higher removal surface area is provided with a more uniform spread.

6.3 – Hypothesis

As mentioned before, the exothermic Fischer-Tropsch reaction (as well as many other applications for which bubble column reactors are preferred) requires heat exchanging internals that cover ~25% of the Cross-Sectional Area (CSA) of the reactor to remove the resulting heat generation and maintain a safe operation. The positions of these tubes might be configured in multiple arrangements. Can they be arranged so that they in effect form small internal bubble columns within the large scale reactor walls? If so, can they, in such a configuration, mimic the behavior of columns of the same small diameter having a solid wall instead? The answer to this question forms the basis for the hypothesis of our proposed methodology for minimizing the risks associated with scaling. In other words, it is to be investigated whether the commercial reactor can be formed of multiple smaller scale reactors in parallel created by means of the necessary heat exchanging internals. Therefore, controlling the effect of scale using internals by means of reactor compartmentalization is proposed in this study.

As noted earlier, Shaikh (2007) suggested that dynamic similarity can be achieved as follows: "Overall gas holdup and its radial profile or cross-sectional distribution should be the same for the two reactors to be dynamically similar." While that assertion is correct, it does not reporesent a scale up rule since both profiles must be measured. We use it here however as a means to assess whether our methodology works. Hence, the hydrodynamics (primarily gas

holdup radial profiles and bubble dynamics) were investigated inside the above mentioned structured column using the four-point optical probe to assess the new design methodology.

The stepwise details of this methodology can be summarized as follows:

- The large reactor diameter is subdivided into similar, vertical compartments by means of the cooling tubes.
- The compartments are to have a diameter similar to that of a small scale column having solid walls on which investigations can be (have been) performed.
- The various hydrodynamic parameters within each compartment are to be compared with those measured in a bubble column of the same diameter.

6.4 – Experimental Setup

The first step of the work was to build an internal circular bundle of 6" diameter arranged concentrically within the 18" diameter column (See Figures 6.2, and 6.3 for detailed design).

The 18" diameter column, shown in Fig. 4.1, made of two Plexiglas sections of 74" height each, was used. The internal circular bundle is composed of 19 PVC rods of 1" diameter each and has an inner diameter of 6". The structure was fixed by means of a top plate as shown in Figure 6.3 (b) and three spacers as shown in Figure 6.3 (a). This tube bundle was allowed to hang 5" above the gas distributor. An air-water system was used with the gas continuously fed through a perforated plate at the bottom of the column into a batch bed of liquid.

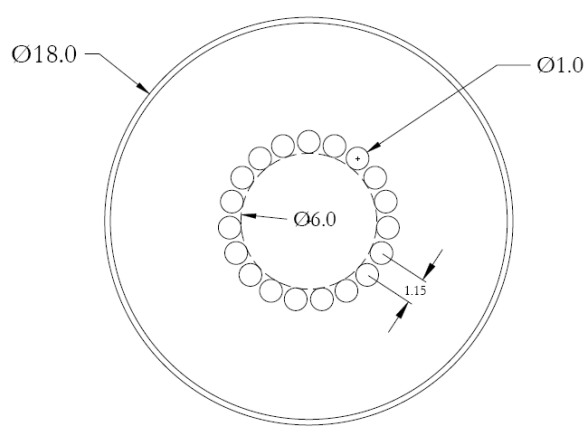

Fig. 6.2 - Schematic diagram of 6" diameter internals bundle inside 18" diameter column

The perforated plate distributor described in Chapter 4 is in use. The four-point optical probe is used to determine the local gas holdup profile at selected conditions within the bundle

(a)

(b)

Fig. 6.3 – Experimental setup for scaling approach, (a) Photo of 6" circular bundle inside 18" bubble column and (b) Photo of top supporting plate

It is to be noted that all holes of the sparger were active (i.e. not only those right below the compartment). The diameter of 6" for the internals circular bundle was chosen to allow comparisons with available database in the Chemical Reaction Engineering Laboratory (CREL). Note that Xue (2004) and Wu (2007) have obtained gas holdup radial profiles by means of the optical probe while Ong (2003) has generated similar data utilizing CT measurements in 6" stainless steel column under a variety of conditions.

6.5 – Preliminary Considerations

For illustration of the viability of this methodology, the case given in Maretto and Piccolo (1998) is taken as a basis, where an industrial reactor of 7 m in diameter and 30 m in height is considered. In this example, the specific exchange surface area per unit volume (a_w) is

given as ~30 m^2/m^3 (heat transfer coefficient=0.39 kcal/m^2.s.K). For a 25% of the total CSA of the column covered with internals, one would need 18987 tubes of 1" diameter each, or 4746 tubes of 2" diameter each or 1186 tubes of 4" diameter each.

Now, using the new design with multiple compartments formed by the heat exchanging tubes, for 1" tubes and 6" ID circular bundles, ~20000 tubes would be needed in the reactor from the example above; while one would need less than 6750 tubes for 2" diameter tubes also with 6" ID circular bundles (see Specht, 2009, for calculation details).

It is to be noted, however, that the above simplified representation involves many of these circles along which the tubes are arranged to touch the outer diameter of the column and, hence, many tubes can be saved by substituting the hexagonal configuration for the cicular in order to also eliminate dead spaces, as pointed out by Kölbel and Ackermann (1958). In other words, it can be safely assumed that there would not be more tubes needed than in a conventional design and hence, no additional costs are involved.

Addressing the pitch issue, Krishna and van Baten (2003) have considered a typical FT case involving 5000-8000 tubes of 5 cm diameter each and with 15 cm pitch in a reactor of 6m in diameter. For the above calculation, the pitch would be ~6 cm for the case of 2" tubes. However, Korte (1987) used pitches as low as 4 cm and 7 cm.

For the mechanical and physical hook up of the new design, Rentech discusses cooling arrangements in FT slurry bubble column reactors (Hawthorne et al., 2006). Their main objective was to simplify removal and reinstallation of cooling tubes for reactor maintenance. They conclude that bundling the tubes is the key solution. They utilize rather different configuration.

The optimum diameter of the compartments is unknown at this stage but Wilkinson (1991) provides an equation for the minimum column diameter needed to avoid wall effects (slugging phenomenon) expressed as follows

$$D_{c,\min} = 20\left(\frac{\sigma^2}{g^2\,\Delta\rho\,\rho_G}\right)$$

Typically, 15 cm diameter is large enough to fulfill this requirement and the maximum diameter is to be determined by the total needed heat transfer surface area within the reactor and the exothermic nature of the chemical reaction.

6.6 – Proof of Concept

One of the first checks required for the validation of this methodology is to verify that the well-known 'parabolic' gas holdup radial profiles can be reproduced inside the compartment despite of the open spaces between the PVC rods allowing for exchange between the flow/bubbles inside and outside the bundle. Figure 6.4 shows the local distribution of the gas holdup at different superficial gas velocities. Qualitatively, it is clear that generated profiles with the tubes compartment are similar to those in solid wall columns. Data is satisfactorily reproduced and the expected increase in gas holdup with the increase of superficial gas velocity is well exhibited. The same observation applies to the specific interfacial area, the radial profiles of which are shown in Figure 6.5.

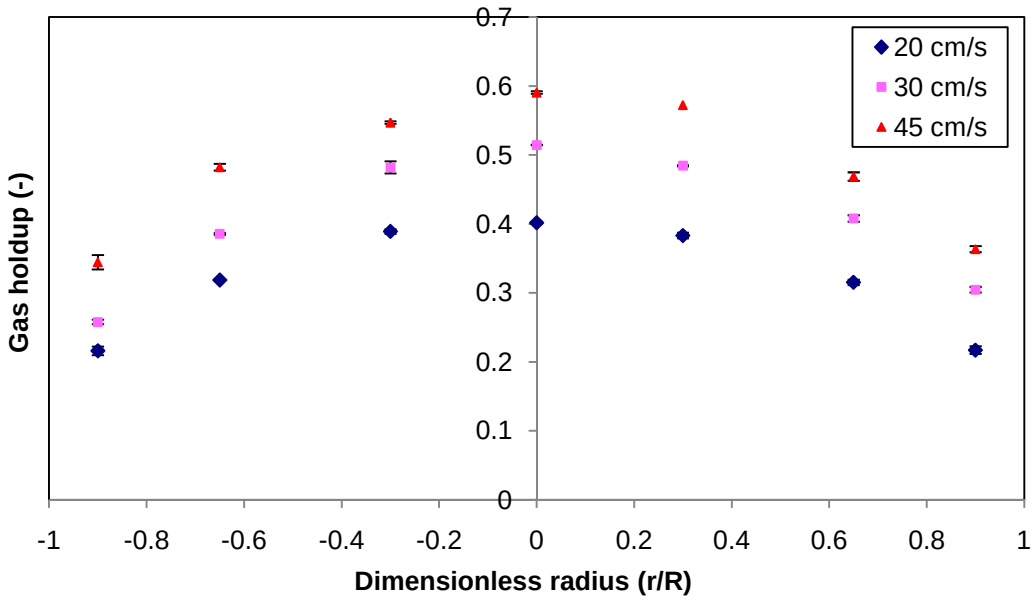

Fig. 6.4 - Radial gas holdup profiles inside the tube bundle

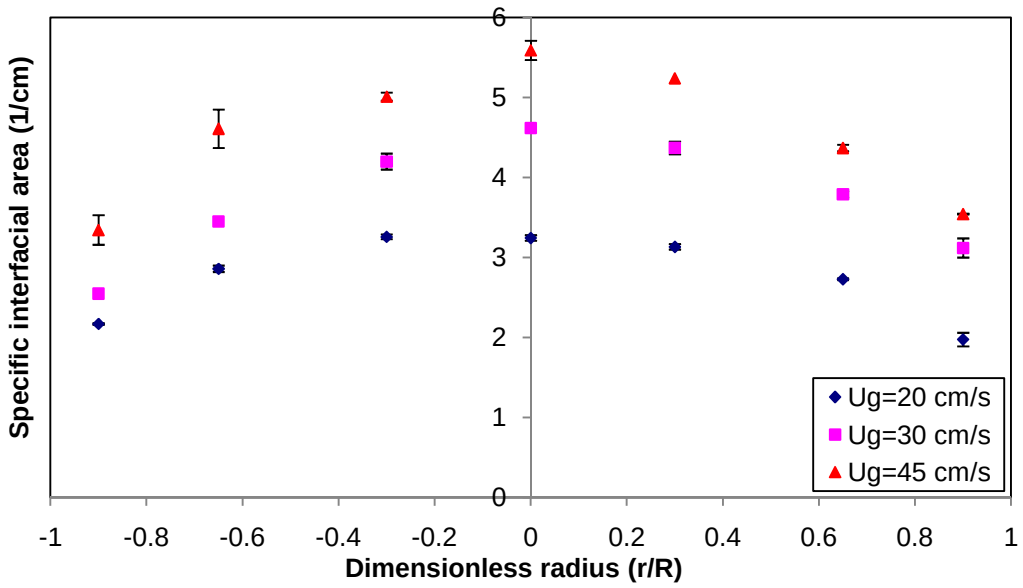

Fig. 6.5 – Specific interfacial area radial profiles inside the tube bundle

Second, an important confirmation relates to how close is the effect of such compartment boundaries formed of tubes when compared to that of a solid wall. Figure 6.6 shows the radial gas holdup inside the tube bundle (blue diamonds and bottom abscissa) compared to that generated in case of an 18" column with no tubes inserted (pink squares and top abscissa).

Obviously, at r/R=0.9 inside the tube bundle (which is equivalent to r/R=~0.3 in case of an empty 18" column), the gas holdup is 0.216 compared to 0.325 at the same locus should the tube bundle not exist. This represents a decrease of about 50% due to the presence of internals at this position. This finding confirms that the impact of the PVC rods in such arrangement is similar to that of a solid wall diminishing the gas holdup in the vicinity of the wall.

In the next section, the comparison between the solid wall column and that formed by the tubes bundle is emphasized.

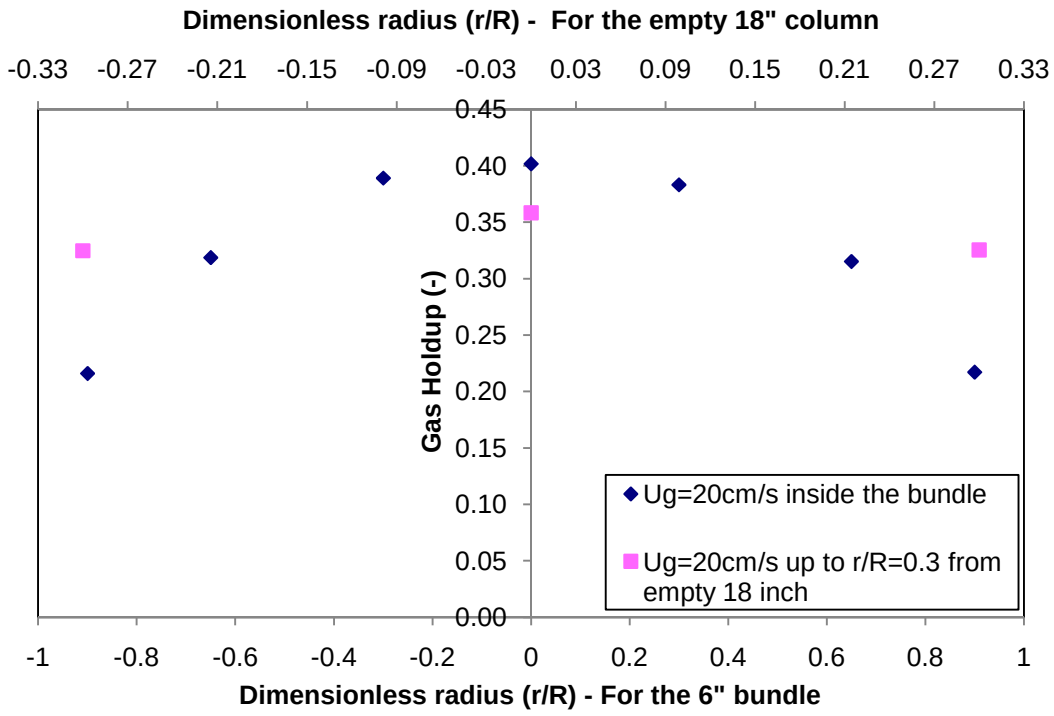

Fig. 6.6 - Comparison of rods vs. solid wall effect

6.7 – Results and Discussion

The above promising results motivated the second step of the scale-up methodology; the actual comparison between data generated within the tubes bundle and that within a solid wall bubble column. This motivation stems from the finding that the proposed arrangement of internals could mimic the solid wall effect as shown above.

Independent results of radial gas holdup profiles obtained by Xue (2004) and Wu (2007) using the optical probe technique in a separate unit consisting of solid wall column of the same diameter as our bundle of tubes are compared with the data generated in the current study.

Figures 6.7, 6.8 and 6.9 illustrate the gas holdup radial profiles in the two systems for Ug=20cm/s, 30cm/s, and 45cm/s, respectively.

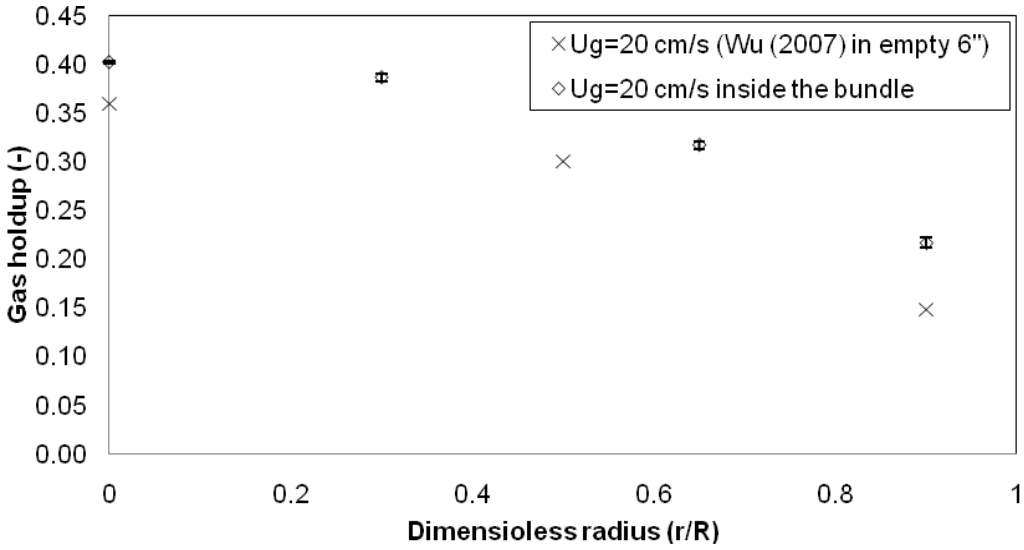

Fig. 6.7 - Radial gas holdup profiles inside circular bundle and in a steel bubble column of 6" diameter at 20 cm/s

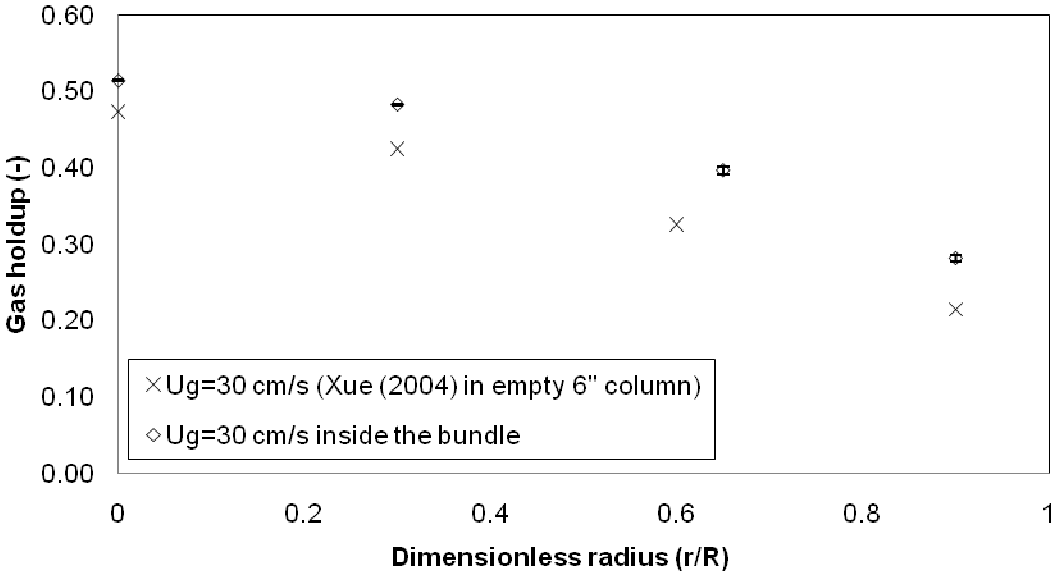

Fig. 6.8 - Radial gas holdup profiles inside circular bundle and in a steel bubble column of 6" diameter at 30 cm/s

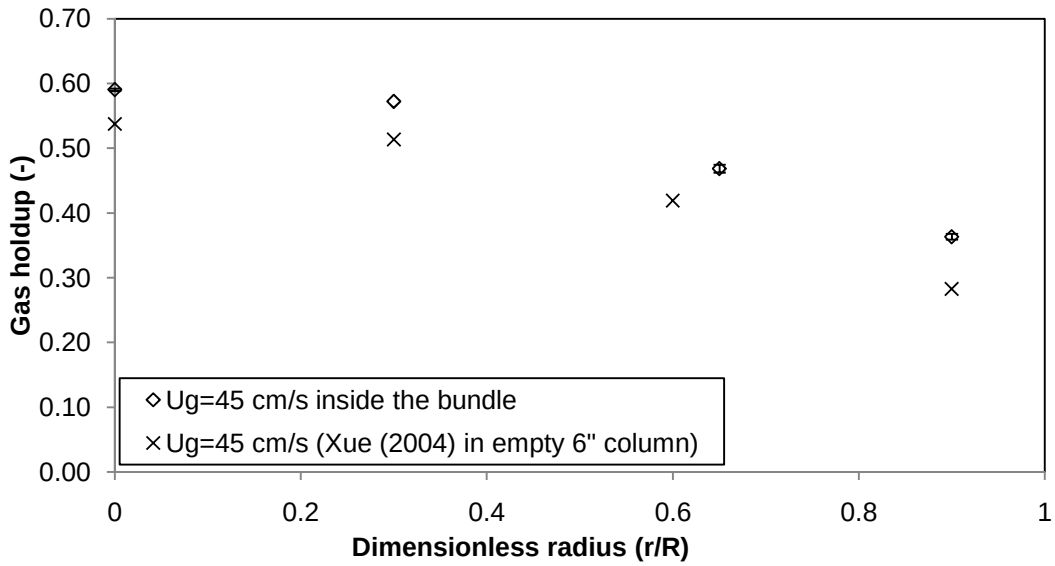

Fig. 6.9 - Radial gas holdup profiles inside circular bundle and in a steel bubble column of 6" diameter at 45 cm/s

The examination of the above figures reveals that the radial gas holdup profiles in the 6" tube bundle is always somewhat higher than the profile in columns of the same diameter with solid walls. The average difference between the two is ~15% while the maximum difference is only observed at the highest r/R. The latter was expected due to the interaction between the inside and outside of the tube bundle (note that in the current arrangement, the center-to-center tube pitch is 1.15"). Therefore, the new methodology adopting a small scale compartment within a large scale unit seems feasible. *A priori* prediction of the gas holdup distribution, the most important parameter in bubble columns, is possible by measurements in separate pilot units.

It should be noted that the relatively larger discrepancy between the holdup values in the column with solid walls and that formed by the tubes bundle can be attributed to the following. In a solid wall column, a 'no slip' boundary condition is valid at r/R=1. However, for the current system under investigation, not all surrounding wall is solid matter. Consequently, the 'no slip' condition is 'weakened'. As a result, the liquid velocity at this locus is not zero but rather has a value which will be denoted here as $u_{l,\ wall}$. In other words, although the absolute value of the gas holdup at the wall is higher for the tubes bundle case,

the liquid recirculation is diminished as a result of a lower gas holdup gradient between the column's center and the 'apparent' wall.

In order to quantify the above postulation, a modification to the One-Dimensional two-fluid model for liquid recirculation (Kumar et al., 1994) is presented below.

The simplified steady, one dimensional, axisymmetric two phase flow Reynolds equation of motion is:

$$-\frac{1}{r}\frac{d}{dr}(r\tau_{rz}) = \frac{dP}{dz} + \rho_l\big(1-\varepsilon(r)\big)g$$

With

$$-\frac{dP}{dz} = \frac{2\tau_w}{R} + \rho_l(1-\bar{\varepsilon})g.$$

Rice and Geary (1990) integrated the first equation above. And using the following gas holdup radial profile:

$$\varepsilon(\varphi) = \bar{\varepsilon}\frac{m+2}{m-2c+2}(1-c\varphi)$$

in which m is an arbitrary constant, c is a parameter allowing the possibility of nonzero void fraction close to the wall, and φ=r/R. The shear stress distribution in the region from the radial position where the liquid downward velocity is maximum to the wall was obtained as:

$$\tau_{rz}(\varphi) = \rho_l gR/2(\frac{\bar{\varepsilon}}{\lambda^2})\left[\frac{\lambda^2-\varphi^2}{\varphi}\right]$$

Then, a 'closure' can be sought by means of a constitutive equation using Prandtl's mixing length (Gupta, 2002) to express the shear stress as follows:

$$\tau_{rz}(\varphi) = \frac{\rho_{l v_m}}{R}(-\frac{du_l}{d\varphi})$$

Making use of the following boundary conditions:

$$u_l = u_l^* \; at \; \varphi = \lambda, and$$

$$u_l = u_{l,wall} \; at \; \varphi = 1$$

combining the above equations followed by integration yields:

$$u_l^*(\varphi) - u_{l,wall} = \bar{\varepsilon}\frac{gR^2}{4\nu_m\lambda^2}\{\varphi^2 - 1 - 2\lambda^2 ln\varphi\}$$

The above expression for the liquid velocity at the wall region implies that a knowledge of $u_{l,\,wall}$ is necessary which can be obtained from CARPT measurements that were not available for the current study.

Furthermore, the various bubble characteristics obtained from the probe measurements are compared between the current reactor configuration and a solid wall 6" diameter column. The p.d.f. of bubble chord lengths at the column's center, at Ug=45 cm/s, for the two cases is almost identical as shown in Figure 6.10.

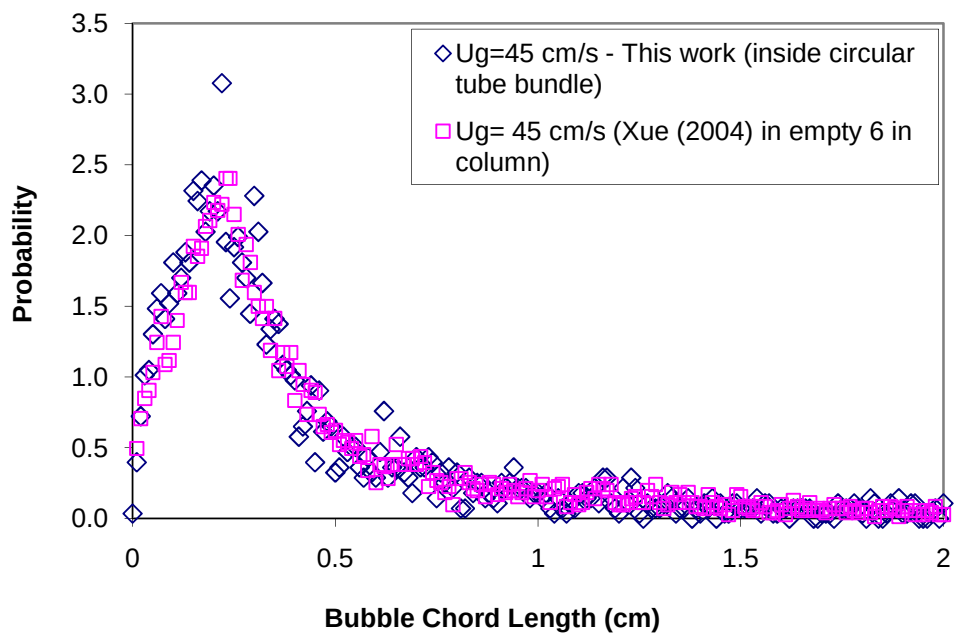

Fig. 6.10 – Bubble chord length distributions at the column's center and Ug=45 cm/s

The examination of the chord length distribution in the wall region (i.e., close to the PVC tubes for the current configuration and in the vicinity of the wall for the solid wall column) is presented in Figure 6.11.

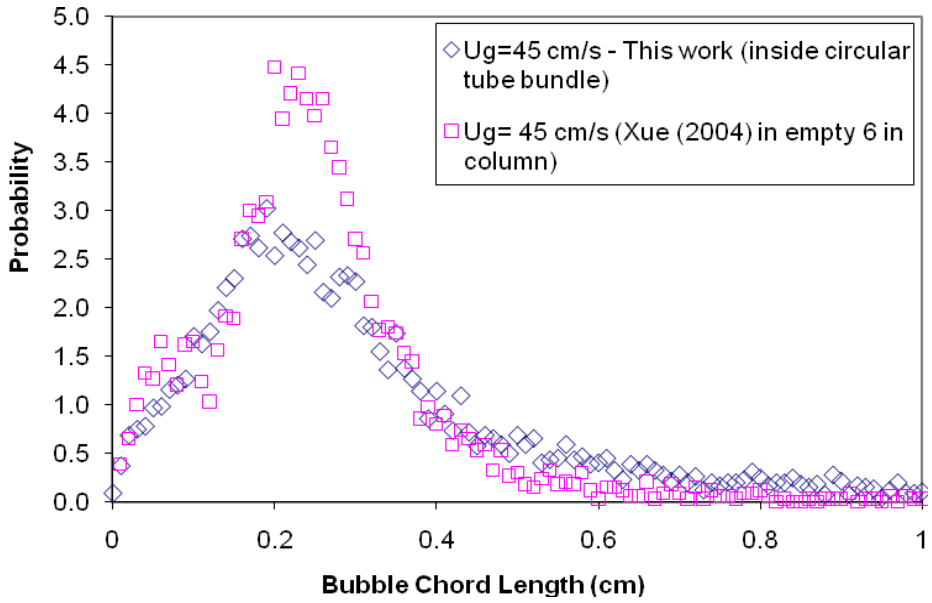

Fig. 6.11 – Bubble chord length distributions at the wall and Ug=45 cm/s

Although the two distributions match in trends, it is obvious that there is a higher probability of finding small chord lengths in the solid wall column. Such difference was expected as demonstrated in the local gas holdup profiles at this location because the flow exchange between the inside and outside of the bundle allows for agglomeration yielding larger bubbles as compared to a solid wall column. In addition, the flow inversion dragging the smaller bubbles in the annular region is somewhat reduced in the case of the circular PVC tubes bundle as further clarified by the following bubble velocity measurements.

The investigation of the bubble velocity probability distributions in both systems, the solid wall 6" column and the 6" circular tubes bundle, at the column's center is shown in Figure 6.12.

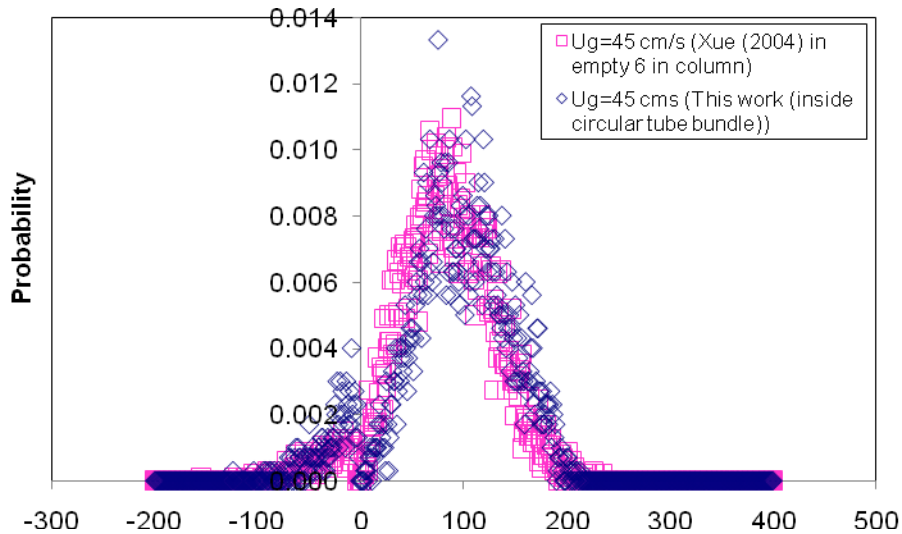

Fig. 6.12 – Bubble velocity distributions at the column's center and Ug=45 cm/s

The above Figure highlights the similarity between the bubble velocity distributions in the column's center. This observation is in line with reported local gas holdup values and chord length distributions in this location. On the other hand, the aforementioned interaction between the flow inside and outside the tube bundle, and the fact that all sparger holes were active resulting in upwards flow in the outer region of the PVC tubes bundle, turned out to be beneficial. Figure 6.13 displays the bubble velocity distributions at the wall region for the two compared systems at Ug=45 cm/s.

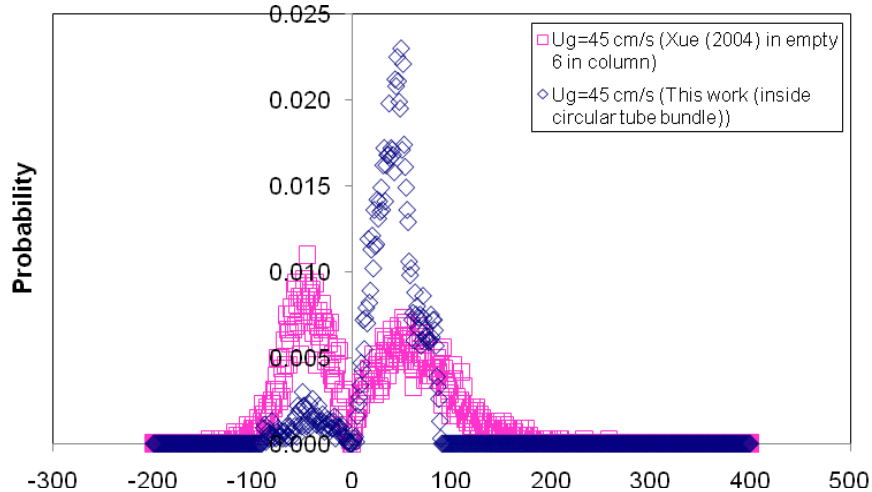

Fig. 6.13 – Bubble velocity distributions at the wall and Ug=45 cm/s

Obviously, there is a higher probability of bubbles moving upwards in the case of the tube bundle and a much smaller fraction of the bubbles move downwards. This observation may be attributed to a decreased backmixing and a more upwardly structured flow behavior throughout the cross section of the tube bundle. Similar conclusions were deduced by Kölbel and Ackermann (1958).

The logical future and final step would be to replicate the single bundle and to investigate the hydrodynamics within each, versus the results obtained in the 6" diameter column. It is noteworthy to mention that the utilization of compartments with hexagonal cross sections might be preferred over the circular ones in order to eliminate the possibility of dead spaces between the compartments and the loss of available heat exchange surface.

6.8 – Conclusions

A new design methodology for minimizing the scale-up risks for bubble column reactors is proposed and is under development. The new approach is sought to offer the following advantages:

- A simple, yet efficient, way of designing large scale bubble column reactors via reactor compartmentalization into small size columns.
- Better prediction of the performance of bubble columns based on a better control on the effect of scale.
- A more uniform bubble size.

However, further work is required in order to compare the gas and liquid phase mixing behavior in the tube bundle and the solid wall column to help validate the methodology.

Chapter 7

Conclusions and Recommendations

7.1 – Summary

This dissertation discussed the bubble dynamics and liquid phase mixing in bubble columns of different diameters with and without heat exchanging internals. A methodology of scaling bubble column reactors up was proposed making use of the presence of internal structures. The main findings of this work are summarized below.

7.2 – Conclusions

7.2.1 – Impact of internals on overall gas holdup

The impact of various configurations of internals was investigated and quantified over a wide range of superficial gas velocities. Increased density internals (i.e. increased percentage coverage of cross sectional area (CSA) by internals) causes an increase in the overall gas holdup values. The results are in agreement with earlier work by Bernemann (1989).

7.2.2 – Study of bubble dynamics in columns with and without internals

The effect of internals on the bubble dynamics in columns of different scales (8" and 18" diameter) was assessed using the four-point optical probe technique. As 22%-25% of the total CSA of the column is obstructed by tubes, an increase in the gas holdup radial profiles was observed. The bubble chord length was smaller with internals as result of an enhancement in bubble break-up rate. Consequently, the specific interfacial area between the gas and liquid phases was higher for systems equipped with internals. In the larger column, the minima of the specific interfacial area radial distributions occurred at the flow inversion point while the maxima were found next to the wall. The bubble velocity probability distributions at the column's center exhibited no significant differences between the case of no internals and that of 25% internals. However, at the 18" diameter column's wall region, a higher probability of bubbles moving downward was obtained. As a matter of fact, in the 18" diameter column, bubble velocity distributions at the wall region showed almost no bubbles moving upwards.

The effect of scale was assessed by comparing measured parameters in the 8" and 18" columns with internals.

7.2.3 – Effect of internals on liquid mixing behavior

A standard liquid tracer/conductivity probe measuring technique was used to evaluate the extent of liquid mixing characteristics with and without internals in an 18" column. Dense packing of internals was found to increase the liquid mixing behavior at various superficial gas and liquid velocities. This finding is in agreement with the work of Bernemann (1989) as well.

7.2.4 – Scale-up of bubble columns

A new approach for a scaling methodology was proposed based on the reactor compartmentalization approach. The proof-of-concept was successfully validated.

7.3 – Recommendations for Future Work

"Science never solves a problem without creating ten more." G. B. Shaw.

Although the current study provides useful information about bubble columns with internals, many questions remain unanswered in topics of relevance to this work. Below are few recommendations for potential future research opportunities to yield a better understanding of the subject.

A) Gas mixing studies in bubble columns with internals

Gas mixing is yet to be discussed in bubble columns with internals. Given the generated database of bubble dynamics, especially bubble velocity and specific interfacial area, it is recommended to conduct a study with state-of-the-art measuring techniques (e.g., Han, 2007) to investigate the extent of gas mixing as a function of internals.

B) Modeling of the liquid phase mixing

The database for liquid phase mixing in bubble columns equipped with internals is still immature due to the scarcity of relevant studies. The current study provides preliminary results assessing the effect of internals on liquid phase mixing characteristics. However, further work is needed at a wider range of superficial gas velocities. It is also of paramount importance to develop a model based on fundamental knowledge to describe the back mixing behavior of the liquid phase.

C) Extension of the scale-up methodology

The scale-up of bubble columns is an ongoing challenge. Chapter 6 presented a methodology for tackling the problem. However, the extension of this investigation is necessary. The multiplication of the inner compartments needs to be evaluated and the testing of cross sections other than circular (e.g., hexagonal) is recommended. Moreover, following Sasol's recent patent (Steynberg et al., 2009), the replacement of the tubes by cooling walls separating the compartments needs to be addressed. Further checks need to be made prior to the commercialization of the methodology including, but not limited to, liquid and gas phase mixing studies.

D) Fischer-Tropsch mimic slurry systems

The current work was limited to air-water systems while the FT synthesis involves a 3-phase system running at high pressures. Therefore, it is important to adopt a study where mimic FT conditions are applied to assure the validity of the current findings and results. Moreover, it is important to discuss in further detail the utilization of superficial gas velocity for open area only and how this affects the bubble dynamics. For the latter to be achieved, investigations using the superficial velocity need to be compared with the results from the data at superficial gas velocity for open area only.

Appendix A

Tabulated Listing of Studies of Bubble Columns with Internals

Research	System	Column and sparger features	Configuration of horizontal internals	Study
Fair et al. (1962)	Air-water	Commercial scale 42" diameter – 10' height/9" ring with 0.03" orifices	20 internal perforated-plate baffles with 5.5" of spacing and open area and hole diameter of 9.5-33% and 0.125-0.312" respectively (sometimes baffles were reciprocally moving)	Heat transfer
Khoze et al. (1971)	Nitrogen-NaOH solution	Alkali-resistant Plastic: 10x10 cm^2 CSA with 30 cm height/dielectric gas distributing grid of 2.4% open area	Glass cylinder tubes in a staggered tube bundle (seven horizontal rows and 14 vertical) s/d=3.5 (s is the pitch between the tubes and d=4 mm)	Heat and mass transfer
Sekizawa and Kubota (1974)	Gas phase: Air Liquid phase: ion-exchanged water, Glycerine aqueous solution (4 different properties variations), and 0.9 wt. % iso-amylalcohol aq. solution	5 cam diameter (100 cm height)/perforated plate distributor	Perforated plates: 10 and 20 cm of spacing, 0.5 cm hole diameter and plate thickness with 0.07 free area fraction of the plate	Liquid mixing and backflow
		10 cm diameter (100 and 120 cm height)/perforated plate distributor	10, 20, and 40 cm of spacing, 0.2, 0.3, 0.5, 1, 1.5, and 2 cm of hole diameter, 0.3 cm 0.5, and 1 cm of plate thickness, and 0.07 to 0.202 free area fraction of the plate	
		20 cm diameter (100 cm height)/perforated plate distributor	20 cm of plate spacing, 0.5 cm hole diameter and plate thickness with 0.0775 to 0.202 free area fraction of the plate.	
Aksel'rod et al. (1976)	Air-water and Air-aqueous glycerin (cross-flow)	Same as Vorotnikova and Aksel'rod. (1975)/sieve tray (6.7% open area)	Single-, two-, and three-row tube bundle of different pitch (1.13 to 1.6 cm)	Heat transfer and hydrodynamics
	Air-water and Air-transformer oil (counter-flow)	Plexiglas: 20cm x 20cm/grid plate (30% open area)	Single tube (12/1.5 mm), in-line tube bundle with spacing 2cm x 2cm, in-line tube bundle with spacing 4cm x 2cm, and staggered tube bundle with spacing 4cm x 4cm	

Blass and Cornelius (1977)	Air-water, Air-water-sand (diameters 60, 78, and 200 μm), Air-water-glass spheres (diameters 48, 78, 800 μm)	Acrylic glass: 14 cm diameter-325 cm height/perforated plate (lowest one of sectionalizing plates)	Perforated plates of 2 and 4 mm diameter holes leading to free cross sectional areas of 0.011-0.36 relative to column cross section	Liquid and solids phase mixing
Chen et al. (1986)	Air-water	Plexiglas: 7.5 cm diameter – 3 m height/gas distributor consisting of four 0.15 cm diameter hyperdermic needles Glass: 5 cm Karr column – 4 m height/same sparger as above	37 plates made of 6 mesh/in stainless steel wire screen were mounted 5 cm apart 84 perforated plates placed at a 2.54 cm interval were attached to the column's central axis made from Teflon sheet with 1.27 cm diameter holes leaving a free area of 53%.	Gas holdup and pressure drop
Chen and Yang (1989)	Air – Water and 0.2% CMC aqueous solution	Plexiglas: 0.05, 0.075, and 0.15 m diameter – 3 m height/four nozzles of 1.5 mm diameter for the first two columns and eight nozzles of the same diameter for the last column	37 circular plates made from 6 mesh stainless steel wire screen sheets with a fractional free area of 0.64 mounted 0.05 m apart on a central shaft of 5 mm diameter – plates were 1.5 mm smaller in diameter than the column.	Gas holdup, bubble size, interfacial area and mass transfer characteristics
Kawasaki et al. (1994)	Air-water	0.15 m diameter-2 m height/single hole sparger	Multiple draft tubes with perforated plates: draft tubes of 0.1 m diameter and length each, perforated plates (0.003 m thick): 1 with 161 holes of 0.003 m diameter each and 0.007 m square pitch, 3 with 161 holes of 0.006 m diameter each and 0.007 pitch, and 5 with 78 holes of 0.009 m each and 0.01 m pitch.	Gas holdup, mass transfer
Al Taweel et al. (1996)	Air-water (with addition of small quantities of polypropylene glycol methyl ether)	0.1 m diameter-2.5 m height/two-phase venture sparger with 0.86, 1.17, and 1.6 mm throat diameters	Honeycomb partitioning plates (2 placed 0.5 apart, and 8 placed 0.2 m apart) each of 50 mm thick and made of extruded aluminum with 0.4 mm wall thickness – 7 mm hexagonal cell structure	Axial mixing
Palaskar et al. (2000)	Air-water	Acrylic: 6.2 cm diameter-77 cm height, and 20 cm diameter-90 cm height/	Acrylic perforated sieve plates with percentage free areas of 0.5%, 1.48%, 10.8%, and 100%	Liquid phase mixing

Kemoun et al. (2001)	Air-water	0.2 m diameter-2.4 m height/10 laterals welded to the main gas manifold with 40 or 200 holes of 350 μm holes in each.	3 sieve trays constructed of 6.35 mm thick acrylic sheet and contained 42 holes of 6.35 diameter each in a triangular pitch	Gas holdup
Colmenares et al. (2001)	Air-water-sieved sand of diameter 130, 510, and 2300	Acrylic: 38cm square-2.2 m height/	49 tubes in an aligned arrangement of seven rows and seven columns (pitch to diameter ratio of 1.75), each tube is of 2.54 cm diameter	Gas and solids concentration distributions
Dreher and Krishna (2001)	Air-water	Polyacrylic: 10, 15, 38 cm diameter – 6, 4, 4 m height/Brass perforated plate with 0.5 mm diameter holes and triangular pitch of 7 mm	Two perforated brass plates of 1 mm thickness and 10 mm diameter holes. Open area of 18.6 and 30.7%	Liquid phase back mixing
Nosier (2003)	Nitrogen-acidified dichromate solution	Prespex: 12x12x80 cm/G4 sintered-glass distributor (pores of 5-10 microns)	Five arrays (6 tubes each) of copper tubes each of 8 mm diameter and 12 cm length with equal longitudinal and transverse pitch of 16 mm	Mass transfer
Pandit and Doshi (2005)	Air-water	0.41 m diameter – 2.87 m height/ sparger with 0.136% free area (25 holes of 3 mm diameter each)	1, 2, or 3 sectionalizing plates with 269, 604, 607, or 617 holes of 5, 8, 6 and 7 mm diameter respectively. The % free area range is 4-23%	Mixing time study
Doshi and Pandit (2005)	Air-water	0.41 m diameter – 2.87 m height/spargers with 0.136% (25 holes of 3 mm diameter each) and 0.6% (251 holes of 2 mm diameter each) free area	3 or 4 sectionalizing plates with 61, 269, 537, 604, 607, or 617 holes of 10, 5, 5, 8, 6, and 7 mm diameter respectively. The % Free area ranged between 4-23%.	Mixing behavior characteristics.
Alvaré and Al-Dahhan (2006a)	Air-water	19 cm diameter – 241 cm height/9.5 mm diameter single point nozzle	4 trays of three different configurations: a) 12 holes, 1.74 cm hole diameter, 10.2% open area; b) 52 holes, 0.6 cm hole diameter, 5.2% open area; and c) 105 holes, 0.6 cm hole diameter, 10.2% open area	Gas holdup
Alvaré and Al-Dahhan (2006b)	Air-water	Same as above	Same as above	Liquid phase mixing
Mecaial and Sadik (2007)	Air-water and air-NaCl solution	PVC: 10 cm diameter-207cm height/single point nozzle (10 mm diameter) and perforated plate (55 holes of 1 mm diameter each giving 0.6% open area)	Two trays with five different configurations each (see Figure 21 for details)	Hydrodynamics and liquid mixing

Research	System	Column and sparger features	Configuration of <u>vertical</u> internals	Study
Hall and Taylor (1955)	Water gas-hydrogen-mill-scale Fe_2O_3	Stainless steel: 7 7/8 " diameter- 7' 6" height/sintered bronze (Porosint) disk 1/8" thick, 12.5μm pore size (effective area = 0.15 ft^2)	Cooling tube bundle: central tube of 2 3/8" OD surrounded by a circular array of 8 tubes of 1 1/16" OD each. The array has a diameter 5 5/8"	Design and operation of FT Synthesis pilot plant
Fair et al. (1962)	Air-water	Commercial scale 42" diameter – 10' height; 9" ring with 0.03" orifices	42 Aluminum tubes of 1.5" diameter in 2 concentric circles	Heat transfer
Voyer and Miller (1968)	Nitrogen-water and Nitrogen-NaOH solution	5.5" diameter-0.67 to 7.8ft/ sieve plate (5% free area, 0.15" diameter holes at ½" triangular pitch)	½" 6 mesh cylindrical screen packing and ½" 6 mesh corrugated screen packing (corrugated and each layer perpendicular to the next one).	Interfacial area
Aksel'rod et al. (1976)	Air-water and air-transformer oil	Plexiglas: 20 x 20 cm square column-height not specified/grid plate distributor	a) single tube, 12/1.5 mm; b) in-line tube bundle with spacing of 20 x 20 mm; c) in-line tube bundle with spacing of 40 x 20 mm; and d) staggered tube bundle with spacing of 40 x 20 mm	Heat transfer
Shah et al. (1978)	Nitrogen-water	Glass: 6.35 cm diameter/sparger details not specified	6, 16 and 23 glass rods (0.004m diameter); 2 and 4 glass rods (0.011 m diameter); 1 glass rod (0.032 m diameter); 1, 2, and 4 screen baskets (0.019 m diameter) and 1 screen basket (0.038 m diameter). The smaller baskets were a) empty, b) filled with 0.0032 m polyethylene packing and c) filled with 0.0159 m diameter glass rods. The larger baskets were a) and b) same as above and c) filled with 0.032 m diameter rod. (Rods were all 1.143 m tall)	Gas holdup and backmixing
Kölbel and Ralek (1980)	Syngas-catalyst slurry	Not Specified	Vertical honeycombed shafts with cooling pipes arranged centrally around or in corners	Liquid backmixing and catalyst efficiency

O'Dowd et al. (1987)	Nitrogen-water-glass spheres	10.8 cm diameter column – 1.94 m height/perforated plate with 72 holes of 0.001 m diameter	Internal baffles: 5 vertical rods (1 central and 4 around at 90 deg. each)of 0.019m diameter and 1.88 m height	Solids dispersion coefficient, local gas holdup and bubble size and interfacial area
Yamashita (1987)	Air-water	31 cm diameter/single nozzle of 60 mm diameter downwards on central axis (10 cm above bottom)	Single rod of 6 mm diameter (hanging 36.5 cm above bottom)	Overall gas holdup
			Multi rods and pipes: *Small separation *(6mm):* 18, 44, 70 and 85 internals of 14mm diameter. *Large separation (≥8mm):* 37, 28, 21 and 10 internals of 22mm diameter. 9 internals of 60 mm diameter. 9 internals of 48 mm diameter.	
		16 cm diameter/single nozzle of 27.6 mm diameter horizontally on side wall (10 cm above bottom)	Single pipe and rod (sitting on bottom)	
			Multi rods and pipes: *Large separation *(≥8mm):* 2 internals of 14, 22, 38 and 20 mm diameter 5, 6, and 11 internals of 22 mm diameter	
		8 cm diameter/single nozzle of 10 mm diameter horizontally on side wall (4.2 cm above bottom)	Single pipe and rod	
Saxena et al. (1990)	Air-water-red iron oxide powder	10.8 cm diameter/perforated plate	Solid cylinder of 19 mm diameter	Heat transfer modeling
Gaspillo and Goto (1991)	Nitrogen-water-resin (Amberlyst 15)	9.7 cm diameter-37 cm height/single nozzle of 1mm diameter and a plastic ball with many fine pres	A static mixer in a draft tube. The mixer was successively composed of right-hand 90°angle corrugated stainless steel sheets	Mass transfer
Saxena and Patel (1991)	Air-water-glass beads	Same as Saxena et al. (1990)	Axial cylindrical probes of 19, 31.8, and 50.8 mm diameter along the central axis of the column	Heat transfer and gas holdup

Saxena et al. (1991)	Nitrogen-Therminol 66-red iron oxide powder	Same as Saxena et al. (1990)	Single cylindrical probe (19, 31.8, and 50.8 mm diameter) and bundle of 7 tubes of 19 mm diameter each in a triangular pitch of 36.5 mm	Heat transfer, gas holdup
Saxena et al. (1992)	Air-water Air-water-glass beads	30.5 cm diameter – 3.3 m height/perforated plate of 0.8mm diameter orifices in square arrangement of 9.5 mm pitch	5, 7, and 37 Stainless Steel tubes (the latter in 3 bundles of 3 concentric hexagonal rows) of 19 mm diameter each and the pitch is 36.5 mm	Overall gas holdup
Saxena and Rao (1993)	Nitrogen-Therminol-Magnetite	Same as Saxena et al. (1992)	37 Stainless Steel tubes in a bundle of 19 mm diameter each in equilateral pitch of 36.5 mm	Overall gas holdup
Saxena (1993)	Air-water Air-water-glass beads Nitrogen-Therminol Nitrogen-Therminol-magnetite	Same as Saxena et al. (1992)	1, 5, 7 and 37 tube bundle (3.25 m in height), pitch as Saxena et. al. (1992)	Heat transfer
Saxena and Chen (1993)	Air-water	Same as Saxena et al. (1992)	1 and 7 tubes bundle	Heat transfer
	Air-water-solids (glass beads (50 μm), magnetite (37.5, 49, 58, 69, 90.5 μm), red iron oxide powder (1.02, 2.38μm)) Nitrogen-Therminol	Same as Saxena et al. (1990) Same as Saxena et al. (1992)		
	Nitrogen-Therminol-Solids (red iron oxide (1.7 μm), magnetite (28, 36.6, 37μm)	Same as Saxena et al. (1990)		
	Nitrogen-Therminol Nitrogen-Therminol-Solids (magnetite (65 μm))	Same as Saxena et al. (1992)	37 tubes bundle, pitch as Saxena et. al. (1992)	
Pradhan et al. (1993)	Air-aqueous CMC solution	0.102 m diameter column – 2.5 m height/64 holes of 1.5mm diameter each in a 1.2 cm triangular pitch	Helical coils (made of 6 mm Co tube) of 3.5 cm and/or 6.8 cm diameter in 2.5 cm pitch and bundles of vertical straight tubes (Stainless Steel with 1.2, 1.5, and 2.0 cm outer diameters)	Overall gas holdup and pressure drop

Thimmarpuram et al. (1993)	Air-water Air-water-glass beads	Same as Saxena et al. (1992)	1, 5, 7, and 37 tubes bundles, pitch as Saxena et al. (1992)	Heat transfer
Schlüter et al. (1995)	Air-water Air-Propylene glycol	0.29 m diameter – 4.27 m height/sieve tray	Longitudinal tube bundle (each of 25 mm diameter) of 40, 70 and 120 mm pitch	Heat transfer
Chen et al. (1999)	Air-water Air-Drakeoil	18" (44cm) diameter/301 holes of 0.77mm diameter each on 14 concentric circular rings at 1.5 cm apart	16 Aluminum tubes of 1" diameter each in two bundles at r/R=0.39 and 0.61	Gas holdup and its radial profile, liquid recirculation velocity, turbulent stresses and eddy diffusivities
De et al. (1999)	Air-sodium sulphate Air-butanol Air-glycerine	0.05 m diameter column – 2.5 m height/plate sparger	Helical coils of 3.5 cm diameter and straight tubes of 1.2 cm and 1.5 cm diameter	Overall gas holdup
Maretto and Krishna (2001)	Syngas-paraffin $C_{16}H_{34}$-Co based catalayst	7 m diameter – 30 m dispersion height	Vertical cooling tubes and spacer sieve trays	Reactor productivity and reaction kinetics modeling
Forret et al. (2003)	Air-water	1 m diameter/perforated plate: 312 holes of 2mm diameter and 50 mm pitch	56 tubes of 63 mm diameter each and a 10.8 cm square pitch	Liquid mixing-axial dispersion coefficient
Nosier and Mohamed (2004)	Air-$K_2Cr_2O_7/H_2SO_4$	Glass: 7.9 cm diameter-50 cm height/G4 sintered glass distributor of 7 cm diameter and 0.5 cm thick. The average diameter of the pores of sintered distributor was 5-10 microns.	One helical coil of copper of ring, diameter 4.7 cm, tube diameter of 0.3 cm and of pitch 0.84 cm. 17 rings in the coils.	Mass transfer
Larachi et al. (2006)	Air-water	Simulated lab scale 19 cm diameter and pilot scale 100 cm diameter	Tubes of 1" diameter and triangular pitch in 4 arrangements: dense (253 tubes), sparse (31 tubes), star/wall clearance (121 tubes), star/core clearance (132 tubes)	CFD simulations (gas holdup, liquid axial velocity and turbulent kinetic energy)
Balamurugan and Subbarao (2006)	Gas (Air) – liquid (NA)	15 cm diameter/perforated plate with 126 holes of 0.2 cm diameter each in 1 cm square pitch	21 and 41 Stainless Steel helical springs of 1.9 cm coil diameter made of 0.5 mm wire	Bubble size and holdup

Youssef and Al-Dahhan (2009)	Air-water	0.19 m diameter – 2 m height/perforated plate: 225 holes of 1.32 mm diameter each in triangular pitch	12 and 48 Plexiglas rods of ½" diameter each located in two concentric circles and in triangular pitch, respectively	Gas holdup and its radial profile, and bubble dynamics.
Kölbel and Langheim (1958) (US 2,852,350)	$CO+H_2$-watery solution of $Fe(NO_3)_3$ and $Cu(NO_3)_2$	1.4 m diameter – 12 m height/NA	360 pipes that reduces to 270 at 3 m above the gas inlet, to 180 after 3 further meters and finally to 90 by moving 3 more meters higher.	Improvement of cooling system design
Kölbel and Ackermann (1958) (US 2,853,369)	Gas-slurry (no details given)	Applicable to any column with diameter 30 cm up to 3m and above, and more than 1.5 m in height	Vertical shafts (circular or hexagonal) with cooling tubes within or in between the circular shafts or various arrangements within the hexagonal ones	Overcoming the liquid recirculation "rolling movement" and backmixing
Hagino et al. (1982) (US 4,327,042)	Seed culture of starting Corynebacterium glutamicum ATCC 21543 - fermentation medium	80 cm diameter – 4m height	Draft device (56 cm diameter-3m height) consisting of 4 vertical plates (50 cm x 3 m) with 1 cm spacing, each of which has one edge in outwardly spaced overlapping relation to a vertical edge of an adjacent plate and has the other vertical edge in inwardly spaced overlapping relation to a vertical edge of the other adjacent plate	Liquid agitation enhancement
Soraker et al. (2005) (WO 2005/065813)	$CO+H_2$-slurry (Co catalyst)	Not specified	Parallel tubes bundle with a header at one end to which 2 or more subheaders are connected and also to the tubes (of triangular, square or rotated square pitch)	Internals design (minimizing cross sectional blockage)
Hawthorne et al. (2006) (US 7,108,835)	FT system	21.5' diameter column	576 cooling tubes of 4" diameter each in bundles of 12 or 4 tubes each in 9 rows	Cooling tube arrangement facilitating the removal of plurality of cooling tubes

Appendix B

Design, Setting and Construction of Internal Structures for Bubble Columns

B.1 – Overview

Since few studies, in the open literature, have discussed the effect of heat exchanger mimic internal structures on the flow field as have been repeatedly pointed in this dissertation, it comes as no surprise that the design features of such bundles for laboratory columns is still immature.

Although the chief criteria associated with the design a bubble column unit equipped with vertical internals have been addressed in Chapters 3 and 4 with regard to heat transfer requirements as well as other mechanical and technical considerations, the main objective of this appendix is to describe in details the steps and guidelines associated with the commissioning phase of such systems.

It should be noted that the emphasis below is given to the internals' systems outlined in Chapter 4 only which can serve a model for extrapolation to other similar systems.

B.2 – System Components

a) Internal rods

The internal rods may ultimately be manufactured from Aluminum. However, PVC and Plexiglas are much cheaper. PVC rods are very flexible and are somewhat lighter. Hence, PVC was chosen for the manufacturing of the rods which are 12 ft. in height yet are made each of 2 pieces that are screwed together via an internal threaded rod. The shortest of the two was 30" tall and was in the lower position. The lower end of the short piece was machined with 45° angle (Figure B.1). The main reason behind the current design is to allow the installation in low ceiling lab spaces. The latter, however, was not needed since the 18" diameter column was located where more than 12 ft. space above is available.

b) Spacers

The spacers are crucial for the stability and fixation of the rods in position. The spacers are made of steel using water jet machining. The designs were prepared utilizing AutoCAD. They can have a diameter larger the column's, sit between the flanges between the column's sections and be supported on a grove in the column's wall or be even of larger diameter and get screwed with the same screws fixing the column's sections together. However, the above

Fig. B.1 – Spacer for 5% internals and lower part of internal rods

design means that for 2-sections columns, only 1 spacer can be utilized which is not enough to provide stability. Consequently, the spacers were of diameter slightly smaller that the column's inner diameter with little plastic pieces to make sure it is firmly touching the walls yet without damaging the Plexiglas (Figure B.1). Three spacers were inserted in the columns at heights 5", 45", and 85" from the lower end of each rod. The spacers are designed to occupy the least possible of the total CSA. Figure A.2 shows the lower spacer in the 25% internals configuration. Only with this dense internals structure, the lower spacer was attached to the sparger with four threaded rods or 'legs' to ensure the rods maintain a vertical setting with no twisting. The latter is very critical since a four point optical probe is inserted between the rods at a height of 56" above the sparger.

Fig. B.2 – Lower spacer for 25% internals attached to distributor

c) Top plate

Since the internal rods are hanging inside the column, a top plate is needed for support. The top plate used for the 5% internals configuration is shown in Figure B.3. The top plate is sitting on four 'legs' while the distance above the top column's flange is adjustable to modify the height of the bundle with respect to the sparger, when needed. Another reason for having these 'legs' supporting the top plate is to be able to check that the bundle is level at all times and make changes accordingly at either angle. Finally, the column must be open at the top to allow gas disengagement and to avoid back pressure effect. The top need to be thick enough (~1/2-3/4") or else an additional piece is needed (Figure B.3). Clearly, the top plate and the spacers must have the same orientation to ensure that the rods are vertically straight.

d) Crane/winch

The top plate may be hooked to a top crane for secondary security measures (Figure B.3). In addition, a top crane can help adjust the height of the bundle considering the large weight of dense bundles.

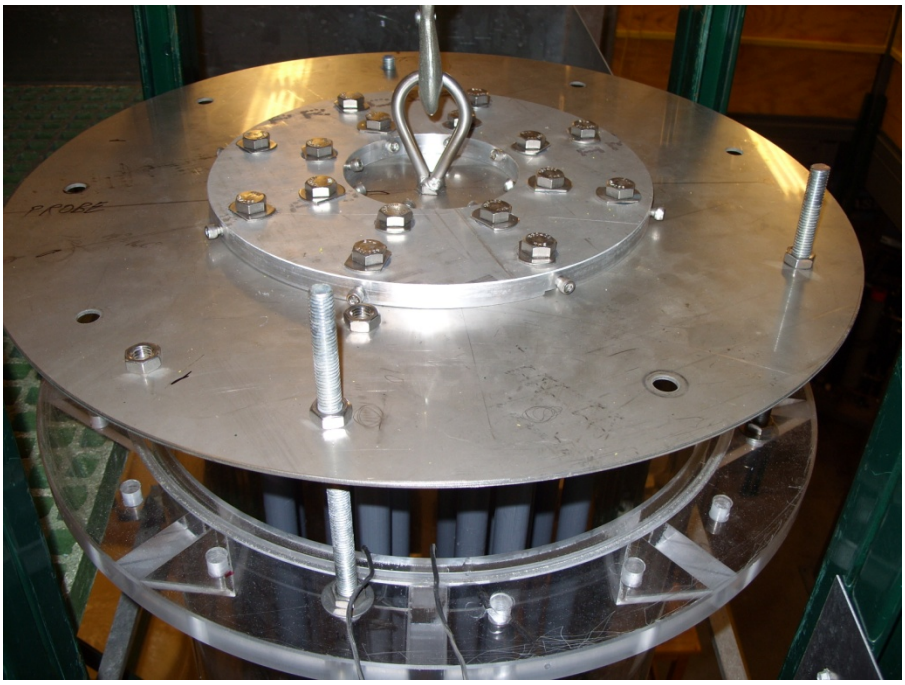

Fig. B.3 – Top plate hooked to top crane.

B.3 – Procedure for Installing the Internal Bundle

If the dense internals structure (25% covered CSA) is installed, the procedure starts by attaching the bottom spacer to the sparger outside of the column which requires the dismantling of the entire system off the plenum chamber. Once the ensemble shown in Figure B.2 is ready, it is inserted to sit on top of the plenum chamber. Note that care must be taken to assure that the orientation of this ensemble (which will guide the insertion of the rods one after the other later on) is in line with the column's ports for the optical probe as the entire system is ready for operation. Hence, it is advisable not to tighten the bolts fixing the bottom column's section and the plenum chamber before making sure that the accurate orientation is reached. Even better, to have a couple of handles screwed to the sparger and outside of the column to rotate this ensemble as needed to adjust its orientation.

Then, the first step of building the bundle is composing the so called 'skeletal structure'. This basically is constituted of the three spacers attached to 3 to 5 (or more) rods. This structure is built outside of the column and one chooses 3 to 5 rods randomly located across the sectional area of the column's yet ensuring that the spacer is maintained somewhat horizontal when the structure is held vertically.

These rods are attached to the spacers by means of tiny threaded pins into the rods above and below the spacer (Figure B.4).

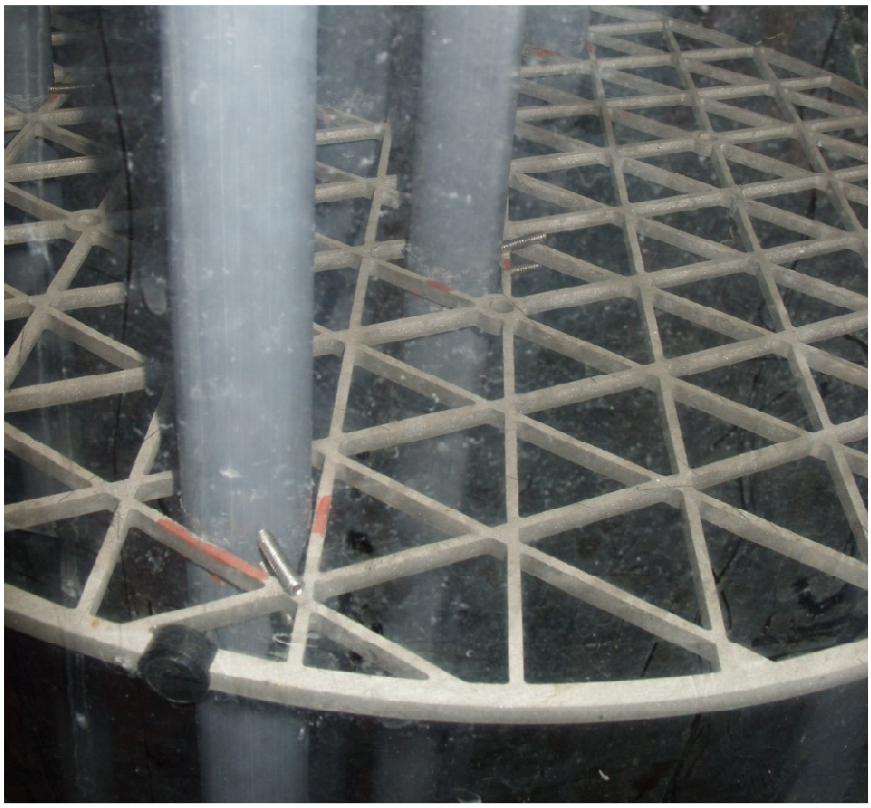

Fig. B.4 – Attachment of the PVC initial rods to the spacers via threaded pins

The 'skeletal structure' is inserted into the column from the top, left to sit on the sparger until the top plate is fixed in place by means of the 'legs' then the rods within the 'skeletal' are pulled through their respective location on the top plate. Each rod is fixed in position using a washer and a bolt that are attached to the top of the rod (Figure B.3).

The crane is to be hooked to the top plate to ensure its stability before the insertion of additional rods.

Next, each of the rods is inserted into the column from the top through its respective opening on the top plate making sure that it goes in its respective position through the three spacers. For the lower one, an available 4" diameter port 'window' at the column's bottom can be used to guide the rod's entry in its correct location. Typically, two persons are to help in this process.

Appendix C

The Estimation of Lumped Parameters from the 4-Point Optical Probe Data

C.1 – Introduction

The main motivation behind the study of bubble dynamics and their local distributions related to their effect on many factors that impact the reactor's performance. For example, the bubble velocity directly relates to the gas holdup in the system since it affects the residence time of the gas phase in the column, while the bubble size (here we measure the chord length as a representation of the size) is amongst the factors on which the bubble velocity depends. In fact, it is well known that the bubble size can be used to distinguish the various flow regimes and to determine the transition point. The interfacial area between the gas and liquid phases influences the mass transfer. Moreover, the local gas holdup is relevant since 2 systems may yield the same overall gas holdup but exhibit very different radial holdup profiles and other hydrodynamic parameters.

It is believed that some of the lumped parameters can be extracted from the bubble characteristics obtained locally using the probe as follows.

C.2 - The determination of the lumped volumetric gas-liquid mass transfer coefficient ($k_l a$)

Assuming an extreme simplified case where the liquid side mass transfer coefficient (k_l) is a constant. This can be calculated following the famous Calderbank and Moo-Young (1961) correlation hat yields k_l=8.5x10^{-5} m/s. In this case, we can use our knowledge of the specific interfacial area (a) between the gas and liquid phases obtained from the probe measurements to investigate the impact of internals on the lumped parameter ($k_l a$) which would yield the radial profiles as shown in Figure C.1 below. Note that the cross-sectional averaged value of $k_l a$ can be readily obtained at any of these conditions via the integration:

$$\overline{k_l a} = 2\int_0^1 \frac{r}{R}.k_l a\left(\frac{r}{R}\right).d(\frac{r}{R})$$

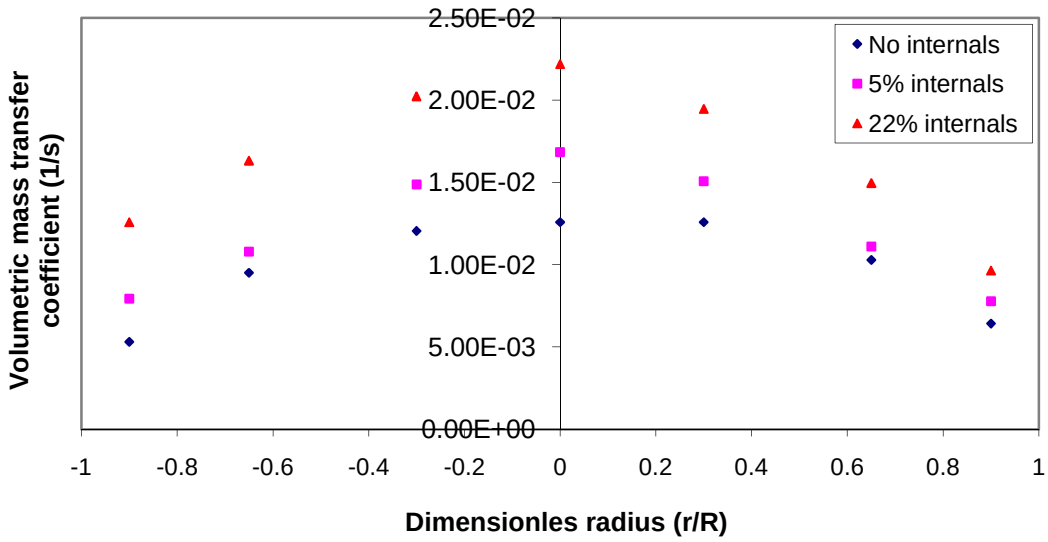

Fig. C.1 – Effect of internals on $k_l a$ in 8" column (Ug= 20cm/s)

Assuming a more complicated case where we utilize Higbie's penetration theory according to which, $k_l = 2\sqrt{\frac{D_{AB}}{\pi . t_e}}$

With t_e being the contact (exposure) time and defined as d_b/u_b. Both these parameters can be obtained from the probe data with an approximation for the bubble diameter. As a matter of fact, the raw data from the probe can provide even a more accurate representation of the contact time since it does collect and report the time step at which the probe tip first pierces the bubbles and the time step at which the bubble exits the tip. This delta t is basically what is used to calculate the gas holdup by relating it to the volume of the gas phase. This can also provide the bubble chord length from each of the 4 tips of the probe. The averaged radial bubble chord length profiles (following proper weighing along the column's cross section) can be used along with these time steps from the probe's raw data to estimate the contact time in a more direct and physically sound manner.

It is noteworthy that the estimated cross-section averaged value of $k_l a$ from the current study in the system with no internals at Ug=20 cm/s ($k_l a$ =0.007 s^{-1}) is two orders of magnitude lower than that obtained by the measurements of Vermeer and Krishna (1981) yet in the same order of magnitude that de Swart (1996) calculates from the surface renewal theory.

C.3 – The determination of axial dispersion coefficient for the liquid phase (D_{ax})

Following Degaleesan's (1997) model development, the representation of liquid backmixing, the 2D convection-diffusion equation is:

$$\frac{1}{r}\frac{\partial}{\partial r}\varepsilon(r)D_{rr}(r)r\frac{\partial C}{\partial r} = \varepsilon(r)u_z(r)\frac{\partial C}{\partial z} - \varepsilon(r)D_{zz}(r)\frac{\partial^2 C}{\partial z^2}$$

Then, using $C_{r,z} = \bar{C}(z) + C'(r)$, where the first term on the RHS represents the cross-sectional average liquid concentration "independent of the radial position" and the second term in the RHS represents the concentration variations around the cross-sectional mean, in the above equation and integrate with proper B.Cs to get:

$$\frac{1}{r}\frac{\partial}{\partial r}\varepsilon(r)D_{rr}(r)r\frac{\partial C'(r)}{\partial r} = \frac{\partial \bar{C}(z)}{\partial z}[\varepsilon(r)u_z(r) - \varepsilon(r)D_{zz}(r).const.]$$

An average flux for the column's cross section can be expressed as:

$$J = -\frac{\partial \bar{C}(z)}{\partial z}[D_{Taylor} + \bar{D}_{zz}]$$

Hence, $D_{eff} = D_{Taylor} + \bar{D}_{zz}$

Full details of the above derivation can be found in Degaleesan and Dudukovic, 1998.

The first term on the RHS is due to the liquid velocity profile while the contribution due to the eddy diffusivity is expressed as

$$D_{zz} = l_z\sqrt{\overline{v_z'^2}}$$

Where l_z is the turbulent length scale which is proportional to the bubble size (recalling Hinze's (1955) break up notions) and the second term is the root mean square of liquid fluctuating velocity.

l_z can be approached, thus, from probe data and it is noteworthy that D_{taylor} becomes of less significance to the axial dispersion coefficient in churn turbulent flow regimes (of industrial interest).

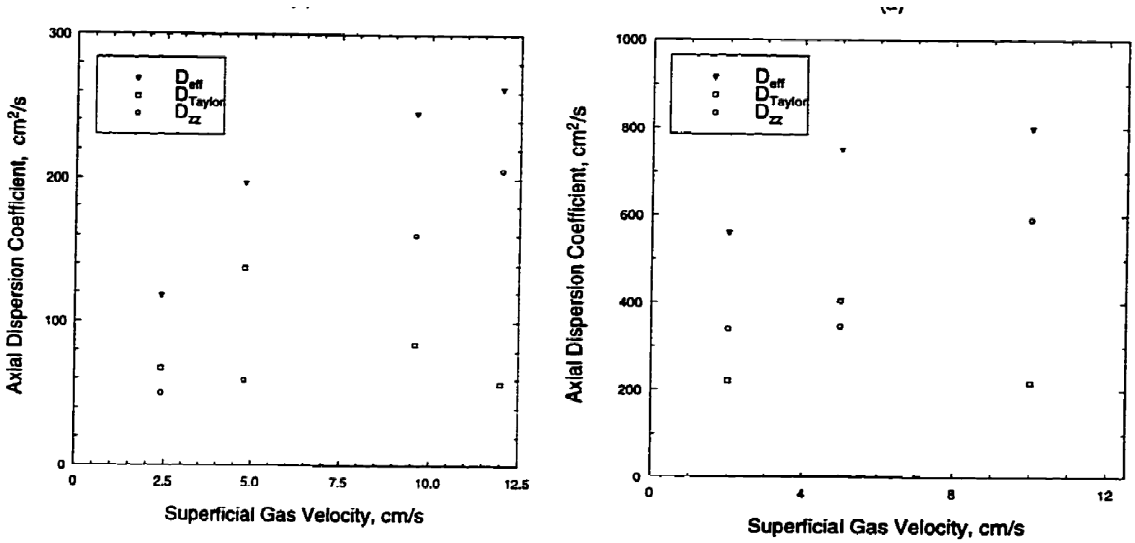

(a) (b)

Fig. C.2 – Axial dispersion coefficients from Degaleesan (1997) for (a) D=14 cm and (b) D=44 cm

References

Akita, K. and Yoshida, F., 1974. Bubble size, interfacial area, and liquid-phase mass transfer coefficient in bubble columns. Ind. Eng. Chem. Process Des. Develop., 13(1), 84-91.

Aksel'rod, L. S., Vorotnikova, N. I., and Kozlov, A. A., 1976. Heat transfer and several aspects of hydrodynamics of bubble beds on sieve trays equipped with tube bundles. Heat Transfer - Soviet Research, 8(6), 25-33.

Al Taweel A. M., Ramadan A. M., Moharam M. R., El Mofty S. M., and Ityokumbul M. T., 1996. Effect of honeycomb inserts on axial mixing in bubble columns, Chemical Engineering Research and Design, 74a, 456-462,

Alvaré, J., 2002. Gas holdup and liquid phase mixing in trayed bubble column reactors, M. Sc. Thesis, Washington University in St. Louis, Saint Louis, MO, USA.

Alvaré, J. and Al-Dahhan, M. H., 2006a. Gas Holdup in Trayed Bubble Column Reactors. Industrial & Engineering Chemistry Research, 45(9), 3320-3326.

Alvaré, J. and Al-Dahhan, M. H., 2006b. Liquid phase mixing in trayed bubble column reactors, Chemical Engineering Science, 61(6), 1819-1835.

Balamurugan, V. and Subbaro, D., Bubble size and holdup in bubble columns with vibrating internals, AIChE Spring National Meeting (2006).

Bankoff, S. V., 1960. A variable Density Single-Fluid Model for Two-Phase flow with Particular Reference to steam-Water Flow, J. Heat Transf., 82, 265-272.

Behkish, A., Men, Z., Inga, J. R., and Morsi, B. I., 2002. Mass transfer characteristics in a large-scale slurry bubble column reactor with organic liquid mixtures. Chemical Engineering Science, 57 (16), 3307-3324.

Bernemann, K., 1989. On the hydrodynamics and mixing of the liquid phase in bubble columns with longitudinal tube bundles, Ph.D. Thesis, University of Dortmund, Germany.

Bhaga D., and Weber M. E., 1981. Bubbles in viscous liquids: shapes, wakes and velocities, J Fluid Mech, 105: 61-85.

Blass, E. and Cornelius, W., 1977. The residence time distribution of solid and liquid in multistage bubble columns in the cocurrent flow of gas, liquid and suspended solid. International Journal of Multiphase Flow, 3(5), 459-469.

Brown, D. M., Bhatt, B. L., Hsiung T. H., Lewnard, J. J., and Waller, F. J., 1991. Novel Technology for the Synthesis of Dimethyl Ether from Syngas, Catalysis Today, 8, 279-304.

Calderbank, P. H., 1987. Gas Absorption from bubbles, Chem. Eng. J., 45, 209-233.

Calderbank, P. H and Moo-Young, M. B, 1961. The continuous phase heat and mass transfer properties of dispersions. Chem. Eng. Sci., 16, 39-54.

Casanave, D., Galtier, P. and Viltard, J.C., 2000. Process and apparatus for operation of a slurry bubble column with application to the Fischer–Tropsch synthesis. US Patent 6 060 524.

Chabot, J. and de Lasa, H.I., 1993. Gas holdups and bubble characteristics in a bubble column operated at high temperature. Industrial and Engineering Chemistry Research, 32, 2595–2601.

Chen, B. H. and Yang, N. S., 1989. Characteristics of a cocurrent multistage bubble column. Industrial & Engineering Chemistry Research, 28(9), 1405-1410.

Chen, B. H., Yang, N. S., and McMillan, A. F., 1986. Gas holdup and pressure drop for air-water flow through plate bubble columns. Canadian Journal of Chemical Engineering, 64(3), 387-392.

Chen R. C., Reese J., and Fan L-S., 1994. Flow structure in a three-dimensional bubble column and three-phase fluidized bed, AIChE J, 40, 1093-1104.

Chen, J., Li, F., Degaleesan, S., Gupta, P., Al-Dahhan, M. H., Dudukovic, M. P. and Toseland, B. A., 1999. Fluid Dynamic Parameters in Bubble Columns with Internals, Chem. Eng. Sci., 54 (13-14), 2187-2197.

Chen, P., Gupta, P., Dudukovic, M. P., and Toseland, B. A., 2006. Hydrodynamics of slurry bubble column during dimethyl ether (DME) synthesis: Gas–liquid recirculation model and radioactive tracer studies, Chem. Eng. Sci., 61(19) 6553-6570.

Chen, P., Sanyal, J., and Dudukovic, M. P., 2005. Numerical simulation of bubble columns flows: effect of different breakup and coalescence closures, Chem. Eng. Sci., 60(4) 1085-1101.

Clift, R., Grace, J. R., and Weber, M. E., 1978. Bubbles, Drops, and Particles. New York, Academic Press.

Colmenares, A., Sevilla, M., Goncalves, J. J., and Gonzalez-Mendizabal, D., 2001. Fluid-dynamic experimental study in a bubble column with internals, International Communications in Heat and Mass Transfer, 28(3), 389-398.

Davis, B., 2005. Fischer–Tropsch synthesis: overview of reactor development and future potentialities, topics in Catalysis 32, 143–168.

De Swart, J. W. A., 1996. Scale up of the Fischer Tropsch slurry reactor, Ph. D. Thesis, University of Amsterdam, The Netherlands.

De, S. K., Ghosh, S., Parichha, R. K. and De, P., 1999. Gas hold-up in two phase system with internals, Indian Chem. Engr. Section A, 41(2), T54-T58.

Deckwer, W.-D., 1992. Bubble column reactors, Chichester.

Deckwer, W.-D. and Schumpe, A., 1993. Improved tools for bubble column reactor design and scale-up. Chemical Engineering Science 48, 889–911.

Deen, N.G., Mudde, R.F., Kuipers, J.A.M., Zehner, P., and Kraume, M., 2010. Bubble Columns, Ullmann's Encylopedia of Industrial Chemistry.

Degaleesan, S., 1997. Turbulence and Liquid Mixing in Bubble Columns, D.Sc. Thesis, Washington University in St. Louis, Saint Louis, MO, USA.

Degaleesan, S., Dudukovic, M. P., and Pan, Y., 2001. Experimental study of gas induced liquid-flow structures in bubble columns, AIChE J., 47, 1913–1931.

Delnoij, E., Kuipers, J. A. M., and van Swaaij, W. P. M., 1997. Computational fluid dynamics applied to gas-liquid contactors, Chemical Engineering Science, 52(21-22), 3623-3638.

Devanathan, N., Moslemian, D., and Dudukovic, M. P., 1990. Flow mapping in bubble columns using CARPT, Chemical Engineering Science, 45(8), 2285-2291.

Diaz, M. E., Iranzo, A., Cuadra, D., Barbero, R., Montes, F. J., and Galan, M. A., 2008. Numerical simulation of the gas-liquid flow in a laboratory scale bubble column: influence of bubble size distribution and non-drag forces, Chemical Engineering Journal, 139, 363-379.

Doshi, Y. K., Pandit, A. B., 2005. Effect of internals and sparger design on mixing behavior in sectionalized bubble column, Chemical Engineering Journal (Amsterdam, Netherlands), 112(1-3), 117-129.

Dreher, A. J. and Krishna, R., 2001. Liquid-phase backmixing in bubble columns, structured by introduction of partition plates, 69(1-4), 165-170.

Duduković, M. P., 2009. Challenges and innovations in reaction engineering, Chem. Eng. Comm., 196:252–266.

Duduković, M. P., 2000. Opaque multiphase reactors: experimentation, modeling and troubleshooting, oil & Gas Science and Technology, 55(2), 135-158.

Duduković, M. P., 2007. Relevance of Multiphase Reaction Engineering to Modern Technological Challenges, *Ind. Eng. Chem. Res.*, 46(25), 8674–8686.

Espinoza, R. L., Styneberger, A. P., Jager, B., and Vosloo, A. C., 1999. Low temperature Fischer-Tropsch synthesis from a Sasol perspective, Applied Catalysis A: General, 186, 13-26.

Euzen, J. P., Trambouze, P., and Wauquier, J. P., 1993. Scale-up Methodology for Chemical Processes, Technip, Paris.

Fair, J. R., Lambright, A. J., and Anderson, J. W., 1962. Heat transfer and gas holdup in a sparged contactor. I & EC Process Design and Development, 1, 33-36.

Fan L.-S. and Tsuchiya K., 1990. Bubble wake dynamics in liquids and liquid-solid suspensions, Butterworth-Heinemann.

Fan, L.-S., 1989. Gas–Liquid–Solid Fluidization Engineering. Butterworth, Stoneham, MA.

Fan, L.-S., Yang, G. Q., Lee, D. J., Tsuchiya, K. and Luo, X., 1999. Some aspects of high-pressure phenomena of bubbles in liquids and liquid-solid suspensions. Chem. Eng. Sci., 54, 4681-4709.

Forret, A., Schweitzer, J. M., Gauthier, T., Krishna, R. and Schweich, D., 2003. Liquid dispersion in large diameter bubble columns with and without internals, the Canadian Journal of Chemical Engineering 81, 360–366.

Forret, A., Schweitzer, J. M., Gauthier, T., Krishna, R., and Schweich, D., 2006. Scale up of slurry bubble reactors, Oil & Gas Science and Technology, 61(3), 443-458.

Frijlink, J. J., 1987. Physical Aspects of Gassed Suspension Reactors, Ph.D. Thesis, Delft University of Technology, The Netherlands.

Fukuma, M., Muroyama, K., Yasunishi, A., 1987. Properties of Bubble Swarm in a Slurry Bubble Column, J. Chem. Eng. Japan., 20, 28-33.

Garnier, C., Lance, M., and MariSe, J. L., 2002. Measurement of local flow characteristics in buoyancy-driven bubbly flow at high void fraction, Experimental Thermal and Fluid Science, 26, 811–815.

Gaspillo, P. D. and Goto, S., 1991. Mass transfer in bubble slurry column with static mixer in draft tube, Journal of Chemical Engineering of Japan, 24(5), 680-692.

Grienberger, J. and Hofmann, H., 1990. Investigations and modelling of bubble columns, Chemical Engineering Science, 47(9-11), 2215-2220.

Groen, J. S., Mudde, R. F., and Van den Akker, H. E. A., 1995. Time dependent behavior of the flow in a bubble column, Trans. I. Chem. E., part A.

Guet, S., Fortunati, R.V., Mudde, R.F., Ooms, G., 2003. Bubble velocity and size measurement with a four-point fiber probe. Particle and Particle Systems Characterization, 20, 219-230.

Gupta, P., 2002. Churn-turbulent bubble columns - experiments and modeling. D. Sc. Thesis, Washington University in St. Louis, Saint Louis, MO, USA.

Gupta, P., Al-Dahhan, M. H., Dudukovic, M. P., and Mills, P. L., 2000. A novel signal filtering methodology for obtaining liquid phase tracer responses from conductivity probes, Flow Measurement and Instrumentation J., 11, 123-131.

Gupta, P., Ong, B. C., Al-Dahhan, M. H., Dudukovic, M. P., and Toseland, B. A., 2001. Hydrodynamics of churn turbulent bubble columns: gas-liquid recirculation and mechanistic modeling, Catalysis today, 64, 253-269.

Hagino H., Odagiri H., and Okutani J., 1980. Draft device for a bubble column. US Patent 4,327,042.

Hall, C. C. and Taylor, A. H., 1955. Design and operation of a fluid catalyst pilot plant for Fischer -Tropsch synthesis, Journal of the Institute of Petroleum, 41, 101-124.

Hamed, M. E. and Al-Dahhan, M. H., 2010. Gas phase mixing in bubble columns with internals (to be submitted).

Han, L., 2007. Hydrodynamics, back-mixing, and mass transfer in a slurry bubble column reactor for Fischer-Tropsch alternative fuels, D. Sc. dissertation, Washington University in St. Louis.

Hawthorne W. H., Ibsen M. D., Pedersen P. S., and Bohn M. S., 2006. Fischer-Tropsch slurry reactor cooling arrangement. US Patent 7,108,835 B2.

Hibiki T. and Ishii, M., 2002. Interfacial Area Concentration of Bubbly Flow Systems, Chem. Eng. Sci., 57: 3967-3977.

Hibiki, T. and Ishii, M., 2001. Interfacial area concentration in steady fully developed bubbly flow Int. J. Heat Mass Transfer, 44, 3443–3461.

Hills, J. H., 1974. Radial non-uniformity of velocity and voidage in a bubble column. Transactions of the Institution of Chemical Engineers, 52, 1–9.

Hinze, J. O., 1955. Fundamentals of the hydrodynamic mechanism of splitting in dispersion processes, AIChE J., 1, 289-295.

Hulet, C., Clement, P., Tochon, P., Schweich, D., Dromard, N., and Anfray, J., 2009. Literature Review on Heat Transfer in Two and Three-Phase Bubble Columns, Int. J. Chem. Reactor Eng., 7.

IEO, 2009. International Energy Outlook, Department of Energy. Washington, DC, USA.

IEO, 2008. International Energy Outlook, Department of Energy. Washington, DC, USA.

Inga, J. R., 1997. Scaleup and scaledown of slurry reactions, Ph.D. Thesis, University of Pittsburgh, PA, USA.

Jakobsen, H. A., Lindborg, H., and Dorao, C. A., 2005. Modeling of bubble column reactors: Progress and Limitations, Ind. Eng. Chem. Res., 44, 5107-5151.

Kafarov, V.V., Kruglik, A.E., and Trofimov, V.I., 1975. Comparative evaluation of the effect of installation of some standard heat exchangers in bubble-type columns on the average gas content and structure of liquid-phase streams, Zhurnal Prikladnoi Khimii, 48, 229–232.

Kawasaki, H., Hirano, H., and Tanaka, H., 1994. Effects of multiple draft tubes with perforated plates on gas holdup and volumetric mass transfer coefficient in a bubble column, Journal of Chemical Engineering of Japan, 27(5), 669-670.

Kemoun, A., Rados, N., Li, F., Al-Dahhan, M. H., Dudukovic, M. P., Mills, P. L., Leib, T. M., and Lerou, J. J., 2001. Gas holdup in a trayed cold-flow bubble column, Chemical Engineering Science, 56(3), 1197-1205.

Khoze, A. N., Burdukov, A. P., Nakoryakov, V. E., Pokusaev, B. G., and Kuz'min, V. A., 1971. Convective heat transfer in a dynamic two-phase bed, Journal of Engineering Physics, 20(6), 759-776.

Koide, K. and Kubota, H., 1966. Gas Holdup Distribution and Liquid Velocity Distribution on Bubble Flow in Vertical Column, Kagaku Kogaku, 30, 806-813.

Kölbel, H. and Ralek, M., 1980. The Fischer-Tropsch synthesis in the liquid phase, Catalysis reviews, science and engineering, 21(2), 225-274.

Kölbel, H., Borchers, E., and Langemann, H., 1961. Grossenverteilung der Gasblasen in Blasensaulen. Chemie-Ing. Technol., 33, 668-675.

Kölbel, H. and Ackermann, P., 1958. Apparatus for carrying out gaseous catalytic reactions in liquid medium. US Patent 2,853,369.

Kölbel, H. and Langheim, R., 1958. Carbon dioxide hydrogenation synthesis reactors. US Patent 2,852,350.

Korte, H., 1987. Heat transfer in bubble columns with and without internals, Ph.D. Thesis, University of Dortmund, Germany.

Krishna, R. and Sie, S. T., 2000. Design and scale-up of the Fischer–Tropsch bubble column slurry reactor, Fuel Processing Technology, 64(1-3), 73-105.

Krishna, R. and van Baten, J. M., 1999. Rise characteristics of gas bubbles in a 2D rectangular column: VOF simulations vs. experiments, International Communications in Heat and Mass Transfer, 26(7), 965-974.

Krishna, R., 2000. A scale-up strategy for a commercial scale bubble column slurry reactor for Fischer-Tropsch synthesis, Oil & Gas Science and Technology-Rev. IFP, 55, 359-393.

Krishna, R. and van Baten, J. M., 2003. A Strategy for Scaling Up the Fischer-Tropsch Bubble Column Slurry Reactor. Topics in Catalysis, 26 (1-4), 21-28.

Krishna, R. and Ellenberger, J., 1996. Gas hold-up in bubble column reactors operating in the churn-turbulent flow regime, American Institute of Chemical Engineers Journal, 42, 2627-2634.

Krishna, R. and Ellenberger, J., 2002. Improving gas–liquid contacting in bubble columns by vibration excitement, International Journal of Multiphase Flow, 28(7), 1223-1234.

Krishna, R., Ellenberger, J. and Maretto, C., 1999. Flow regime transition in bubble columns. International Communications in Heat and Mass Transfer, 26(4), 467-475.

Krishna, R., van Baten, J.M., Urseanu, M.I., and Ellenberger, J., 2001. Design and scale-up of the bubble column slurry reactor for Fischer-Tropsch synthesis, Chem. Eng. Sci., 56, 537-545.

Kulkarni, A.A. and Joshi, J.B., 2005. Bubble formation and bubble rise velocity in gas–liquid systems: a review. Industrial & Engineering Chemistry Research 44, 5873–5931.

Kumar, S. B., Devanathan, N., Moslemian, D., and Dudukovic, M. P., 1994. Effect of scale on liquid recirculation in bubble columns, Chemical Engineering Science, 49(24), 5637-5652.

Kumar, S. B., Moslemian, D., Dudukovic, M. P., 1995. γ-ray tomographic scanner for imaging void fraction distribution in bubble column, Flow Measurement and Instrumentation, 6, 61-73.

Kumar, S., Dudukovic, M. P., and Toseland, B. A., 1998. Measurement Techniques for local and global fluid dynamic quantities in two and three phase systems. Topical report.

Kwon, H. W., Y. Kang, S. D. Kim, M. Yashima, and Fan, L. T., 1994. Bubble-Chord Length and Pressure Fluctuations in Three-Phase Fluidized Beds, Ind. Eng. Chem. Res., 33, 1852-1857.

Lapin, A. and Lübbert, A., 1994. Numerical simulation of the dynamics of two-phase gas—liquid flows in bubble columns, Chemical Engineering Science, 49(21), 3661-3674.

Lapin, A.; Paaschen, T.; Junghans, K.; and Lübbert, A., 2002. Bubble column fluid dynamics, flow structures in slender columns with large-diameter ring-spargers, Chemical Engineering Science, 57(8), 1419-1424.

Larachi, F., Desvigne, D., Donnat, L., Schweich, D., 2006. Simulating the effects of liquid circulation in bubble columns with internals, Chemical Engineering Science, 61(13), 4195-4206.

Lee, S., 1990. Methanol Synthesis Technology, CRC Press, Boca Raton, FL.

Lee, S.L.P. and De Lasa, H.I., 1987. Phase holdups in three-phase fluidized beds, AIChE J. 33, 1359–1370.

Levenspiel, O., 1999. Chemical reaction Engineering, 3rd ed., Wiley, New York.

Li, H., and Prakash, A., 2001. Survey of heat transfer mechanisms in a slurry bubble column. The Canadian Journal of Chemical Engineering, 79, 717-725.

Liu W., Clark N. N., and Karamavruc A. I., 1998. Relationship between bubble size distribution and Chord-length distribution in heterogeneously bubbling systems, Chem. Eng Sci., 53, 1267-1276.

Luewisutthchat, W., Tsutsumi, A., and Yoshida, K., 1997. Bubble characteristics in multiphase flow systems: bubble sizes and size distributions. Journal of Chemical Engineering of Japan, 30 (3), 461-466.

Luo, H., Svendsen, H. F., *1996*. A Theoretical Model for Drop or *Bubble* Breakup in Turbulent Dispersions. AIChE J., 42(5), 1225-1233.

Luo, X., Zhang, J., Tsuchiya, K., and Fan, L.-S., 1997. On the rise velocity of bubbles in liquid-solid suspensions at elevated pressure and temperature. 52 (21-22), 3693-3699.

Macchi, A., 2002. Dimensionless Hydrodynamic Simulation of High Pressure multiphase reactors Subject to Foaming, Ph. D. Thesis, University of British Columbia, Vancouver, Canada.

Macchi, A., Bi, H., Grace, J. R., McKnight, C. A., and Hackman, L., 2001. Dimensional hydrodynamic similitude in three-phase fluidized beds, Chemical Engineering Science, 56 (21-22), 6039-6045.

Maretto, C. and Krishna, R., 2001. Design and optimisation of a multi-stage bubble column slurry reactor for Fischer-Tropsch synthesis, Catalysis Today, 66(2-4), 241-248.

Maretto, C. and Piccolo, V., 1998. Fischer-Tropsch process with a multistage bubble column reactor, US Patent 5,827,902.

Mashelkar, R. A. and Sharma, M. M., 1970. Mass transfer in bubble and packed bubble columns, Transactions of the Institution of Chemical Engineers, 48(4-6), 162-172.

Matsuura, A. and Fan, L-S., 1984. Distribution of bubble properties in a gas-liquid-solid fluidized bed, AIChE J., 30, 894-903.

Mecaial, N. and Sadik, B., 2007. Hydrodynamic and RTD of Sectionalized Bubble Column, Proceedings of the 12th International Conference on Fluidization - New Horizons in Fluidization Engineering.

Millies, M. and Mewes, D., 1995. Calculation of circulating flows in bubble columns, Chemical Engineering Science, 50(13), 2093-2106.

Mudde, R. F., 2005. Gravity-driven bubbly flows, Annual Reviews of Fluid Mechanics, 37, 393-423.

Nishikawa, M., Kato, H., and Hashimoto, K., 1977. Ind. Eng. Chem. Recess Des. Dev., 16, 133-139.

Nosier, S. A., 2003. Solid-liquid mass transfer at gas sparged tube bundles, Chemical Engineering & Technology, 26(11), 1151-1154.

Nosier, S. A. and Mohamed, M. M., 2004. Mass transfer at helical coils in bubble columns, Chemical and Biochemical Engineering Quarterly, 18(3), 235-239.

Nottenkämper, R., 1983. Zur Hydrodynamic in Blasensauelnreaktoren, Ph. D. Thesis University of Dortmund, Germany.

O'Dowd, W., Smith, D., N., Ruether, J. A. and Saxena, S., C., 1987. Gas and solids behavior in a baffled and unbaffled slurry bubble column, AIChE J., 33(12), 1959-1970.

Olmos, E., 2002. Etude expérimentale et numérique des écoulements gaz-liquide en colonnes à bulles. Ph. D. Thesis, Institut National Polytechnique de Lorraine, Nancy, France.

Ong, B. C., 2003. Experimental investigation of bubble column hydrodynamics –effect of elevated pressure and superficial gas velocity-, D. Sc. Thesis, Washington University in St. Louis, USA.

Ong, B. C., Gupta, P., Youssef, A., Al-Dahhan, M. and Dudukovic, M. P., 2009. Computed Tomographic Investigation of the Influence of Gas Sparger Design on Gas Holdup Distribution in a Bubble Column, Ind. Eng. Chem. Res., 48, 58–68.

Palaskar, S. N., De, J. K., Pandit, A. B., 2000. Liquid phase RTD studies in sectionalized bubble column. Chemical Engineering & Technology, 23(1), 61-69.

Pan, Y. and Dudukovic, M. P., 2000. Numerical Investigation of Gas-Driven Flow in 2-D Bubble Columns", AIChE J., (46) 3, 434-449.

Pan, Y., Dudukovic, M. P., and Chang, M., 1999. Dynamic simulation of bubbly flow in bubble columns, Chemical Engineering Science, 54(13-14), 2481-2489.

Pandit, A. B. and Doshi, Y. K., 2005. Mixing time studies in bubble column reactor with and without internals, International Journal of Chemical Reactor Engineering, 3.

Patel, S.A., Daly, J.G., and Bukur, D.B., 1990. Bubble-size distribution in Fischer-Tropsch-derived eaxes in a bubble column. AIChE J., 36(1), 93-105.

Pohorecki, R., Moniuk, W., Bielski, P., Zdrójkowski, A., 2001. Modelling of the coalescence/redispersion processes in bubble columns. Chemical Engineering Science 56, 6157–6164.

Pradhan A., K., Parichia, R., K. and De, P., 1993. Gas hold-up in non Newtonian solutions in a bubble column with internals, The Canadian journal of chemical engineering, 71, 468-471.

Prenosil, J. and Novosad, Z., 1968. Coll. Czech. Chem. Commun., 33, 376.

Rados, N., 2003. Slurry bubble column hydrodynamics: experimentation and modeling, DSc thesis, Washington University in St. Louis, Saint Louis, MO, USA.

Rafique, M., Chen, P., and Dudukovic, M. P., 2004. Computational, Modeling of Gas-Liquid Flow in Bubble Columns. Rev. Chem. Eng., 20 (3/4), 225-375.

Ranade, V. V., 1992. Flow in bubble columns: some numerical experiments, Chemical Engineering Science, 4(8), 1857-1869.

Reilly, I. G., Scott, D. S., de Bruijn, T. J. W., Jain, A., and Piskorz, J., 1986. Correlation for gas holdup in turbulent coalescing bubble columns, Canadian Journal of Chemical Engineering, 64, 705-717.

Rice, R. G. and Geary, N. W., 1990. Prediction of liquid recirculation in viscous bubble columns, AIChE J., 36, 1339-1348.

Safoniuk, M., 1999. Dimesnional Similitude and the hydrodynamics of three-phase fluidized beds, Ph. D. Thesis, University of British Columbia, Vancouver, Canada.

Safoniuk, M.; Grace, J. R.; Hackman, L.; McKnight, C. A., 1999. Use of dimensional similitude for scale-up of hydrodynamics in three-phase fluidized bed, Chemical Engineering Science, 54 (21), 4961-4966.

Sannaes B. H., 1997. Solids movement and concentration in column slurry reactors, Dr. Ing. Thesis, Norwegian University of Science and Technology, Trondheim, Norway.

Sanyal, J., Vásquez, S., Roy, S., and Dudukovic, M. P., 1999. Numerical simulation of gas–liquid dynamics in cylindrical bubble column reactors, Chemical Engineering Science, 54(21), 5071-5083.

Saxena, S. C., 1995. Bubble column reactors and Fischer-Tropsch synthesis. Catal.. Rev.- Sci. Eng., 37(2), 227-309.

Saxena, S. C., 1993. A novel heat exchanger design for slurry bubble columns. Transp. Phenom. Therm. Eng., Proc. Int. Symp., 6th, 896-901.

Saxena, S.C. and Chen, Z.D., 1994. Hydrodynamics and heat transfer of baffled and unbaffled slurry bubble columns, Reviews in Chemical Engineering, 10(3-4), 193-400.

Saxena, S.C. and Rao, N. S., 1993. Estimation of gas holdup in a slurry bubble column with internals: nitrogen–therminol–magnetite system. Powder Technology 75, 153–158.

Saxena, S. C. and Chen, Z. D., 1993. Heat transfer in baffled bubble columns of dilute slurries of fine powders and viscous liquids. Exp. Heat Transfer, Fluid Mech. Thermodyn., Proc. World Conf., 3rd, 2, 1451-1458.

Saxena, S. C. and Patel, B. B., 1991. Heat transfer investigations in a bubble column with immersed probes of different diameters, International Communications in Heat and Mass Transfer, 18(4), 467-478.

Saxena, S. C., Rao, N. S., and Yousuf, M., 1991. Hydrodynamic and heat transfer investigations conducted in a bubble column with fine powders and a viscous liquid Powder Technology, 67(3), 265-275.

Saxena, S. C., Rao, N. S., and Saxena, A. C., 1990. Estimation of heat transfer coefficient for immersed surfaces in bubble columns involving fine powders, Powder Technology, 63(2), 197-202.

Saxena, S. C., Rao, N. S., and Thimmapuram, P. R., 1992. Gas phase holdup in slurry bubble columns for two- and three-phase systems, Chemical Engineering Journal, 49(3), 151-159.

Schlüter, S., Steiff, A., and Weinspach, P.-M., 1995. Heat transfer in two- and three-phase bubble column reactors with internals, Chemical Engineering and Processing, 34(3), 157-172.

Schügerl, K., Lucke, J., and Oels, U., 1977. Bubble Column Bioreactors, Adv. Biochem. Eng., 7, 1-84.

Sekizawa, T. and Kubota, H., 1974. Liquid mixing in multistage bubble columns, Journal of Chemical Engineering of Japan, 7(6), 441-446.

Shah, Y. T., Ratway, C. A., and Mcilvried, H. G., 1978. Back-mixing characteristics of a bubble column with vertically suspended tubes, Transactions of the Institution of Chemical Engineers, 56(2), 107-112.

Shaikh, A. and Al-Dahhan, M. H., 2007. A Review on Flow Regime Transition in Bubble Columns, *International Journal of Chemical Reactor Engineering, 5.*

Shaikh, A., 2007Bubble and slurry bubble column reactors for syngas to liquid fuel conversion: mixing, flow regime transition, and scale-up, D.Sc. Thesis, Washington University in St. Louis, Saint Louis, MO, USA.

Shetty, S. A., Kantak, M. V., and Kelkar, B. G., 1992. Gas-phase backmixing in bubble - column reactors, AIChE J., 38(7), 1013-1026.

Sokolichin, A. and Eigenberger, 1994. G., Gas—liquid flow in bubble columns and loop reactors: Part I. Detailed modelling and numerical simulation, Chemical Engineering Science, 49(24), 5735-5746.

Soraker, P., Lian, P., and Vankan, S., Heat exchange system for a slurry bubble column reactor, 2005. WO Patent 2005/065813 A1.

Spect, E., 2009. http://hydra.nat.uni-magdeburg.de/packing.

Steynberg, A., and Dry, M., 2004. Fischer-Tropsch technology, Amsterdam: Elsevier.

Svendsen, H. F., Jakobsen, H. A., and and Torvik, R., 1992. Local flow structures in internal loop and bubble column reactors, Chemical Engineering Science, 47(13-14), 3297-3304.

Thimmapuram, P. R., Rao, N. S., and Saxena, S. C., 1993. Heat transfer from immersed tubes in a baffled slurry bubble column. Chemical Engineering Communications, 120, 27-43.

Thyn, J., Zitny, R., Kluson, J., and Cechak, T., 2000. Analysis and Diagnostics of industrial processes by radiotracers and radioisotope sealed sources, Vydavatelstvi CVUT, Praha.

Tsuchiya, K., Furumoto, A., Fan, L.-S., and Zhang, J., 1997. Suspension viscosity and bubble velocity in liquid-solid fuidized beds. Chemical Engineering Science, 52, 3053-3066.

Ueyama, K. and Miyauchi, T., 1979. Properties of recirculating turbulent two phase flow in gas bubble columns. AIChE J., 25, 258-266.

Ueyama, K., 2006. Force Balance Controlling Radial Gas Holdup Distribution for the Recirculating Turbulent Flow in Bubble Columns, Journal of Chemical Engineering of Japan, 39, 1, 1-6.

Ueyama, K., Morooka, S., Koide, K., Kaji, H., Miyauchi, T., 1980. Behavior of gas bubbles in bubble columns, Ind. Eng. Chem. Process Des. Dev., 19, 592-599.

Van den Bleek, C. M.; Schouten J. C., 1993. Can deterministic chaos create order in fluidized-bed scale-up?, Chemical Engineering Science 48, 2367-2373.

Vermeer, D.J. and Krishna, R., 1981. Hydrodynamics and. Mass Transfer in Bubble ColumnsOperating in the Churn-Turbulent Regime, Ind. Eng. Chem. Des. Dev., 20, 475-482.

Voyer, R. D. and Miller, A. I., 1968. Improved gas-liquid contacting in co-current flow, Canadian Journal of Chemical Engineering, 46(5), 335-341.

Warsito, W. and Fan, L.-S., 2005. Dynamics of spiral bubble plume motion in the entrance region of bubble columns and three-phase fluidized beds using 3D ECT. Chemical Engineering Science, 60 (22), 6073-6084.

Wender, I., 1996. Reactions of Synthesis Gas, Fuel Processing Technology, 48, 189-297.

Westerterp, K. R., van Swaaij, W. P. M., and Beenackers, A. A. C. M., 1987. Chemical reactor design and operation, Chicester: Wiley.

Wild, G., Poncin, S., Li, H., and Olmos, E., 2003. Some aspects of the hydrodynamics of bubble columns, International Journal of chemical reactor engineering, 1.

Wilkinson, P., 1991. Physical aspects and scale-up of high pressure bubble columns, Ph. D. Thesis, University of Groningen, The Netherlands.

Wilkinson, P. M., Spek, A. P., and Van Dierendonck, L. L., 1992. Design parameters estimation for scale-up of high-pressure bubble columns. AIChE J., 38(4), 544-554.

Wu, C., 2007. Heat Transfer and Bubble Dynamics in Slurry Bubble Columns for Fischer-Tropsch Clean Alternative Energy, Ph.D. Thesis, Washington University in St. Louis, Saint Louis, MO, USA.

Wu, C., Suddard, K., and Al-Dahhan, M., 2008. Bubble dynamics Investigation in a slurry bubble column, 54, 5, 1203-1212.

Xu, S., Qu, Y., Chaouki, J., and Guy, C., 2005. Characterization of Homogeneity of Bubble Flows in Bubble Columns Using RPT and Fiber Optics. International Journal of Chemical Reactor Engineering, 3, 16.

Xue, J., Al-Dahhan, M., Dudukovic, M., P., and Mudde, R., F., 2008. Bubble velocity, size, and interfacial area measurements in a bubble column by four-point optical probe, AIChE J., 54(2), 350-363.

Xue, J., Al-Dahhan, M., Dudukovic, M.P., and Mudde, R.F., 2003. Bubble dynamics measurements using four-point optical probe, The Canadian Journal of Chemical Engineering, 81, 1-7.

Xue, J., 2004. Bubble velocity, size and interfacial area measurements in bubble columns, D. Sc. Thesis, Washington University in St. Louis, Saint Louis, MO, USA.

Yamashita F., 1987. Effects of vertical pipe and rod internals on gas holdup in bubble columns, Journal of Chemical Engineering of Japan, 20(2), 204-206.

Yang, G. Q., Fan, L. S., 2003. Axial liquid mixing in high-pressure bubble columns. AIChE J., 49 (8), 1995-2008.

Yang, G. Q., Du, B., and Fan L. S., 2007. Bubble formation and dynamics in gas–liquid–solid fluidization—A review, Chemical Engineering Science, 62(1-2), 2-27.

Yasunishi, A., Fukuma, M., and Muroyama, K., 1986. Measurement of behavior of gas bubbles and gas holdup in a slurry bubble column by a dual electroresistivity probe method. 19 (5), 444-449.

Yoshida, F. and Akita, K., 1965. Performance of Gas bubble columns: Volumetric Liquid-Phase Mass transfer Coefficient and Gas Holdup, AIChE J., 11, 9-13.

Youssef, A. A. and Al-Dahhan, M. H., 2009. Impact of Internals on the Gas Holdup and Bubble Properties of a Bubble Column, Industrial & Engineering Chemistry Research, 48(17), 8007-8013.

Youssef, A. A., Al-Dahhan, M. H., and Dudukovic, M. P., 2010. Bubble Columns with Internals: A Review, International Journal of Chemical Reactor Engineering (Submitted).

Vita

Ahmed Abouelfetouh Youssef

Date of Birth	January 15, 1984
Place of Birth	Alexandria, Egypt
Degrees	B.Sc. Degree of Honor, Chemical Engineering, June 2006. Alexandria University, Alexandria, Egypt. M.Sc., Chemical Engineering, December 2008. Washington University, Saint Louis, MO, USA. Ph.D., Energy, Environmental and Chemical Engineering, August 2010. Washington University, Saint Louis, MO, USA.
Industrial Experience	Bayer Technology Services GmbH, Leverkusen, Germany (2009) Sasol Technology Netherlands bv., Enschede, The Netherlands (2009)
Professional Societies	Water Environment Federation

Publications

Youssef, A. A., Al-Dahhan, M. H., and Dudukovic, M. P., 2010. Bubble Columns with Internals: A Review, International Journal of Chemical Reactor Engineering (Submitted).

Youssef, A.; Hamed, M., Dudukovic, M. and Al-Dahhan, M. "Novel scale-up methodology for bubble column reactors" (2009), International Journal of Chemical Reactor Engineering (accepted).

Youssef, A. A. and Al-Dahhan, M. H., 2009. Impact of Internals on the Gas Holdup and Bubble Properties of a Bubble Column, Industrial & Engineering Chemistry Research, 48(17), 8007-8013.

Ong, B. C., Gupta, P., Youssef, A., Al-Dahhan, M. and Dudukovic, M. P., 2009. Computed Tomographic Investigation of the Influence of Gas Sparger Design on Gas Holdup Distribution in a Bubble Column, Industrial & Engineering Chemistry Research, 48, 58–68.

Presentations

Youssef, A.; Dudukovic, M. and Al-Dahhan, M. "Novel scale-up methodology for bubble column reactors" – GLS9 (8th World Congress of Chemical Engineering 2009 – Montreal, Canada, August 23-27, 2009.

Youssef, A.; Dudukovic, M. and Al-Dahhan, M. "On the Hydrodynamics of Bubble Columns with Internals for Liquid Fuels Syntheses" – AIChE Spring National Meeting 2009 – Tampa, FL, April 26-30, 2009.

Youssef, A.; Dudukovic, M. and Al-Dahhan, M. "Novel Design of Multiphase reactors for Biomass-to-Liquid Synthesis" – Bioenergy II: Chemicals and Fuels from Renewable Resources – Rio de Janeiro, Brazil, March 8-13, 2009.

Youssef, A.; Dudukovic, M. and Al-Dahhan, M. "Novel reactor design for clean alternative fuels synthesis" - 2nd International Symposium of Energy and Environment – Hong Kong, December 8-10, 2008.

May, 2010